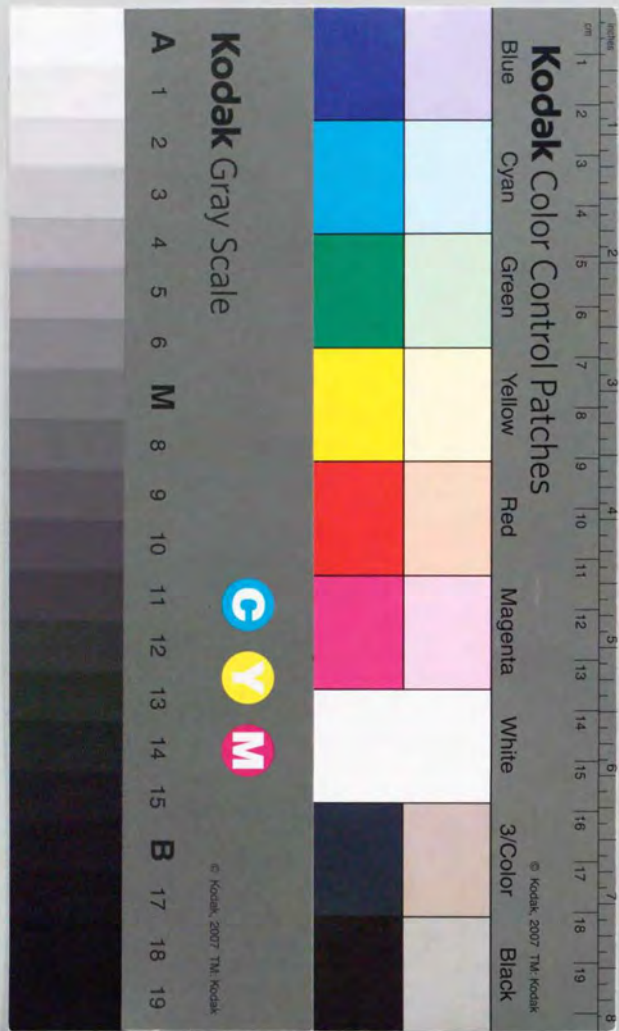Polymerized Membranes and Their Phase
Transitions

高分子膜とその相転移

平成　7 年　1 0 月　理学博士　申請

東京大学大学院理学系研究科

物理学専攻

守　真太郎

THESIS

Polymerized Membranes
and Their Phase Transitions

Shintaro Mori

Department of Physics, Graduate School of Science
University of Tokyo

October, 1995

Acknowledgements

The author * expresses his sincerest gratitude to Professor Miki Wadati for useful discussions, suggestions, and above all constant encouragements during his graduate study.

He also thanks Prof. S.Komura for several guidances and suggestions about tethered membrane and its numerical studies. He also benefited from useful and instructive discussions with Prof.D.R.Nelson, Prof.E.Guitter, Prof.M.Plischke, Prof.M.Kardar, Prof.L.Peliti, Prof.F.David, Prof.T.Eguchi, Prof.M.Doi, Prof.Y.Saito and Dr.Y.Ozeki and expresses his great gratitude to them. Especially, discussions with Prof.D.R.Nelson and Prof.E.Guitter are very helpful and he thinks that it is impossible to make these works complete without them.

He also thanks Dr.K.Nakayama and Mr.Y.Kajinaga for useful discussions and helps in preparing several figures in this work. He also expresses his gratitude to the superusers Mr.H.Mizuta and Dr.K.Tsurusaki for preparing convenient circumstance of using work stations. And he thanks workstation DEC 3000 "Monet", "Renoir" and "Cezanne" for performing numerical studies. Without their helps, the works in chapter 3 has not been finished.

He would like to acknowledge fruitful discussions with all members of the informal seminar "maku no kenkyuukai" and expresses his sincere gratitude to them.

Finally, he thanks his parents for mental and financial support.

---

*e-mail address : mori@monet.phys.s.u-tokyo.ac.jp.

i

Abstract

In this thesis we discuss the statistical properties of polymerized membranes. In particular we concentrate on the phase transitions of polymerized membranes, wrinkling transition of randomly polymerized membrane and flat- compact phase transition of polymerized membrane in poor solvent.

In chapter 1, we review several fundamental results about polymerized membranes. After presenting the definition of the polymerized membrane and explaining notations in Sec.1.2, we review its phase transition, known as crumpling transition, from a crumpled phase to a flat phase as we increase its bending rigidity in Sec.1.3. In Sec.1.4, we discuss the effect of self-avoiding interaction. The membrane with self-avoiding interaction is flat when embedded in 3-dimensional space. We explain the mechanism that the "entropic" bending rigidity induced by self-avoiding interaction causes the crumpling transition like crossover. We also present a theoretical approach that explain the mechanism and a related phenomenon. In Sec.1.5, we discuss the polymerized membranes with long-range repulsive interactions ($r^{-\gamma}$). We briefly explain the method of the large-d limit, which will be used in later chapters. Sec.1.6 is devoted to the discussions on the effects of quenched in-plane disorders. We explain the condition of the buckling transition and the stability of the flat phase with respect to weak random stress.

The following chapters are the main part of the thesis. Chap. 2 and Chap. 3 are devoted to theoretical and numerical studies of self-avoiding randomly polymerized membranes. In Sec.2.2 we study the D-dimensional randomly polymerized membrane with long-range repulsive interactions ($r^{-\gamma}$) using the large-d limit analysis. The phase diagram in the (γ, D) plane is obtained. Due to the random stress, the flat phase becomes unstable and the crumpled glass phase takes over. The crumpled phases are not affected in the large-d limit. In order to discuss the effect of quenched randomnesses on the crumpled phases, we study the generalized Edwards model with disorders in Sec.2.3. Using the replica field theory we estimate the exponent for the radius of gyration. We show that even a short-range disorder is relevant at $d < 8$ and crumpled phase exists at $2 < d < 4$. This means that the self-avoiding polymerized membrane with short-range disorder can be crumpled

at $d = 3$. On the other hand, as has been explained in Sec.1.6, the flat phase of the rigid membrane is stable with respect to weak randomnesses at $T > 0$. Based on these results, we propose the possibility that there exists a phase transition between the crumpled phase and the flat phase in the self-avoiding randomly polymerized membrane as we change its bending rigidity or the strength of random stress.

In order to study the above possibility, especially the possible crumpled phases, we perform numerical studies in Chap.3. In Sec.3.2, we describe models and numerical procedures. We study two types of self-avoiding tethered membrane with random stress. The "effective" bending rigidity of the membrane are controlled by changing their reference bond length b between monomers. The results are summarized as follows: (1) The membrane with "strong" self-avoidance is asymptotically flat and the quenched in-plane disorders only cause local bucklings. (2) The membrane with "weak" self-avoidance shows large shrink even if the strength of disorder is weak. The membrane with strong disorder is crumpled with the exponent $\nu = 0.84 \sim 0.90 (R_G \sim L^\nu)$. The result is in good accordance with the theoretical value $\nu = 6/7$. The membrane with weak disorder is flat with small roughness exponent $\nu_\perp = 0.3 \pm 0.1$. In Sec.3.4, we discuss implications of the results, in particular its relevance to the wrinkling transition of partially polymerized membranes.

In Chap.4 we discuss phase transitions of polymerized membrane with attractive interactions. We summarize previous numerical results in Sec.4.1. Depending on the local flexibility of the membrane, it shows two-types of phase transitions. When the membrane is less flexible, it shows a first-order transition frrom the flat phase to the compact phase as the temperature decreases. If the membrane has open boundary it shows a sequential folding transition. When the membrane is very flexible, it seems to show a ccontinuous phase transition from the flat phase to the compact phase passing through a intermediate crumpled phase. In Sec.4.2, we review the Landau model for the phase transitions. Sec.4.3 is devoted to a theory for D-dimensional polymerized membrane with attractive long-range interactions ($r^{-\gamma}$). Using the large-d limit analysis, we solve the model and discuss possible phases and phase transitions in the (γ, D) plane. When the interaction is short-ranged, the membrane shows a continuous phase transition from the flat phase to the compact phase passing through a critical crumpled phase. Based on the result, we propose a theoretical interpretations about the above flexible case. In particular we emphasize on the viewpoint of the cancellation between the "entropic" bending rigidity and the negative bending rigidity from attractive interactions which causes the crumpling transition of the membrane. In order to describe the sequential folding transition of the membrane with attractive interaction, we study the effect of attractive ($\omega < 0$)and repulsive ($\omega > 0$) interactions on the square lattice model, which is introduced by David and

Guitter in Sec.4.4. We obtain the phase diagrams in the (u, ω) plane and showd that this model describes the sequential folding transition of the polymerized membrane.

List of Publications

List of papers submitted for the requirement of the Degree

Chapter 2:

1. S.Mori and M.Wadati: Randomly Polymerized Membranes with Long-range Interactions, Phys.Lett.**A185**.(1994)206.

2. S.Mori and M.Wadati: Tethered Membranes with Quenched Random Internal Disorders and Long range interactions, J.Phys.Soc.Jpn.**63**(1993)3864.

3. S.Mori and M.Wadati: Crumpled Phases of Self-Avoiding Randomly Polymerized Membranes, Phys.Rev.**E50**(1994)867.

Chapter 3:

4. S.Mori: Conformation of Self-Avoiding Randomly Tethered Membrane
, Phys.Lett.**A207**(1995)87.

5. S.Mori: Conformation of Self-Avoiding Randomly Tethered Membrane, preprint submitted to J.Phys.Soc.Jpn.

6. S.Mori: Self-Avoiding Tethered Membrane with Quenched Random Internal Disoreders, preprint submitted to Phys.Rev.**E**.

Chapter 4:

7. S.Mori and M.Wadati: Phase Transitions of Polymerized Membranes with Attractive Long-range Interactions, Phys.Lett.**A201**(1995)61.

8. S.Mori and Y.Kajinaga: Square Lattice with Attractive Interactions, Phys.Rev.**E** (1996)in press.

Other references:

1. S.Mori and M.Wadati: Curvature Instability induced by Diffusing Particles, J.Phy.Soc.Jpn.**63**(1993)3557.

2. S.Mori and M.Wadati: Spherical Model and Curvature Instability, J.Phys.Soc.Jpn.**63**(1993)3565.

3. K.Kawanishi, S.Mori and M.Wadati: Crumpling Transition of Self-Avoiding Tethered Membranes Caused by Screening, Phys.Lett.**A190**(1994)439.

4. S.Mori, K.Kawanishi and M.Wadati: Dilute and Semi-dilute Solutions of Randomly Polymerized Membranes, J.Phys.Soc.Jpn.**64**(1994)64.

5. S.Mori and S.Komura : Self-Avoiding Tethered Membrane with Negative Bending Rigidity, preprint.

Contents

Chapter 1

Polymerized Membranes

1.1 Genesis

Statistical properties of membranes and surfaces has been studied extensively during these twenty years [1]. Membranes can be regarded as a two-dimensional generalization of linear polymer chains, which have a long history of extensive researches. However, membranes are very different from linear polymers. One of the most important difference is that constituent molecules of membranes can be in several different phases and the difference in the internal properties causes very different physical properties. For example, the molecules in fluid membranes can be in liquid or hexatic phase [2, 3, 4, 5]. The fluid membrane with hexatic order has long-range correlation between normals of the membrane [5]. On the other hand, the fluid membrane with no internal order is crumpled with no such correlation [6]. Another example of membranes is polymerized (or tethered) membrane, where connections between monomers are fixed and its local order is crystalline [6]. Such membrane has a nonzero shear modulus and shows different behavior from their liquid counterparts. One of the differences is that the membrane with bending rigidity shows a flat phase at sufficiently low temperature [6]. The flat phase is stabilized by the presence of long-range force which is induced by the coupling of undulation modes with the elastic phonon modes. Theoretically, at high temperature it was considered that a crumpled phase does exists [7, 8]. However, a crumpled phase does only appear in computer simulation of a "phantom" membrane or at the "Θ point of flat-compact phase transition of an attractive polymerized membrane [9]. Now it is widely believed that self-avoiding tethered membranes are always flat due to large entropically induced bending rigidity [10, 11]. In this chapter, we briefly review some theoretical results of polymerized membranes.

1.2 Generalities and Definitions

Here we define the polymerized membrane with a lattice model of a flexible D-dimensional sheet of interconnected particles embedded in the d-dimensional space [1, 7, 8]. The configuration of a polymerized membrane is given, once the location of each monomers in the d-dimensional space is known. The fixed connectivity of the polymerized membrane allows us to label the constituent particles with a D-dimensional vector $\vec{\sigma}$,

$$\vec{\sigma} \equiv (\sigma_\alpha), \quad (\alpha = 1, 2, \cdots, D). \tag{1.2.1}$$

We specify the embedding of these particles inside the d-dimensional space with a continuous d-dimensional vector fields $\vec{X}(\sigma)$,

$$\vec{X} \equiv (X^i) \ (i = 1, 2, \cdots, d). \tag{1.2.2}$$

Because here we are only interested in the large distance physics, with the usual coarse graining, we pass to a continuum field theoretic model. We assume that the configuration $\vec{X}_0(\sigma)$ of minimal energy is flat. We can select coordinates σ_α such that the configuration

$$\vec{X}_0 = \zeta(\sigma_1, \sigma_2, \cdots, \sigma_D, 0, 0, \cdots, 0) \tag{1.2.3}$$

minimize the free energy. The induced metric $g_{\alpha\beta}$ is defined by

$$g_{\alpha\beta} = \partial_\alpha \vec{X} \cdot \partial_\beta \vec{X}, \tag{1.2.4}$$

and the corresponding ground state metric is

$$g_{0\alpha\beta} = \partial_\alpha \vec{X}_0 \cdot \partial_\beta \vec{X}_0 = \zeta^2 \delta_{\alpha\beta}. \tag{1.2.5}$$

The curvature tensor $\vec{K}_{ij}$ is defined by

$$\vec{K}_{ij} = D_i D_j \vec{X} \tag{1.2.6}$$

where D_i denotes the covariant derivative.

1.3 Phantom Polymerized Membranes

Here we introduce a model for polymerized membranes [4, 13]. We require that the continuum field theoretical model respects all the original symmetries of the underlying lattice model and construct an effective free energy that is invariant under translation and rotation in the embedding d-dimensional space and is $O(D)$ invariant. From the

translational invariance, the effective Hamiltonian $\mathcal{H}_{eff}$ of an arbitrary configuration $\vec{X}(\sigma)$ can be expressed as a Taylor series in $\partial_\alpha \vec{X}$ and its derivatives,

$$\mathcal{H}_{eff}(\vec{X}) = \int d^D\sigma[\frac{1}{2}\kappa(\partial_\alpha^2 \vec{X})^2 + \frac{1}{2}t(\partial_\alpha \vec{X})^2 + u(\partial_\alpha \vec{X} \cdot \partial_\beta \vec{X})^2 + v(\partial_\alpha \vec{X} \cdot \partial_\alpha \vec{X})^2. \quad (1.3.1)$$

The terms neglected here are of higher order in $\vec{X}$ or involve higher derivatives, and may be shown to be irrelevant. We also exclude distant-neighbor interactions, restricting our attention to phantom membrane or the flat phase of self-avoiding ones [7, 8].

Upon identifying the tangent vectors $\vec{t}_\alpha \equiv \partial_\alpha \vec{X}$ as the order parameters of this field theory, an analogy with the usual ϕ^4 theories of critical phenomena becomes apparent [14]. Within mean-field theory the high-temperature crumpled phase is characterized by a positive t and the low-temperature flat phase is characterized by a negative t. It can be shown that the order parameter ζ behaves as

$$\zeta = \frac{1}{2}\sqrt{(\frac{-t}{u + Dv})}. \quad (1.3.2)$$

The nonlinear quartic term are now essential to stabilize the membrane.

When $T > T_C$ or $t > 0$, the membrane is crumpled. A usual measure of the size of the membrane in this high temperature phase is the correlation function

$$< |\vec{X}(\vec{\sigma}) - \vec{X}(0)|^2 > = 2\frac{1}{(2\pi)^2}\int d^2q < \vec{X}(q) \cdot \vec{X}(-q) > (1 - \exp(i\vec{q}\cdot\vec{\sigma})), \quad (1.3.3)$$

where the brackets represent a thermal average and we consider two-dimensional membrane case. At high temperature, the term proportional to κ, u and v in eq.(1.3.1) produce only small corrections to the basic result,

$$< \vec{X}(\vec{q}) \cdot \vec{X}(-\vec{q}) > = \frac{1}{tq^2}, \quad (1.3.4)$$

and it follows that

$$\lim_{\sigma\to\infty} < |\vec{X}(\vec{\sigma}) - \vec{X}(0)|^2 > \simeq \frac{1}{t\pi}\ln(\sigma/a), \quad (1.3.5)$$

where a is a microscopic cutoff. A measure of the membrane size R_G is this correlation function evaluated at $\sigma \sim L$, where L is a typical membrane internal dimension [7, 8]:

$$R_G \simeq \frac{1}{\sqrt{(\pi t)}}\ln^{1/2}(L/a). \quad (1.3.6)$$

The exponent ν for the radius of gyration $R_G(R_G \sim L^\nu)$ is zero.

In order to see the meaning of the original Hamiltonian (1.3.1) in the flat phase ($t < 0$), we rewrite it in the following form,

$$\mathcal{H}_{eff}(\vec{X}) = \int d^D\sigma[\frac{1}{2}\kappa(\partial_\alpha^2 \vec{X})^2 + \mu(u_{\alpha\beta})^2 + \lambda(u_{\alpha\alpha})^2]. \quad (1.3.7)$$

where μ and λ are Lamé coefficients, related to the previous couplings by $\mu = 4u\zeta^4$ and $\lambda = 8v\zeta^4$. The quantity $u_{\alpha\beta}$ is the strain tensor, defined by

$$u_{\alpha\beta} = \frac{1}{2\zeta^2}(g_{\alpha\beta} - g_{0\alpha\beta}). \quad (1.3.8)$$

The strain tensor measures the local deformation of the membrane relative to the metric in the ground state. For the pure system this reference metric $g_{0\alpha\beta}$ is always taken to be flat. However, as we will discuss later, the disorder will modify the reference metric.

Hereafter, we discuss the thermal fluctuations in the flat polymerized membrane [4, 13]. We concentrate on the case of experimental interest $(D, d) = (2, 3)$. Upon setting

$$\vec{X}(\sigma) = \zeta\{[\sigma_\alpha + u_\alpha(\sigma)]\vec{e}_\alpha + f(\sigma)\vec{e}_3\}, \quad (1.3.9)$$

with $\alpha = 1, 2$ and $\vec{e}_3 = \vec{e}_1 \times \vec{e}_2$, the Hamiltonian (1.3.7), to leading order in the gradients of the $u_\alpha(\sigma)$ and $f(\sigma)$, reduces to

$$\mathcal{H}_{eff} = \int d^2\sigma[\frac{1}{2}\kappa(\partial_\alpha^2 f)^2 + \mu(u^0_{\alpha\beta})^2 + \lambda(u^0_{\alpha\alpha})^2], \quad (1.3.10)$$

with

$$u^0_{\alpha\beta}(\sigma) = \frac{1}{2}(\partial_\alpha u_\beta + \partial_\beta u_\alpha + \partial_\alpha f\partial_\beta f). \quad (1.3.11)$$

After integrating out the phonon fields u_α, the Hamiltonian has two parameters, the bending rigidity κ and the elastic parameter $K_0 \equiv 4\mu(\mu + \lambda)/(2\mu + \lambda)$.

We now evaluate the renormalized wave vector dependent bending rigidity $\kappa_R(\vec{q})$ and the elastic parameter $K_R(\vec{q})$ by caluculating the two and four point connected correlation function as,

$$< |f(\vec{q})|^2 >_C \equiv \frac{k_B T}{\kappa_R(q)|q|^4}, \quad (1.3.12)$$

$$< f(\vec{q}_1)f(\vec{q} - \vec{q}_1)f(\vec{q}_2)f(\vec{q}_2 - \vec{q}) >_C \equiv k_B T K_R(q)P^T_{\alpha\beta}(\vec{q})P^T_{\gamma\delta}(\vec{q})q_{1\alpha}q_{1\beta}q_{2\gamma}q_{2\delta} \quad (1.3.13)$$

where $P^T_{\alpha\beta}$ is the transverse projection operator, $P^T_{\alpha\beta} \equiv \delta_{\alpha\beta} - \partial_\alpha\partial_\beta/\Delta$ and Δ is the Laplacian.

To leading order in $k_B T$, we obtain the renormalized bending rigidity and elastic parameter as [6]

$$\kappa_R(q) = \kappa + k_B T\frac{1}{(2\pi)^2}\int d^2p\frac{K_0[\hat{q}_\alpha P^T_{\alpha\beta}(\vec{p})\hat{q}_\beta]^2}{\kappa|\vec{q} + \vec{p}|^4} \quad (1.3.14)$$

$$K_R(q) = K_0 - \frac{k_B T}{2}P^T_{\alpha\beta}(\vec{q})P^T_{\gamma\delta}(\vec{q})\frac{1}{(2\pi)^2}\int d^2p\frac{K_0^2 p_\alpha p_\beta p_\gamma p_\delta}{\kappa|\vec{p}|^4\kappa|\vec{q} - \vec{p}|^4}, \quad (1.3.15)$$

where there is an implicit upper cutoff Λ in the integrals. Although the above perturbation series is infrared divergent, we can still extract the qualitative effects of thermal fluctuations. A simple self-consistent theory which replace κ by κ_R in the integrand of eq.(1.3.14) and assumes no significant renormalization of K_0 gives

$$\kappa_R(q) \sim \sqrt{T}q^{-1}. \qquad (1.3.16)$$

This means long-range order in the normals and thermal reduction of effective bending rigidity. The equation (1.3.15) means that to one-loop order K_R is reduced by thermal fluctuations. More precisely, these parameters $\kappa_R(p)$ and $K_R(p)$ are expected to be singular as p tends to zero, with $\kappa_R(p) \sim p^{-\eta_k}$ and $K_R(p) \sim p^{\eta_u}$. From a rotational invariance, these exponents satisfy the scaling relation $2\eta_K + \eta_u = 2$ and are estimated using ϵ-expansion etc [13].

1.4 Self-Avoiding Polymerized Membranes: Short-Range Interaction Case

In a pioneer work [7, 8], Kantor et.al. studied the effect of self-avoiding interaction on a phantom polymerized membrane numerically and it was shown only to swell the membrane and the exponent for the radius of gyration is obtained as $\nu \sim 0.8$. In order to discuss the self-avoiding effect, they have introduced the generalized Edwards model for D-dimensional manifold in the d-dimensional space as

$$\mathcal{H}[\vec{X}(\sigma)] = \int d^D\sigma \frac{1}{2}\partial_\alpha X^i \partial_\alpha X^i + u \int d^D\sigma \int d^D\sigma' \delta^d(X^i(\sigma) - X^i(\sigma')). \qquad (1.4.1)$$

The first term is the "entropic" gaussian potential term, which appears in the previous section. The second term means the excluded volume interaction by assigning a positive energetic penalty u whenever two elements of the surface occupy the same position in the d-dimensional embedding space.

Scaling behavior of a self-avoiding tethered membrane can be studied by Flory-type approximation. Assume a D-dimensional manifold of internal size L occupying a region of size R_G in the d-dimensional embedding space. According to Flory, the free energy $\mathcal{F}$ is estimated as

$$\mathcal{F}/k_BT = \frac{1}{2}L^D(\frac{R_G}{L})^2 + u(\frac{L^D}{R_G^d})^2 R_G{}^d. \qquad (1.4.2)$$

Here, R_G is the radius of gyration of the manifold and the second term is the mean field estimate of the self-avoiding interaction. By balancing two terms in the free energy and assuming the scaling form $R_G \sim L^{\nu_F}$, the exponent ν_F is

$$\nu_F = \frac{D+2}{d+2}. \qquad (1.4.3)$$

In the case of membrane in three dimensional space $(D,d) = (2,3)$, $\nu_F = 4/5$ and this result is in good agreement with the numerical data $\nu \sim 0.8$.

However, after the work, extensive numerical studies has been performed and now it was widely believed that the self-avoiding membrane is always flat even if its "bare" bending rigidity is zero [17, 18, 19]. This means that the crumpling transition does not occur in self-avoiding membranes and there does not exist any crumpled phase. The flat phase observed in these computer simulations was partly explained in terms of the crumpling transition induced by the implicit bending rigidity ("entropic" rigidity) from self-avoidance [10]. In fact, the restriction of the excluded volume interactions between next nearest neighbor particles with hard core potential prevents the membranes from bending freely and induce the bending rigidity. This discussion also means that the hard sphere model has inevitably large bending rigidity and that these simulations did not study the "pure" self-avoiding polymerized membrane. In other words, this argument clarified the possibility of attributing the flatness to the model-dependent problems in numerical simulations. On the other hand, there reported an interesting result that the tethered membranes with the excluded volume interactions are always flat even for small diameters of hard cores [19]. With hard spheres of smaller diameters, it is possible to reduce the entropic bending rigidity and to study the effect of the "pure" self-avoidance. The "plaquette" membrane model [20, 21], which has incorporated the effect of self-avoidance by prohibiting all intersections of each plaquette instead of hard sphere, was also shown to be asymptotically flat. In Ref. [11], the model tethered membrane was described by a local Hamiltonian with the repulsive interactions acting only between atoms whose degree of neighborhood does not exceed a certain value l. It was found that the hard-core diameter σ has a critical value $\sigma_c(l)$ at which the membranes undergo a crumpling transition. Moreover a relation $\sigma_c(l)^3 l^4 = $ Constant was also discovered. This indicates that the membrane becomes flat when the excluded volume interactions are active even for the case with small diameter. Thus it was concluded that the flatness is an inherent property of self-avoiding tethered membranes. In addition, Kantor and Kremer proposed the following picture about the behavior of the self-avoiding membrane: On very short length scale self-avoidance is not felt and the surface is crumpled. Then, the self-avoidance begin to modify the behavior of the membrane. Up to certain length scales l_C, self-avoiding interactions produce effective rigidity that suffices to keep the entire membrane flat. In a sense, the crumpling transition-like crossover occurs through the effective rigidity. Beyond the scale l_C the self-avoiding interaction no longer plays an essential role.

While the flatness of the tethered membranes with the excluded volume interactions

is established in numerical simulations, there is no satisfactory theory that explains such behavior of the membranes with self-avoidance. We have only Gaussian variational approach to obtain sensible results [22, 23, 24]. This is a variational approach and the best quadratic Hamiltonian is determined by finding an upper bound for the exact free energy $\mathcal{F}$,

$$\mathcal{F} = -\ln Z, \quad Z = \int \mathcal{D}[\vec{X}]e^{-\mathcal{H}}. \tag{1.4.4}$$

Here $\mathcal{H}$ is the Hamiltonian of the generalized Edwards model. The most general trial hamiltonian, quadratic in the fields, is

$$\mathcal{H}_0 = \int d^D k \{X^i(-k)g(k)X^i(k)\}. \tag{1.4.5}$$

From the analysis, it was found that the membranes are crumpled above $d = 4$ and R_g scales as $R_g \sim L^{\nu_G}$ with $\nu_G = 4/d$. The exponent ν_G gives a good estimate to the results of computer simulations in higher dimensions $d \geq 4$ [25](Table 1.1).

Table 1.1: Self-Avoiding Tethered Membrane in Higher Dimensional Space

Dimension	Numerical Result	Gaussian Approx.	Flory Approx.
3	Flat	Flat	0.8
4	Flat	1.0	0.666
5	0.82 ± 0.05	0.8	0.571
6	0.69 ± 0.05	0.666	0.50
8	0.60 ± 0.03	0.5	0.40

These theories only treat the crumpled phases and does not describe the crumpling transition induced by the entropic rigidity. However, we can derive the scaling relation obtained by Kantor and Kremer as follows [26]. According to the above picture, at short length scale, the membrane is crumpled. We assume that at this scale we can use the generalized Edwards model (1.4.1) and that, the interaction $\delta^d(X^i(\sigma) - X^i(\sigma'))$ is valid only when $(\sigma - \sigma')^2$ is smaller than some length scale $l_C{}^2$. When $(\sigma - \sigma')^2$ is greater than $l_C{}^2$, the interaction vanishes. From the self-consistent equation for the propagator $g(k)$, it is possible to obtain the effective rigidity κ_{eff} from the self-avoidance with strength u as

$$\kappa_{eff} = \text{const.} \times u \int d^D \sigma \sigma^4 \langle (\vec{X}(\vec{\sigma}) - \vec{X}(0))^2 \rangle^{-1-d/2}, \tag{1.4.6}$$

where $\langle (\vec{X}(\vec{\sigma}) - \vec{X}(0))^2 \rangle$ is the two-point function and we simply assume that $\langle (\vec{X}(\vec{\sigma}) - \vec{X}(0))^2 \rangle = A\sigma^2$ with some constant A, because near the length scale l_C, the membrane is almost flat. The length scale l_C is determined by the condition that the effective

bending rigidity becomes large enough for the crumpling transition to occur. Therefore, the value of the effective rigidity (1.4.6) is almost fixed at the critical value κ_C of the crumpling transition of the phantom tethered membrane. In the work [11], the range of the neighborhood l and the critical diameter of the hard sphere σ_c are determined by the condition that the crumpling transition occurs. In this case, the range l can be identified with the length l_C and u corresponds to $\sigma_c{}^d$. Then the integral at $d \leq 4$ behaves as

$$\int d^2 \sigma \sigma^4 (\frac{1}{\sigma^2})^{1+d/2} \sim l_C{}^{4-d}, \tag{1.4.7}$$

and we obtain the following relation at $d \leq 4$,

$$B l_C{}^{4-d} u = \kappa_C, \tag{1.4.8}$$

where B is a positive constant. Kantor and Kremer obtained the following relation

$$l_C^4 u \sim 1 \quad \text{in } d = 3. \tag{1.4.9}$$

The exponent $4 - d$ is very different from their numerical result [11], this is the relation obtained by Kremer and Kantor.

From this result, we can rely on the results of the gaussian approximation, or at least, we think it gives some insights into the behavior of self-avoiding tethered membrane.

1.5 Self-Avoiding Polymerized Membranes: Long-Range Case

In this section, we review the results about tethered membranes with long-range repulsive interaction [22, 24]. The interaction between different positions, which is rotationally-invariant, is represented by V and we take $V(r^2) = u/(r^2)^{\frac{3}{2}}$, r and u being the distance and some positive constant, respectively. The Hamiltonian of the tethered membrane with long range interaction is given by

$$\begin{aligned} \mathcal{F}[\vec{X}(\sigma)] &= \int d^D \sigma [\frac{1}{2}\kappa \triangle \vec{X} \cdot \triangle \vec{X} + \frac{1}{4}\mu \{\partial_\alpha \vec{X} \cdot \partial_\beta \vec{X} - \delta_{\alpha\beta}\}^2 \\ &+ \frac{1}{8}\lambda \{\partial_\alpha \vec{X} \cdot \partial_\alpha \vec{X} - D\}^2] \\ &+ \int d^D \sigma \int d^D \sigma' V((\vec{X}(\sigma) - \vec{X}(\sigma'))^2). \end{aligned} \tag{1.5.1}$$

The first local term is the Hamiltonian for the phantom polymerized membrane which has been introduced previously. Le Doussal, Guitter and Palmeri solved this model exactly in the large-d limit [22, 24]. Here we explain it shortly.

After rescaling all physical constants, for instance, $\kappa \to d\kappa$, in order to obtain sensible and nontrivial results in the limit $d \to \infty$, we introduce several auxiliary fields $\chi_{\alpha\beta}, A, B$ and rewrite the above Hamiltonian into

$$\mathcal{H}_{C,\tilde{H}}[\vec{X}, \chi_{\alpha\beta}, A, B] = d \int d^D\sigma[\frac{1}{2}\kappa\triangle\vec{X} \cdot \triangle\vec{X} + \frac{1}{2}\chi_{\alpha\beta}(\partial_\alpha\vec{X} \cdot \partial_\beta\vec{X} - \delta_{\alpha\beta})$$
$$- \rho\frac{1}{2}(\chi_{\alpha\beta})^2 - \eta\frac{1}{2}(\chi_{\alpha\alpha})^2]$$
$$- d \int d^D\sigma \int d^D\sigma'\{\frac{1}{4}[(\vec{X}(\sigma) - \vec{X}(\sigma'))^2 - A]B(\sigma, \sigma')$$
$$- V(A(\sigma, \sigma'))\}, \tag{1.5.2}$$

where $\rho = 1/2\mu$ and $\eta = -\lambda/(2\mu(2\mu + d\lambda))$. When we carry out functional integrations over $\chi_{\alpha\beta}, A, B$, we recover the original expression (1.5.1).

By integrating out the fluctuations in the $\vec{X}$ degrees of freedom around the ground state $\vec{X}^0$ ($\vec{X} = \vec{X}^0 + \delta\vec{X}$), we calculate the effective free energy. In the calculation, we evaluate the auxiliary fileds χ, A, B at their saddle points χ^0, A^0, B^0. We look for the following homogeneous solution,

$$\vec{X}^0 = \zeta\sigma^\alpha\vec{e}_\alpha \quad \chi_{\alpha\beta}^{\ 0} = \chi\delta_{\alpha\beta} \tag{1.5.3}$$

$$B^0(\sigma, \sigma') = B(\sigma - \sigma') \quad A^0(\sigma, \sigma') = A(\sigma - \sigma'). \tag{1.5.4}$$

We refer to ζ as flatness order parameter.

From the effective free energy, we obtain the saddle point equations for $\delta A, \delta B, \delta\chi$ and $\delta\zeta$. From the convergence criteria, we can study the possible asymptotic behaviours of the membrane. The membrane has mainly two phases, flat phase ($\zeta > 0$) and crumpled phase ($\zeta = 0$). In Fig. 1, we depict the phase diagram in the (γ, D) plane.

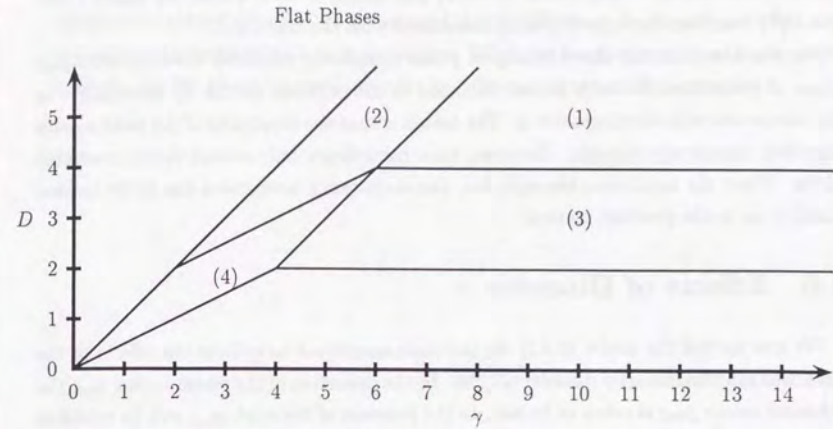Figure 1a: The flat phases in the (γ, D) plane: (1) SRSF(short range superflat) phase; (2) LRSF(long range superflat) phase; (3) SRF(short range flat) phase; (4) LRF(long range flat) phase.
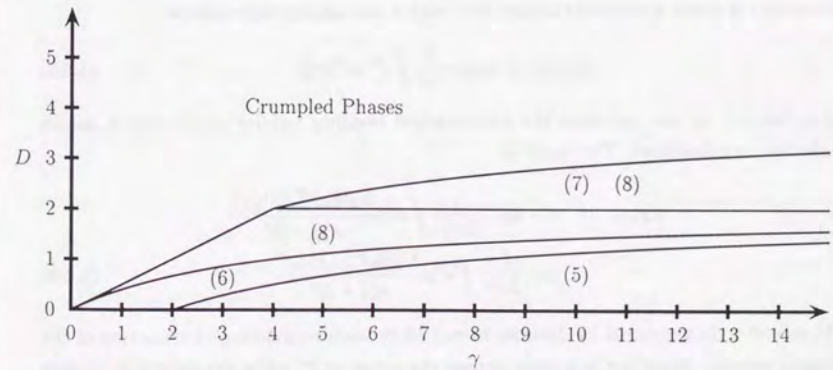

Figure 1b: The crumpled phases in the (γ, D) plane: (5) NG(normal Gaussian) phase; (6) AG(anomalous Gaussian) phase; (7) IC(intermediate crumpled) phase; (8) SC(swollen crumpled) phase.

We note that in several parts of the (γ, D) plane, some phases coexist. In the region $D > 2$ and $D < \frac{4\gamma}{4+\gamma}$, the three phases (3:SRF), (7:IC) and (8:SC) coexist. There exists a phase transition between (3:SRF: $\nu = 1$) and (8:SC: $\nu = \frac{2D}{\gamma}$) and the phase (7:IC: $\nu = \frac{4-D}{2}$) describes the behavior being associated with the transition.

We also note that the above crumpled phase completely coincides with the crumpled phase of generalized Edwards model discussed in the previous section by replacing γ in the interaction with the dimension d. The reason is that the structures of the saddle point equations completely coincide. However, such coincidence only occurs in the crumpled phase. When the membrane becomes flat, the short-range interaction has to be treated carefully as in the previous section.

1.6   Effects of Disorder

We now extend the model (1.3.7) for the pure membrane to include the effects of the quenched random impurity disorder [27, 28]. In the definition of the strain tensor $u_{\alpha\beta}$, the reference metric $g_{0\alpha\beta}$ is taken to be flat. In the presence of disorder, $g_{0\alpha\beta}$ will be modified to reflect local deformations of the membrane to accommodate defects and impurities. This leads us to model the effects of disorders by taking $g_{0\alpha\beta}$ to be

$$g_{0\alpha\beta} = \zeta^2 \delta_{\alpha\beta}[1 + 2c(\sigma)], \tag{1.6.1}$$

where $c(\sigma)$ is a new quenched random field with a probability distribution

$$P[c(\sigma)] \propto \exp[-\frac{1}{2\alpha} \int d^D\sigma c^2(\sigma)]. \tag{1.6.2}$$

As in Sec.1.3, we can calculate the renormalized bending rigidity $\kappa_R(q)$ from a simple perturbative calculation. The result is

$$
\begin{aligned}
\kappa_R(q) &= \kappa + k_B T \frac{1}{(2\pi)^2} \int d^2p \frac{K_0[\hat{q}_\alpha P_{\alpha\beta}^T(\vec{p})\hat{q}_\beta]^2}{\kappa|\vec{q}+\vec{p}|^4} \\
&- (\alpha) \frac{1}{(2\pi)^2} \int d^2p \frac{K_0^2[\hat{q}_\alpha P_{\alpha\beta}^T(\vec{p})\hat{q}_\alpha]^2}{\kappa|\vec{q}+\vec{p}|^4}
\end{aligned} \tag{1.6.3}
$$

The second term generated by disorder in eq.(1.6.3) leads to a divergent reduction of the bending rigidity. Since the first term carries the factor of T, while the second term does not depend on T, the effect of disorder will dominate at low-temperature [28].

Replacing the wavevector dependent quantities $\kappa_R(q) \sim p^{-\eta_\kappa}$ and $K_R(q) \sim p^{\eta_u}$ which are assumed to be renormalized only by thermal fluctuation and using the scaling relation $2\eta_k + \eta_u = 2$, Nelson and Radzihovsky concluded that weak disorder will produce only a

small singular correction. More precise study showed that the instability occurs only at $T = 0$ and weak disorder is irrelevant in the flat phase at $T > 0$ [28]. In order to break the flat phase of polymerized membrane, it is considered that long-range correlation of disorders or strong disorder are necessary [28, 29]. However, as we will see later, these conclusion are restricted to a rigid membrane. When the bending rigidity of the membrane is small, the flat phase becomes unstable and the membrane can be crumpled.

Chapter 2

Self-Avoiding Randomly Polymerized Membrane I : Theoretical Approach

2.1 Genesis

The statistical properties of polymerized membranes, or tethered surfaces have been widely discussed in the past few years [1, 7, 8, 15, 16]. The polymerized membrane is a two dimensional generalization of linear polymers. At low temperature T a membrane with bending rigidity is asymptotically flat, and its radius of gyration R_G increases as the linear dimension L of the surface [4, 15, 16]. As the temperature increases the phantom membranes shows a crumpling transition between the flat phase and a crumpled phase $(R_G \sim \sqrt{\ln L})$ [15, 16]. The properties of the flat phase has been studied extensively [4, 13, 30]. It is characterized by a divergent bending rigidity κ, vanishing shear and compression moduli μ and λ, and a nonlinear stress-strain relation.

One of the surprising characters of the membrane is that the self-avoiding tethered membrane is flat when embedded in the three-dimensional space [17, 18, 19]. Abraham and Nelson [10] discussed the origin of this phenomena and pointed out that entropic rigidity induced by the (next-nearest neighbor) self-avoidance causes the crumpling transition [1] and the membrane becomes flat. This means that the flat phase of the self-avoiding tethered membrane is described by the fixed point associated with the flat phase of the phantom membrane [30]. Their discussion also means that the hard sphere model has inevitably large bending rigidity originated from the next nearest neighbor interactions and that these simulation did not purely investigate the effect of self-avoidance. That is, the hard sphere model becomes very rigid when self-intersection is completely prohibited. In order to study the "genuine" self-avoidance effect, tethered membrane with hard

spheres of smaller diameter ("weak" self-avoidance) [11, 19], and "plaquette" membrane model [20, 21] has been employed. Even in these cases, the membrane becomes flat and it was concluded that the self-avoiding tethered membrane is flat. Theoretically, using the gaussian variational method, Guitter and Palmeri [22], Le Dousaal [24] and Goulian [23] discussed the existence region of the crumpled phase and showed that the self-avoiding tethered membrane is flat in three dimensional space. Higher dimensional cases are also well described in the same frame work [25]. However, up to now, we have no complete theory which describe the crumpling transition like cross-over of the membrane by the entropic bending rigidity which originates from the distant neighbor self-avoidance [11].

Recently, studies on the effects of quenched in-plane disorders have been performed. One of the most important effect of the disorder is the buckling transition [4, 31]. Although the stable phase of a defect free polymerized membrane is flat, strains induced by a defect, such as a dislocation or disclination, can be accomodated by displacements in the normal direction, resulting in the buckling of the membrane. This process, which depends on the balance between in-plane stretching energy and curvature energy, occurs when

$$K_0 l^2 / \kappa > \gamma. \tag{2.1.1}$$

Here, K_0 is Young's modulus, κ is the bending rigidity, l is a length scale, and γ is a dimensionless constant of order 10^2 [29, 31]. The length scale l depends on the nature of the defect. In membranes of size R, $l = R$ for disclinations, and $l = \sqrt{Rb}$ for a dislocation with burger's vector $\vec{b}$. Thus, these defects always buckle in sufficiently large membranes, irrespective of the value of the elastic constants. In the case of finite energy defects, such as vacancies or tightly bound dislocation pairs, l is of order a lattice constant and the stability of the flat phase in the presence of such defects is determined by the actual value of the elastic constants. This leads to the following possibility of thermal buckling transition in an infinite system. As the temperature decreases, κ decreases and K_0 increases [4]. At some temperature T_B, the condition (2.1.1) is satisfied and the membrane shows buckling transition.

Experimentally, Mutz, Bensimon and Brienne discovered the "wrinkling transition" in partially polymerized lipid vesicles [32, 33]. The membrane undergoes a reversible phase transition from a high-temperature phase where the membrane is smooth and very fluctuating to a low-temperature phase characterized by a rigid and highly wrinkled surface. Nelson and Radzihovsky [27, 28] and Morse, Lubensky and Grest [34, 35] analyzed the stability of the flat phase of the (phantom) tethered membrane with randomnesses of the locally preferred metric and spontaneous curvature by the field theoretical method. It was concluded that weak short-range disorder is irrelevant and that the rigid membrane

at $T > 0$ is described by the pure flat phase. In order to explain the wrinkling transition, two possibilities are presented. One is the strong disorder [36, 37] and the other is the long-range correlation of the disorder [28, 38] which is induced by unscreened disclinations [28, 39]. On the other hand, the fact that the flat phase of the rigid polymerized membrane is stable with respect to weak disorders at $T > 0$ seems to mean that the flat phase of the self-avoiding tethered membrane is stable with respect to the randomnesses, however the situation is not so simple. Mori and Wadati [40, 41, 42] discussed the existence region of the crumpled phase of the self-avoiding tethered membrane with disorders and showed the possibility that the membrane is crumpled with $\nu = 6/7$ at $d = 3$.

This analysis does not contradict with the above analyses of the flat phase, because it does not forbid the existence of any flat phase. That is, when the membrane is very rigid, the membrane may become flat and crumpled phase only occurs when the bending rigidity of the membrane is small. In fact, Morse, Petsche, Grest and Lubensky [43] carried out molecular dynamics simulation for self-avoiding polymerized fluid membrane. They have studied hard-sphere model with a diameter which completely prohibit the intersection of the membrane. They concluded that the membrane is asymptotically flat and those sites which have more than six neighbors buckled only locally. In order to conclude whether the "genuine" self-avoiding tethered membrane with randomnesses is crumpled or not, it is necessary to investigate very soft (small bending rigidity) membranes with randomnesses. That is, we need to study the hard sphere model with smaller diameter [19] or plaquette membrane [20, 11]. Following this point of view, Mori have performed the numerical studies of a model randomly tethered membrane and a model tethered membrane with quenched random internal disorder with several strength of disorder and self-avoiding interaction [44, 45, 46]. When the self-avoiding interaction is strong, both models show small shrink and random stress does not cause any large buckling. And the membrane is asymptotically flat. When the self-avoiding interaction is weak and the bending rigidity of the membrane is small, the membrane shows large bucklings and large shrink is found (densiy changes order of a magnitude in some case) irrespective of the strength of disorder. However, when the disorder is weak, the membrane is asymptotically flat and theoretically predicted crumpled phase only appears when the disorders are very strong.

In these models, "weak" self-avoiding case was studied and there remains the possibility that such large shrink is an artifact of the model, because the self-intersection is not necessarily prohibited. It is impossible to exclude such possibility in the hard sphere model when we analyze the self-avoiding membrane with small bending rigidity. However, it is important that such large shrink occurs even in the weak self-avoiding case. Because, up to now, almost all theoretical works treat the stability of (phantom) rigid polymerized

membrane (or stability of AL fixed point). Even if the self-intersection is not completely forbidden, when the usual flat phase becomes unstable in numerical studies, it means that AL fixed point becomes unstable by randomnesses. And we can say that the randomnesses are relevant for the behavior of the membrane. The second reason is that from the condition (2.1.1) the buckling transition occurs more and more easily when the bending rigidity is small. If there occurs a large conformational transformation in the model only with self-avoiding interaction and disorders, thermal phase transition from the flat phase to some other phase is possible by introducing the bending rigidity and temperature T. And it may be related to the wrinkling transition [32].

In the following two chapters, we discuss the behavior of self-avoiding randomly polymerized membrane. In this chapter, we study its behavior theoretically and next chapter is devoted to its numerical analyses. The organization of this chapter is as follows. In Sec.2.2, we shall study the randomly polymerized membranes with long-range repulsive interactions $r^{-\gamma}$ using the large-d limit analysis. Due to the randomness in the metric, the flat phase becomes unstable and the spin-glass phase takes over. The phase diagram in the (γ, D) plane is obtained. The crumpled phase is not affected by the randomnesses and the exact exponent for the radius of gyration in the spin-glass phase is given. In order to discuss the effect of disorders on the crumpled phase, we analyze the generalized Edwards model with quenched random internal disorders in Sec.2.3. In subsec.2.3.1, using the gaussian variational method (or Replica field theory) we obtain the saddle point equations. We discuss the difference between the saddle point equations with and without disorders. In subsec.2.3.2, we obtain the large distance behaviors of the membrane for several types of the randomnesses by analyzing the saddle point equations. We show that even a short-range stress disorder is relevant at $d < 8$ and the crumpled phase exists at $2 < d \leq 4$. This means that the self-avoiding polymerized membranes with short-range stress disorder can be crumpled at the physical dimension ($d = 3$). We also obtain the phase diagrams of the crumpled phases of the self-avoiding polymerized membranes with long-range disorders. Sec.2.4 contains summary and concluding remarks.

2.2 Randomly Polymerized Membrane with Long-range Interactions

In this section we study the randomly polymerized membrane with long-range repulsive ($r^{-\gamma}$) interactions. This model can be solved exactly in the large-d limit and we can discuss the possible phases and phase diagrams in the (γ, D) plane.

2.2.1 Randomly polymerized membrane with long-range interactions

We prepare some notations. The position of the D-dimensional membrane in a d-dimensional space is described by d bulk coordinates $X^i(\sigma^\alpha)(i = 1, \cdots, d)$, where $\sigma^\alpha(\alpha = 1, \cdots, D)$ are the internal manifold coordinates. We denote the bending rigidity of the membrane by κ and the elastic Lamé coefficients by μ and λ. The interaction between different positions, which is rotationally-invariant, is represented by V and we take $V(r^2) = u/(r^2)^{\frac{z}{2}}$, r and u being the distance and some positive constant, respectively. The Hamiltonian for the tethered membrane with long range interaction is given by

$$
\begin{aligned}
\mathcal{H}[\vec{X}(\sigma)] &= \int d^D\sigma[\frac{d}{2}\kappa\triangle\vec{X}\cdot\triangle\vec{X} + \frac{1}{4}\mu d\{\partial_\alpha\vec{X}\cdot\partial_\beta\vec{X} - \delta_{\alpha\beta}\}^2 \\
&+ \frac{1}{8}\lambda d\{\partial_\alpha\vec{X}\cdot\partial_\alpha\vec{X} - D\}^2] \\
&+ d\int d^D\sigma\int d^D\sigma' V((\vec{X}(\sigma) - \vec{X}(\sigma'))^2).
\end{aligned} \tag{2.2.1}
$$

The first term represents the bending elasticity, the second and third terms correspond to the stretching elasticity and the last term represents the long-range interactions. In order to consider the randomnesses of the preferred internal metric and the spontaneous curvature of the membrane, we introduce the fields $\delta c(\sigma)$ and $H^i(\sigma)$ which are random variables obeying the Gaussian probability distributions with variance α and J/d, i.e.

$$
P[\delta c(\sigma)] \propto \exp[-\frac{1}{2\alpha}\int d^D\sigma\delta c(\sigma)^2], \tag{2.2.2}
$$

$$
P[H^i(\sigma)] \propto \exp[-\frac{d}{2J}\int d^D\sigma H^i(\sigma)^2]. \tag{2.2.3}
$$

We start with the following Hamiltonian:

$$
\begin{aligned}
\mathcal{H}_{C,\vec{H}}[X(\sigma)] &= \int d^D\sigma[\frac{d}{2}\kappa\triangle\vec{X}\cdot\triangle\vec{X} + \frac{1}{4}\mu d\{\partial_\alpha\vec{X}\cdot\partial_\beta\vec{X} - \delta_{\alpha\beta}[1 + 2\delta c(\sigma)]\}^2 \\
&+ \frac{1}{8}\lambda d\{\partial_\alpha\vec{X}\cdot\partial_\alpha\vec{X} - D[1 + 2\delta c(\sigma)]\}^2] \\
&+ d\int d^D\sigma\int d^D\sigma' V((\vec{X}(\sigma) - \vec{X}(\sigma'))^2) + d\int d^D\sigma\triangle\vec{X}\cdot\vec{H}. \tag{2.2.4}
\end{aligned}
$$

We have rescaled all physical constants, for instance, $\kappa \to d\kappa$, in order to obtain sensible and nontrivial results in the limit $d \to \infty$. To simplify the calculation we introduce several auxiliary fields $\chi_{\alpha\beta}, A, B$ as in [13, 22, 24, 36] and rewrite the above Hamiltonian into

$$
\begin{aligned}
\mathcal{H}_{C,\vec{H}}[\vec{X}, \chi_{\alpha\beta}, A, B] &= d\int d^D\sigma[\frac{1}{2}\kappa\triangle\vec{X}\cdot\triangle\vec{X} + \frac{1}{2}\chi_{\alpha\beta}(\partial_\alpha\vec{X}\cdot\partial_\beta\vec{X} - \delta_{\alpha\beta}) \\
&- \rho\frac{1}{2}(\chi_{\alpha\beta})^2 - \eta\frac{1}{2}(\chi_{\alpha\alpha})^2 - \frac{1}{2}(\lambda D + 2\mu)\delta c\partial_\alpha\vec{X}\cdot\partial_\alpha\vec{X}]
\end{aligned}
$$

$$
\begin{aligned}
&- d\int d^D\sigma\int d^D\sigma'\{\frac{1}{4}[(\vec{X}(\sigma) - \vec{X}(\sigma'))^2 - A]B(\sigma, \sigma') \\
&- V(A(\sigma, \sigma'))\} \\
&+ d\int d^D\sigma\triangle\vec{X}\cdot\vec{H}, \tag{2.2.5}
\end{aligned}
$$

where $\rho = 1/2\mu$ and $\eta = -\lambda/(2\mu(2\mu + d\lambda))$. When we carry out functional integrations over $\chi_{\alpha\beta}, A, B$, we recover the original expression (2.2.4). The disorder-averaged effective free energy $\mathcal{F}_{eff}$ is given by the average of the logarithm of the partition function $Z_{C,\vec{H}}$ for each configuration of the randomnesses with the weights $P[\delta c]$ and $P[\vec{H}]$. We use the replica formalism [48] and introduce n copies of the fields $\vec{X}, \chi_{\alpha\beta}, A, B$ labelled by replica index a. The total free energy is the replicated version of the free energy (2.2.5). We take an average of the replicated partition function over the randomnesses to get the replicated free energy,

$$
\begin{aligned}
< Z_{C,\vec{H}}{}^n >_{\delta c,\vec{H}} &= \int \mathcal{D}[\vec{X}_a]\mathcal{D}[\chi_{a\alpha\beta}]\mathcal{D}[A_a]\mathcal{D}[B_a] \\
&\exp\{-\mathcal{F}_{rep}[\vec{X}_a, \chi_{a\alpha\beta}, A_a, B_a]\}, \tag{2.2.6}
\end{aligned}
$$

$$
\begin{aligned}
\mathcal{F}_{rep}[\vec{X}_a, \chi_{a\alpha\beta}, A_a, B_a] &= \sum_{a=1}^n \mathcal{F}_0[\vec{X}_a, \chi_{a\alpha\beta}, A_a, B_a] \\
&- \frac{d^2\alpha'}{8}\sum_{a\neq b}\int d^D\sigma(\partial_\alpha\vec{X}_a\cdot\partial_\alpha\vec{X}_a)(\partial_\beta\vec{X}_b\cdot\partial_\beta\vec{X}_b) \\
&- dJ^2\int d^D\sigma(\sum_a\triangle\vec{X}_a)^2, \tag{2.2.7}
\end{aligned}
$$

where

$$
\begin{aligned}
\mathcal{F}_0[\vec{X}, \chi_{\alpha\beta}, A, B] &= d\int d^D\sigma[\frac{1}{2}\kappa\triangle\vec{X}\cdot\triangle\vec{X} + \frac{1}{2}\chi_{\alpha\beta}(\partial_\alpha\vec{X}\cdot\partial_\beta\vec{X} - \delta_{\alpha\beta}) \\
&- \rho\frac{1}{2}(\chi_{\alpha\beta})^2 - \eta'\frac{1}{2}(\chi_{\alpha\alpha})^2] \\
&- d\int d^D\sigma\int d^D\sigma'\{\frac{1}{4}[(\vec{X}(\sigma) - \vec{X}(\sigma'))^2 - A]B(\sigma, \sigma') \\
&- V(A(\sigma, \sigma'))\}, \tag{2.2.8}
\end{aligned}
$$

with $\alpha' = (2\mu + D\lambda)^2\alpha$, $\lambda' = \lambda - d\alpha'$ and $\eta' = -\lambda'/(2\mu(2\mu + d\lambda'))$. We introduce the spin-glass order parameter $Q_{ab\alpha\beta ij}$, as the thermal average of a composite quadratic operator of tangent fields from different replicas $\partial_\alpha X_{ia}\partial_\beta X_{jb}$ [36]. Integrating out the fluctuations in the $\vec{X}_a$ degrees of freedom around the ground state $\vec{X}_a^0$ ($\vec{X}_a = \vec{X}_a^0 + \delta\vec{X}_a$), we calculate the effective free energy to be

$$
\begin{aligned}
&n\mathcal{F}_{eff}[\vec{X}_a^0, \chi_{a\alpha\beta}{}^0, Q_{ab\alpha\beta ij}{}^0, A_a^0, B_a^0] \\
&= d\int d^D\sigma\sum_a[\frac{1}{2}\kappa\triangle\vec{X}_a^0\cdot\triangle\vec{X}_a^0 + \frac{1}{2}\chi_{a\alpha\beta}^0(\partial_\alpha\vec{X}_a^0\cdot\partial_\beta\vec{X}_a^0 - \delta_{\alpha\beta})
\end{aligned}
$$

$$- \rho \frac{1}{2}(\chi_{a\alpha\beta}{}^0)^2 - \eta' \frac{1}{2}(\chi_{a\alpha\alpha}{}^0)^2]$$

$$+ dJ^2 \int d^D\sigma (\sum_a \triangle \vec{X}_a{}^0)^2$$

$$- d \int d^D\sigma \int d^D\sigma' \sum_a \{\frac{1}{4}[(\vec{X}_a^0(\sigma) - \vec{X}_a^0(\sigma'))^2 - A_a^0(\sigma, \sigma')]B_a^0(\sigma, \sigma')$$

$$- V(A_a{}^0(\sigma, \sigma'))\}$$

$$+ \sum \int d^D\sigma [\frac{\alpha'}{8}Q_{ab\alpha\beta ij}{}^{0^2} - \frac{d\alpha'}{4}Q_{ab\alpha\beta ij}{}^0 \partial_\alpha X_{ai}{}^0 \partial_\beta X_{bj}{}^0]$$

$$+ \sum \int d^D\sigma \frac{1}{2}\mathrm{Tr}\ln\{M_{abij}\}, \tag{2.2.9}$$

where M_{abij} stands for

$$M_{abij} = \delta_{ab}\delta_{ij}(\kappa\triangle^2 - \partial_\alpha \chi_{a\alpha\beta}{}^0 \partial_\beta) + \frac{\alpha'}{2}\partial_\alpha Q_{ab\alpha\beta ij}{}^0 \partial_\beta$$

$$+ (B_a^0(k) - B_a^0(0))\delta_{ab}\delta_{ij} - J^2\triangle^2\delta_{ij}, \tag{2.2.10}$$

and χ_a^0, A_a^0, B_a^0 are the saddle points of this effective action. Assuming that the replica symmetry breaking occurs in higher orders in $1/d$, we look for the following homogeneous and replica symmetric solution,

$$\vec{X}_a^0 = \zeta\sigma^\alpha \vec{e}_\alpha \quad \chi_{a\alpha\beta}{}^0 = \chi\delta_{\alpha\beta} \tag{2.2.11}$$

$$Q_{ab\alpha\beta ij}^0 = q\delta_{\alpha\beta}\delta_{ij}(1 - \delta_{ab}) \tag{2.2.12}$$

$$B_a{}^0(\sigma, \sigma') = B(\sigma - \sigma') \quad A_a{}^0(\sigma, \sigma') = A(\sigma - \sigma'). \tag{2.2.13}$$

We refer to ζ as the flatness order parameter. Then the effective free energy is evaluated as

$$\mathcal{F}_{eff}[\zeta, \chi, q]/L^D = \frac{d}{n}[\frac{1}{2}nD\chi(\zeta^2 - 1) - \frac{n}{2}D\chi^2(\rho + \eta'D)$$

$$+ n(n-1)\frac{D\alpha'}{8}(q^2 - 2q\zeta^2)$$

$$- n \int d^D\sigma \{\frac{1}{4}[\zeta^2\sigma^2 - A(\sigma)]B(\sigma) - V(A(\sigma))\}$$

$$+ \frac{1}{2}\int \frac{d^Dk}{(2\pi)^D}\{\ln[\kappa k^4 + \chi k^2 - J^2 k^4$$

$$- (n-1)(\frac{\alpha'}{2}qk^2 + J^2k^4 + B(k) - B(0)]$$

$$+ (n-1)\ln[\kappa k^4 + \chi k^2 + \frac{\alpha'}{2}qk^2 + B(k) - B(0)]\}]. \tag{2.2.14}$$

We now take the limit $n \to 0$ as usual in the replica trick and arrive at a final expression for the effective free energy of the membrane in the large d limit:

$$\mathcal{F}_{eff}[\zeta, \chi, q]/L^D = d[\frac{1}{2}D\chi(\zeta^2 - 1) - \frac{1}{2}D\chi^2(\rho + \eta'D)$$

$$- \frac{D\alpha'}{8}(q^2 - 2q\zeta^2)$$

$$- \int d^D\sigma \{\frac{1}{4}[\zeta^2\sigma^2 - A(\sigma)]B(\sigma) - V(A(\sigma))\}$$

$$+ \frac{1}{4}\int \frac{d^Dk}{(2\pi)^D}\{2\ln[\kappa k^4 + \chi k^2 + \frac{\alpha'}{2}qk^2 + B(k) - B(0)]$$

$$- \frac{\alpha'qk^2 + 2J^2k^4}{\kappa k^4 + \chi k^2 + \frac{\alpha'}{2}qk^2 + B(k) - B(0)}\}]. \tag{2.2.15}$$

For a later convenience, we write

$$K(k) = \kappa k^4 + \chi k^2 + \frac{\alpha'}{2}qk^2 + B(k) - B(0), \tag{2.2.16}$$

which is approximately the full inverse propagator $< \vec{X}(k) \cdot \vec{X}(-k) >_C^{-1}$. Note that, as seen in (2.2.12), q is considered to be the spin-glass order parameter.

From the effective free energy (2.2.15), we have the saddle point equations for $\delta A, \delta B, \delta\chi, \delta q$ and $\delta\zeta$:

$$K(k) = \kappa k^4 + \chi k^2 + \frac{\alpha'}{2}qk^2 + 4\int d^D\sigma(1 - \cos(\vec{k}\cdot\vec{\sigma}))V'(A(\sigma)). \tag{2.2.17}$$

$$A(\sigma) = \zeta^2\sigma^2 + 2\int \frac{d^Dk}{(2\pi)^D}(1 - \cos(\vec{k}\cdot\vec{\sigma}))[\frac{1}{K(k)} + \frac{\alpha'qk^2 + 2J^2k^4}{K(k)^2}]. \tag{2.2.18}$$

$$(\zeta^2 - 1) - 2\chi(\rho + D\eta') = \frac{1}{2D}\int \frac{d^Dk}{2\pi^D}[\frac{k^2}{K(k)} + \frac{\alpha'qk^4 + 2J^2k^6}{K(k)^2}]. \tag{2.2.19}$$

$$\zeta^2 = q(1 - \frac{1}{2D}\int \frac{d^Dk}{2\pi^D}\frac{\alpha'k^4 + 2J^2k^6/q}{K(k)^2}). \tag{2.2.20}$$

$$\zeta = 0 \quad \text{or/and} \quad \partial_{q^2}K(q) = 0. \tag{2.2.21}$$

Equation (2.2.21) indicates that the solution with the broken symmetry($\zeta > 0$) is possible only if the coefficient of k^2 term in $K(k)$ is 0. We can formally expand (2.2.17) in powers of k:

$$K(k) = \tau_{eff}k^2 + \kappa_{eff}k^4, \quad \text{for small} \quad k, \tag{2.2.22}$$

where the effective surface tension τ_{eff} and the effective rigidity κ_{eff} are given by

$$\tau_{eff} = \chi + \frac{\alpha'}{2}q - \frac{\gamma u}{D}\int d^D\sigma\sigma^2(A(\sigma))^{-1-\frac{3}{2}}. \tag{2.2.23}$$

$$\kappa_{eff} = \kappa + \frac{\gamma u}{4(D^2 + 2D)}\int d^D\sigma\sigma^4(A(\sigma))^{-1-\frac{3}{2}}. \tag{2.2.24}$$

2.2.2 Large distance behavior

We analyze the large distance (infrared) behaviors of $A(\sigma)$ and $K(k)$ from convergence criteria and discuss the possible phases in the (γ, D) plane [22]. Convergence criteria insist that the integrals appearing in (2.2.17)~(2.2.20) are infrared-convergent. We first assume the following forms of K and A in the infrared limit:

$$K(k) \sim \tau_{eff} k^2 + \kappa_0 k^{2+\theta}. \tag{2.2.25}$$

$$A(\sigma) \sim \zeta^2 \sigma^2 + A_0 \sigma^\omega. \tag{2.2.26}$$

When the manifold is in the crumpled state ($\zeta = 0, q = 0$), the exponent ω is related to the standard exponent ν for the radius of gyration ($R_G^2 \sim L^{2\nu}$) by $\nu = \omega/2$. In the case $\zeta > 0$, this exponent is also related to the roughening exponent ξ by $\xi = \omega/2$. It is convenient to introduce θ_0 and ω_0 by

$$
\begin{aligned}
\theta_0 &= 0 \quad \text{if} \quad \tau_{eff} > 0 \\
&= \theta \quad \text{if} \quad \tau_{eff} = 0, \\
\omega_0 &= 2 \quad \text{if} \quad \zeta > 0 \\
&= \omega \quad \text{if} \quad \zeta = 0.
\end{aligned}
\tag{2.2.27}
$$

We substitute the dominant behavior $K(k) \sim k^{2+\theta_0}(k \to 0)$ into the integrals in (2.2.18). We find that

$$\int \frac{d^D k}{(2\pi)^D} \frac{1}{K(k)} \text{ is infrared convergent when } 2 - D + \theta_0 < 0,$$

$$\text{otherwise} \int \frac{d^D k}{(2\pi)^D} \frac{1}{K(k)}(1 - \cos(\vec{k} \cdot \vec{\sigma})) \sim \sigma^{2-D+\theta_0}. \tag{2.2.28}$$

$$\int \frac{d^D k}{(2\pi)^D} \frac{\alpha' q k^2}{K(k)^2} \text{ is infrared convergent when } 2 - D + 2\theta_0 < 0,$$

$$\text{otherwise} \int \frac{d^D k}{(2\pi)^D} \frac{\alpha' q k^2}{K(k)^2}(1 - \cos(\vec{k} \cdot \vec{\sigma})) \sim \sigma^{2-D+2\theta_0}. \tag{2.2.29}$$

$$\int \frac{d^D k}{(2\pi)^D} \frac{2J^2 k^4}{K(k)^2} \text{ is infrared convergent when } -D + 2\theta_0 < 0,$$

$$\text{otherwise} \int \frac{d^D k}{(2\pi)^D} \frac{2J^2 k^4}{K(k)^2}(1 - \cos(\vec{k} \cdot \vec{\sigma})) \sim \sigma^{-D+2\theta_0}. \tag{2.2.30}$$

From these conditions, we see that when the membrane is in the $q > 0$ phase, ω is given by

$$\omega = \max(0, 2 - D + 2\theta_0). \tag{2.2.31}$$

and when the membrane is in the crumpled phase, ω is given by

$$\omega = \max(0, 2 - D + \theta_0, 2\theta_0 - D). \tag{2.2.32}$$

As will be shown shortly, θ_0 is always equal to or smaller than 2, so the third term in the r.h.s. of (2.2.32) is not relevant. This indicates that the randomness of the spontaneous curvature does not play an essential role in contrast with the result of [34]. Inserting the dominant behavior $A(\sigma) \sim \sigma^{\omega_0}$ in (2.2.18), we find [22] that θ satisfies

$$\theta = \min(2, -2 - D + (1 + \frac{\gamma}{2})\omega_0), \tag{2.2.33}$$

which implies $\theta_0 \leq 2$. We can also derive the following restrictions [22];

$$\omega < 2, \quad \theta > 0. \tag{2.2.34}$$

2.2.3 Phase diagram and possible phase transitions

The membrane has mainly three different phases depending on the flatness order parameter ζ and the spin-glass order parameter q, that is, flat phase ($\zeta > 0, q > 0$), crumpled spin-glass phase ($\zeta = 0, q > 0$) and crumpled phase ($\zeta = 0, q = 0$). Each phase is further characterized by the exponents θ and ω, and whether τ_{eff} vanishes or not. Summarizing the above maximum or minimum conditions and the constraints, we end up with four flat phases, four crumpled phases and four crumpled spin glass phases.

1. The flat phases:

(1) short range superflat (SRSF) phase, $\theta = 2, \omega = 0$. Then $K(k) \sim \kappa_{eff} k^4$ and $A(\sigma) \sim \zeta^2 \sigma^2 + A_0$. This phase exists for $D > 6$ and $D < \gamma - 2$.

(2) long range superflat (LRSF) phase, $\theta = -D + \gamma, \omega = 0$. Then $K(k) \sim \kappa_0 q^{2+\theta}$ and $A(\sigma) \sim \zeta^2 \sigma^2 + A_0$. This phase exists for $D > \frac{1}{3}(2 + 2\gamma), D > \gamma - 2$ and $D < \gamma$.

(3) short range flat (SRF) phase, $\theta = 2, \omega = 6 - D$. Then $K(k) \sim \kappa_{eff} q^4$ and $A(\sigma) \sim \zeta^2 \sigma^2 + A_0 \sigma^\omega$. This phase exists for $D < \gamma - 2$ and $4 < D < 6$.

(4) long range flat (LRF) phase, $\theta = -D + \gamma, \omega = 2 - 3D + 2\gamma$. Then $K(k) \sim \kappa_0 k^{2+\theta}$ and $A(\sigma) \sim \zeta^2 \sigma^2 + A_0 \sigma^\omega$. This phase exists for $D > \gamma - 2, D < \gamma, D < \frac{1}{3}(2 + 2\gamma)$ and $D > \frac{2}{3}\gamma$.

2. The crumpled phases:

(5) normal Gaussian (NG) phase, $\theta = 2, \omega = 2 - D$. Then $K(k) \sim \kappa_{eff} k^4 + \tau_{eff} k^2$ and $A(\sigma) \sim \sigma^\omega$. This phase exists for $D < \frac{2(\gamma-2)}{4+\gamma}$.

(6) anomalous Gaussian (AG) phase, $\theta = -2D + \frac{\gamma}{2}(2 - D), \omega = 2 - D$. Then $K(k) \sim \kappa_0 k^{2+\theta} + \tau_{eff} k^2$ and $A(\sigma) \sim \sigma^\omega$. This phase exists for $\frac{-4+2\gamma}{4+\gamma} < D < \frac{2\gamma}{4+\gamma}$.

(7) intermediate crumpled (IC) phase, $\theta = 2, \omega = 4 - D$. Then $K(k) \sim \kappa_{eff} k^4$ and $A(\sigma) \sim \sigma^\omega$. This phase exists for $2 < D < \frac{4\gamma}{4+\gamma}$.

(8) swollen crumpled (SC) phase, $\theta = D - 2 + \frac{4D}{\gamma}, \omega = \frac{4D}{\gamma}$. Then $K(k) \sim \kappa_0 k^{2+\theta}$ and $A(\sigma) \sim \sigma^\omega$. This phase exists for $D < \frac{\gamma}{2}, D < \frac{4\gamma}{\gamma+4}$ and $D > \frac{2\gamma}{\gamma+4}$.

3. The crumpled spin-glass phases:

(9) normal Gaussian spin-glass (NGSG) phase, $\theta = 2, \omega = 2 - D$. Then $K(k) \sim \kappa_{eff} k^4 + \tau_{eff} k^2$ and $A(\sigma) \sim \sigma^\omega$. This phase exists for $D < \frac{2(\gamma-2)}{4+\gamma}$.

(10) anomalous Gaussian spin-glass (AGSG) phase, $\theta = -2D + \frac{\gamma}{2}(2 - D), \omega = 2 - D$. Then $K(k) \sim \kappa_0 k^{2+\theta} + \tau_{eff} k^2$ and $A(\sigma) \sim \sigma^\omega$. This phase exists for $\frac{-4+2\gamma}{4+\gamma} < D < \frac{2\gamma}{4+\gamma}$.

(11) crumpled spin-glass 1 (SG1) phase, $\theta = 2, \omega = 6 - D$. Then $K(k) \sim \kappa_{eff} k^4$ and $A(\sigma) \sim A_0 \sigma^\omega$. This phase exists for $4 < D < \frac{4+6\gamma}{4+\gamma}$.

(12) crumpled spin-glass 2 (SG2) phase, $\theta = -2 - D + (1 + \frac{\gamma}{2})(\frac{2+3D}{1+\gamma}), \omega = \frac{2+3D}{1+\gamma}$. Then $K(k) \sim \kappa_0 k^{2+\theta}$ and $A(\sigma) \sim A_0 \sigma^\omega$. This phase exists for $D < \frac{2}{3}\gamma$ and $\frac{2\gamma}{4+\gamma} < D < \frac{4+6\gamma}{4+\gamma}$.

The phase diagrams are summarized in Figures 1. The flat phase is unstable to the randomness of the preferred metric, which is consistent with the previous analyses. The spin-glass phase replaces the flat phase [36] and the exponent $\nu = \omega/2$ for the radius of gyration is given explicitly. The crumpled phase is not affected by the randomnesses and coincides with that of the tethered membrane with long-range interactions [22]. However, the lower critical dimension of the spin-glass phase is 0 in our case as in [36]. Therefore the existence of the crumpled spin-glass phases, especially NGSG and AGSG phases, below 2 dimension is unlikely. Furthermore, the instability of the flat phase is a (known) artifact of keeping only the zero-th order in a $1/d$ expansion. Therefore when we consider the finite d case, there remains the possibility that the flat phase is stable and at large enough disorder strength the crumpled glass phase appears. This picture is also supported by the field theoretical studies and one interpretation about the above spin-glass phase is that it only appears when the strength of disorder is strong. When the strength is weak, the result of "pure" polymerized membrane with long-range interaction applys (Chap.1). Or there also remains the possibility that the short-range disorder is irrelevant and long-range disorder becomes important in order to cause the crumpled glass phase [28].

We also note that in several parts of the (γ, D) plane, some phases coexist. We think that all these phases are stable except for the crumpled spin-glass phases NGSG and AGSG. We give a conjectural picture. In the region $D > 4$ and $D < \frac{4\gamma}{4+\gamma}$, the three phases (3:SRF), (11:SG1) and (12:SG2) coexist with decreasing values of $\nu(\nu = 1, \frac{6-D}{2}, \frac{2+3D}{2+2\gamma})$. The transition occurs in this region, separating a large u and small disorder flat phase (3:SRF) from a small u and large disorder crumpled glass phase (12:SG2), the behavior (11:SG1) being associated with the transition point. In the region $D > 2$ and $D < \frac{4\gamma}{4+\gamma}$,

the three phases (12:SG2), (7:IC) and (8:SC) coexist. There exists a phase transition between (12:SG2: $\nu = \frac{2+3D}{2+2\gamma}$) and (8:SC: $\nu = \frac{2D}{\gamma}$) and the phase (7:IC: $\nu = \frac{4-D}{2}$) describes the behavior being associated with the transition. However in this region, the behavior of ν is $\nu_{SG2} < \nu_{SC} < \nu_{IC}$ and the size of the membrane becomes small in the crumpled spin-glass phase. This behavior is interesting.

2.2.4 Discussions

As has been discussed in Chap.1, it is possible to make some conjecture about the short-range self-avoiding interaction case by replacing the number γ with the dimension of the embedding space d. From our study, the crumpled phase is not affected by the randomnesses. If we assume it remains so at finite d, the physical point $(3, 2)$ is outside the boundary of the crumpled phase and the membrane can not be in the crumpled phase. That is, the self-avoiding randomly polymerized membrane ($d = 3, D = 2$) is in the crumpled spin-glass phase or in the flat phase. However, as we shall see in section 2.3, the assumption that the randomnesses are irrelevant on the crumpled phase of the membrane at finite d is not right. In the next section, we discuss the effect of randomnesses on the crumpled phase.
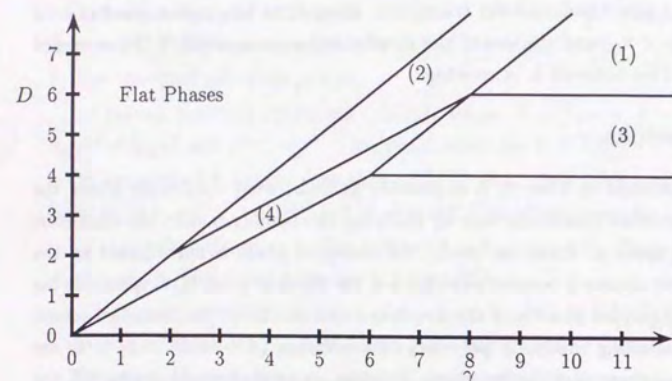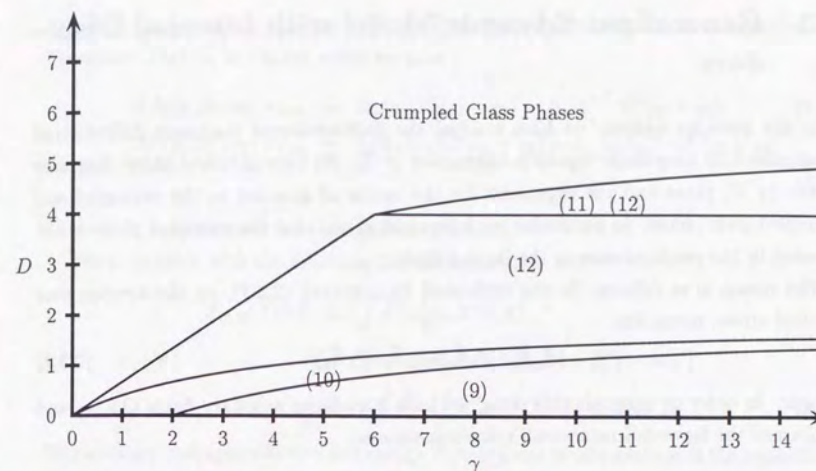
Figure 1a: The flat phases in the (γ, D) plane:

(1) SRSF(short range superflat) phase; (2) LRSF(long range superflat) phase; (3) SRF(short range flat) phase; (4) LRF(long range flat) phase.
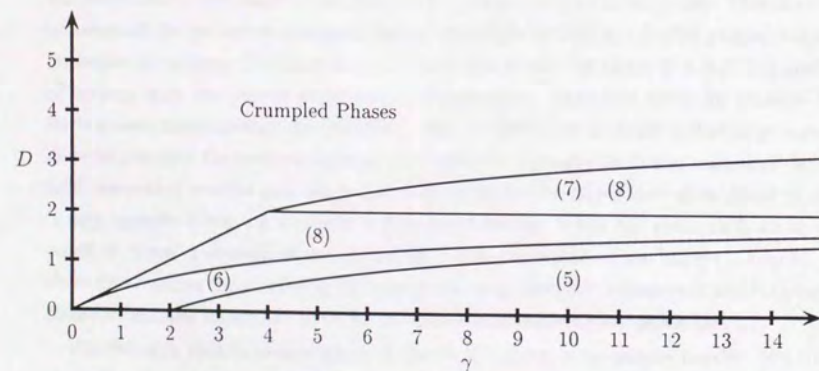
Figure 1b: The crumpled phases in the (γ, D) plane:

(5) NG(normal Gaussian) phase; (6) AG(anomalous Gaussian) phase; (7) IC(intermediate crumpled) phase; (8) SC(swollen crumpled) phase.

Figure 1c:The crumpled spin-glass phases in the (γ, D) plane:

(9) NGSG(normal Gaussian spin-glass) phase; (10) AGSG(anomalous Gaussian spin-glass) phase; (11) SG1(spin-glass 1) phase; (12) SG2(spin-glass 2) phase.

2.3 Generalized Edwards Model with Internal Disorders

In the previous section, we have studied the D-dimensional randomly polymerized membrane with long-range repulsive interaction ($r^{-\gamma}$). We have obtained phase diagrams in the (γ, D) plane and the exponents for the radius of gyration in the crumpled and crumpled glass phases. In particular, we have pointed out that the crumpled phase is not affected by the randomnesses in the large-d limit.

The reason is as follows. In the replicated Hamiltonian (2.2.7), by the average over random stress, terms like

$$(\partial_\alpha \vec{X}_a \cdot \partial_\alpha \vec{X}_a)(\partial_\beta \vec{X}_b \cdot \partial_\beta \vec{X}_b) \qquad (2.3.1)$$

appear. In order to decouple this term, we have introduced auxiliary fields $Q_{ab\alpha\beta ij}$ and performed the Havard-Stratonovich transformation as,

$$Q_{ab\alpha\beta ij}^2 + Q_{ab\alpha\beta ij}\partial_\alpha X_{ia}\partial_\beta X_{jb}. \qquad (2.3.2)$$

After the transformation, the quartic terms (2.3.1) becomes quadratic terms in the field $\vec{X}$ and we can perform the integration over the fields $\vec{X}$. And the integration over the auxiliary fields $Q_{ab\alpha\beta ij}$ is replaced by the estimation at its saddle point. If one consider the crumpled phase, the value of the fields $Q_{ab\alpha\beta ij}$ is zero and the disorder has no play any more. However, it is true only in the large-d limit case and in the finite d case, the random stress becomes relevant. In this section, we will study the effect of random stress and random spontaneous curvature on the crumpled phase.

2.3.1 Replica field theory for S.-A. randomly polymerized membrane

We consider a D-dimensional membrane in a d-dimensional space. The position of the membrane is described by d bulk coordinates $X^i(\sigma^\alpha)(i = 1, \cdots, d)$, where $\sigma^\alpha(\alpha = 1, \cdots, D)$ are the internal manifold coordinates. We denote by u the strength of the "excluded volume" interaction. The Hamiltonian for the generalized Edwards model is given by [1]

$$\mathcal{F}[\vec{X}(\sigma)] = \int d^D\sigma \frac{1}{2}\partial_\alpha X^i\partial_\alpha X^i + u\int d^D\sigma \int d^D\sigma' \delta^d(X^i(\sigma) - X^i(\sigma')). \qquad (2.3.3)$$

The first term corresponds to the Gaussian potential of a free tethered manifold. In order to take into account the randomnesses of the stress and spontaneous curvature of the

manifold, we introduce random fields $\delta c(\sigma)$ and $H^i(\sigma)$ [27, 28] whose distributions are Gaussian: That is, in Fourier space we have

$$< \delta c(q_1)\delta c(q_2) >_{Dis} = \Delta_\mu(q_1)\delta^D(q_1 + q_2) = \Delta_\mu' q_1^{-Z_\mu}\delta^D(q_1 + q_2). \qquad (2.3.4)$$

$$< H^i(q_1)H^j(q_2) >_{Dis} = \delta_{ij}\Delta_K(q_1)\delta^D(q_1 + q_2) = \delta_{ij}\Delta_K' q_1^{-Z_K}\delta^D(q_1 + q_2). \qquad (2.3.5)$$

Here $< \quad >_{Dis}$ denotes the average over disorders.

Then, we start with the following Hamiltonian:

$$\begin{aligned}
\mathcal{F}_{C,\vec{H}}[\vec{X}(\sigma)] &= \int d^D\sigma \frac{1}{2}\partial_\alpha X^i\partial_\alpha X^i \\
&+ \int d^D\sigma[\delta c(\sigma)\partial_\alpha X^i\partial_\alpha X^i + H^i(\sigma)\Delta X^i] \\
&+ u\int d^D\sigma \int d^D\sigma' \delta^d(X^i(\sigma) - X^i(\sigma')). \qquad (2.3.6)
\end{aligned}$$

The disorder-averaged effective free energy $\mathcal{F}_{eff}$ is given by the average of the logarithm of the partition function $Z_{C,\vec{H}}$ for each configuration of the randomnesses . We have recourse to the replica formalism [48] and introduce n copies of the fields $\vec{X}$ labelled by replica index a. The total hamiltonian is the replicated version of the Hamiltonian (2.3.6),

$$\mathcal{F}_{total} = \sum_{a=1}^n \mathcal{F}_{C,\vec{H}}[\vec{X}_a]. \qquad (2.3.7)$$

We take an average of the replicated partition function over the randomnesses to get the replicated hamiltonian $\mathcal{F}_{rep}$,

$$< e^{-\mathcal{F}_{total}} >_{Dis} = e^{-\mathcal{F}_{rep}}, \qquad (2.3.8)$$

where

$$\begin{aligned}
\mathcal{F}_{rep} &= \frac{1}{2}\int d^D k K_{ab}(k)X_a^i(-k)X_b^i(k) \\
&- \frac{1}{2}\sum_{a,b=1}^n \int_{q=k_1+k_2, k_1+k_2=-(k_3+k_4)} d^D k_1 d^D k_2 d^D k_3 d^D k_4 \\
&\quad \Delta_\mu(q)k_1^\alpha k_2^\alpha X_a^i(k_1)X_a^i(k_2)k_3^\beta k_4^\beta X_b^j(k_3)X_b^j(k_4) \\
&+ \sum_{a=1}^n u\int d^D\sigma \int d^D\sigma' \delta^d(X_a^i(\sigma) - X_a^i(\sigma')). \qquad (2.3.9)
\end{aligned}$$

In the above, $K_{ab}(k) = k^2\delta_{ab} - \Delta_K(k)k^4 J_{ab}$, where $J_{ab} = 1$ for all a, b. To calculate the effective free energy we use the gaussian variational approximation [49, 23, 50]. The method consists in choosing as a variational hamiltonian the most general quadratic form.

$$\mathcal{H}_{var} = \frac{1}{2}\int d^D k X_a^i(-k)G_{ab}^{-1}(k)X_b^i(k). \qquad (2.3.10)$$

That is, two-point correlation function is given by

$$< X_a^i(-k) X_b^j(k) >_{var} = \delta_{ij} G_{ab}(k), \qquad (2.3.11)$$

where $< \quad >_{var}$ means the thermal average with the trial hamiltonian(2.3.10). Then the effective free energy is given by [49]

$$\frac{1}{L^D} \mathcal{F}_{eff} = \lim_{n \to 0} \frac{1}{n} \left[\frac{1}{L^D} < \mathcal{F}_{rep} - \mathcal{F}_{var} >_{var} - \frac{d}{2} \mathrm{Tr} \ln G_{ab}(k) \right], \qquad (2.3.12)$$

where L is the linear size of the membrane. It is easy to carry out this calculation to find

$$\begin{aligned}
& \frac{1}{L^D} < \mathcal{F}_{rep} - \mathcal{F}_{var} >_{var} + \frac{d}{2} \mathrm{Tr} \ln G_{ab}^{-1}(k) \\
& = \frac{d}{2} \int \frac{d^D k}{(2\pi)^D} [K_{ab}(k) G_{ab} - 1] \\
& \quad - \frac{d}{2} \int \frac{d^D k_1}{(2\pi)^D} \frac{d^D k_3}{(2\pi)^D} [n^2 \Delta_\mu(0) \vec{k_1}^2 \vec{k_3}^2 G_{aa}(k_1) G_{bb}(k_3)] \\
& \quad - \frac{d^2}{2} \int_{q=k_1+k_2} \frac{d^D k_1}{(2\pi)^D} \frac{d^D k_2}{(2\pi)^D} \Delta_\mu(q) \sum_{a,b} [2(\vec{k_1} \cdot \vec{k_2})^2 G_{ab}(k_1) G_{ab}(k_2)] \\
& \quad - \frac{d}{2} \int \frac{d^D k}{(2\pi)^D} \mathrm{Tr} \ln G_{ab}^{-1}(k) \\
& \quad + \frac{u}{(2\pi)^d} \int d^D \sigma \left(\frac{\pi}{K(\sigma)} \right)^{\frac{d}{2}}, \qquad (2.3.13)
\end{aligned}$$

where $K(\sigma)$ is the two-point correlation function for the trial hamiltonian,

$$\begin{aligned}
K(\sigma) & = \lim_{n \to 0} \frac{1}{n} \sum_{a=1}^n \frac{1}{2d} < (X_a^i(\sigma) - X_a^i(0))^2 >_{var} \\
& = \lim_{n \to 0} \frac{1}{n} \sum_{a=1}^n \int \frac{d^D k}{(2\pi)^D} (1 - \cos(\vec{k} \cdot \vec{\sigma})) G_{aa}(k). \qquad (2.3.14)
\end{aligned}$$

We now look for a replica symmetric solution

$$G_{ab}(k) = g_K(k) \delta_{ab} + g_\Delta(k) J_{ab}. \qquad (2.3.15)$$

For later convenience, we introduce the following expression for the "bare " propagators

$$K_{ab}(k) = \delta_{ab} h_K(k) - J_{ab} h_\Delta(k). \qquad (2.3.16)$$

With these propagators, the effective free energy is evaluated as

$$\begin{aligned}
\frac{1}{L^D} \mathcal{F}_{eff} = & \frac{d}{2} \int \frac{d^D k}{(2\pi)^D} \left\{ [h_K(k) - h_\Delta(k)][g_K(k) + g_\Delta(k)] + \frac{d}{2} g_\Delta(k) h_\Delta(k) \right\} \\
& - \frac{d}{2} \int \frac{d^D k}{(2\pi)^D} \left[\ln g_K(k) + \frac{g_\Delta(k)}{g_K(k)} \right]
\end{aligned}$$

$$\begin{aligned}
& - d \int_{q=k_1+k_2} \frac{d^D k_1}{(2\pi)^D} \frac{d^D k_2}{(2\pi)^D} \Delta_\mu(q) (\vec{k_1} \cdot \vec{k_2})^2 \\
& \quad \{ [g_K(k_1) + g_\Delta(k_2)][g_K(k_2) + g_\Delta(k_2)] - g_\Delta(k_1) g_\Delta(k_2) \} \\
& + \frac{u}{(2\pi)^d} \int d^D \sigma \left(\frac{\pi}{K(\sigma)} \right)^{d/2}, \qquad (2.3.17)
\end{aligned}$$

and the two-point correlation function $K(\sigma)$ reduces to

$$K(\sigma) = \int \frac{d^D k}{(2\pi)^D} (1 - \cos(\vec{k} \cdot \vec{\sigma})) (g_K(k) + g_\Delta(k)). \qquad (2.3.18)$$

For disorder fluctuations [38] we also introduce the following function $L(\sigma)$,

$$\begin{aligned}
L(\sigma) & = < \frac{1}{2d} < (X^i(\sigma) - X^i(0)) >^2 >_{Dis} \\
& = \int \frac{d^D k}{(2\pi)^D} (1 - \cos(\vec{k} \cdot \vec{\sigma})) g_\Delta(k). \qquad (2.3.19)
\end{aligned}$$

Here $< \quad >$ means the thermal average. Note that the second equality is correct only in the gaussian variational approximation. These two functions are characterized by two exponents ω and ω': $K(\sigma) \sim A_0 \sigma^\omega$ and $L(\sigma) \sim A_0' \sigma^{\omega'}$.

Taking the variational derivatives of (2.3.17) with respect to $g_K(k)$ and $g_\Delta(k)$ and setting the results equal to zero, we find that

$$\begin{aligned}
\frac{1}{g_K} = & h_K - 4 \int \frac{d^D q}{(2\pi)^D} \Delta_\mu(q) g_K(k-q) ((\vec{k} - \vec{q}) \cdot \vec{k})^2 \\
& - \frac{u}{2(2\pi)^d} \int d^D \sigma \left(\frac{1}{K(\sigma)} \right)^{\frac{d}{2}+1} (\pi)^{d/2} (1 - \cos(\vec{k} \cdot \vec{\sigma})), \qquad (2.3.20)
\end{aligned}$$

and

$$\frac{g_\Delta}{g_K^2} = h_\Delta + 4 \int \frac{d^D q}{(2\pi)^D} \Delta_\mu(q) g_\Delta(k-q) ((\vec{k} - \vec{q}) \cdot \vec{k})^2. \qquad (2.3.21)$$

The saddle point equation (2.3.20) is different from that of the pure self-avoiding tethered membrane [22, 23] by the second term. This term comes from the stress disorder term and as we shall see below, we can also interpret it as the contribution from the fluctuations of the spin-glass operator in the short-range disorder case. We note that these saddle point equations have essentially the same structure with the integral equations studied in [38].

In the short-range disorder case, we can incorporate the spin-glass phase. As in [36], we consider the ground state $X_{a,cl}$,

$$\partial_\alpha X_{a,cl}^i \partial_\beta X_{b,cl}^j = q \delta_{\alpha\beta} \delta_{ij} \quad (a \neq b) \qquad (2.3.22)$$

and fluctuations about the ground state,

$$X_a^i(\sigma) = X_{a,cl}^i(\sigma) + \delta X_a^i(\sigma). \qquad (2.3.23)$$

The thermal average is calculated by use of the following trial hamiltonian,

$$\mathcal{H}_{var} = \frac{1}{2}\int d^D k (X_a^i(-k) - X_{a,cl}^i(-k))G_{ab}^{-1}(k)(X_b^i(k) - X_{b,cl}^i(k)). \qquad (2.3.24)$$

Then, we have

$$\frac{1}{L^D} < -\frac{1}{2}\sum_{a,b=1}^{n}\Delta_\mu \int d^D\sigma \partial_\alpha X_a^i \partial_\alpha X_a^i \partial_\beta X_b^j \partial_\beta X_b^j >_{var}$$

$$= -2d\sum_{a\neq b=1}^{n}\Delta_\mu q \int \frac{d^D k}{(2\pi)^D}k^2 G_{ab}(k)$$

$$- \sum_{a\neq b=1}^{n} d\Delta_\mu D q^2$$

$$- \frac{1}{2}d^2 \int \frac{d^D k_1}{(2\pi)^D}\frac{d^D k_3}{(2\pi)^D}[n^2\Delta_\mu \vec{k}_1^2 \vec{k}_3^2 G_{aa}(k_1)G_{bb}(k_3)]$$

$$- \frac{1}{2}d^2 \int_{q=k_1+k_2}\frac{d^D k_1}{(2\pi)^D}\frac{d^D k_2}{(2\pi)^D}\Delta_\mu\sum_{a,b}[2(\vec{k}_1 \cdot \vec{k}_2)^2 G_{ab}(k_1)G_{ab}(k_2)]. \qquad (2.3.25)$$

In this case, the saddle point equations are

$$\frac{1}{g_K} = h_K + 2\Delta_\mu q k^2 - 4\int\frac{d^D q}{(2\pi)^D}\Delta_\mu g_K(k-q)((\vec{k}-\vec{q})\cdot\vec{k})^2$$

$$- \frac{u}{2(2\pi)^d}\int d^D\sigma(\frac{1}{K(\sigma)})^{\frac{d}{2}+1}(\pi)^{d/2}(1-\cos(\vec{k}\cdot\vec{\sigma})), \qquad (2.3.26)$$

and

$$\frac{g_\Delta}{g_K^2} = h_\Delta + 4\int\frac{d^D q}{(2\pi)^D}\Delta_\mu g_\Delta(k-q)((\vec{k}-\vec{q})\cdot\vec{k})^2 + 2\Delta_\mu q k^2. \qquad (2.3.27)$$

From these calculations, we can identify the contributions from the stress disorder with the fluctuation of the spin-glass operator. It is interesting to note that, except for the contributions from the stress disorder, these saddle point equations (2.3.26),(2.3.27) are the same with those of the randomly polymerized membrane with long-range interactions [40].

2.3.2   Solutions to saddle point equations

In this subsection, we restrict our interest to the 2-dimensional membranes in d-dimension and examine the large distance (infrared) behaviors of $K(\sigma)$, $L(\sigma)$, $g_K(k)$ and $g_\Delta(k)$. We first study the crumpled phases of self-avoiding tethered membranes with long-range disorders and then the crumpled-glass phase ($q \neq 0$) in the case of the short-range disorder.

Large distance behaviors of crumpled phases

To find the possible phases we analyze the saddle point equations (2.3.20) and (2.3.21) through convergence criteria. We assume the following forms of $g_K(k)$, $g_\Delta(k)$, $K(\sigma)$ and $L(\sigma)$ in the infrared limit:

$$g_K(k)^{-1} \sim k_0 k^{2+\alpha}.$$

$$g_\Delta(k)^{-1} \sim k_0' k^{2+\alpha'}.$$

$$K(\sigma) \sim A_0 \sigma^\omega.$$

$$L(\sigma) \sim A_0' \sigma^{\omega'}.$$

The exponent ω is related to the standard exponent ν for the radius of gyration ($R_G^2 \sim L^{2\nu}$) by $\nu = \omega/2$. We then have

$$\int\frac{d^2 k}{(2\pi)^2}g_K(k)(1-\cos(\vec{k}\cdot\vec{\sigma})) \sim \sigma^\alpha.$$

$$\int\frac{d^2 k}{(2\pi)^2}g_\Delta(k)(1-\cos(\vec{k}\cdot\vec{\sigma})) \sim \sigma^{\alpha'}. \qquad (2.3.28)$$

If $\alpha > \alpha'$, the thermal fluctuations take over disorder fluctuations; $K(\sigma) \sim \sigma^\alpha$ and $\omega = \alpha$ hold . We name such a regime temperature-dominated phase [38]. On the other hand, if $\alpha < \alpha'$, disorder fluctuations take over the thermal fluctuations and two-point correlation function is determined by the disorder fluctuations. That is, $K(\sigma) \sim L(\sigma) \sim \sigma^{\alpha'}$ and $\omega = \alpha'$. We call such a regime disorder-dominated phase. These suggest that $\omega = \max(\alpha, \alpha')$. We now analyze the crumpled phases of the membrane. We assume the following constraints on the values of the above exponents,

$$0 < \omega, \omega' < 2,$$

$$0 < \alpha, \alpha' < 2. \qquad (2.3.29)$$

Inserting the dominant behaviors $g_K(k)^{-1} \sim k^{2+\alpha}$ and $g_\Delta(k)^{-1} \sim k^{2+\alpha'}$ in the integrants, we find that

$$\int\frac{d^2 q}{(2\pi)^2}\Delta_\mu(q)g_K(\vec{k}-\vec{q})((\vec{k}-\vec{q})\cdot\vec{k})^2 \sim k^{4-Z_\mu-\alpha}. \qquad (2.3.30)$$

$$\int\frac{d^2 q}{(2\pi)^2}\Delta_\mu(q)g_\Delta(\vec{k}-\vec{q})((\vec{k}-\vec{q})\cdot\vec{k})^2 \sim k^{4-Z_\mu-\alpha'}. \qquad (2.3.31)$$

From the dominant behavior $K(\sigma) \sim \sigma^\omega$, we also find that

$$h_K(k) - \frac{u}{2(2\pi)^d}\int d^2\sigma(\frac{1}{K(\sigma)})^{1+\frac{d}{2}}(\pi)^{d/2}(1-\cos(\vec{k}\cdot\sigma)) \sim k^{2+\theta} \qquad (2.3.32)$$

and

$$\theta = -4 + (1 + \frac{d}{2})\omega \leq 2. \qquad (2.3.33)$$

The condition $\theta \leq 2$ comes from the followings. If $\theta > 2$ the coefficient of the k^4 term in the lhs of (2.3.32) becomes finite and the infrared behavior is $\sim k^4$ [22], which implies $\theta = 2$. From these considerations we determine the infrared behaviors, that is, ω, α and α' of the membranes in several cases.

1. Pure case (no disorder).

For readers' convenience, we summarize the results of the gaussian variational approximation for the 2-dimensional self-avoiding tethered membranes in d-dimension [22, 23, 24]. In this case, the equalities $\theta = \alpha = \omega$ hold and from (2.3.33) we obtain $\omega = 8/d$. This means that the crumpled phases exist only at $d > 4$ and the membrane at $d \leq 4$ is in the flat phase. In [22], more careful discussions have been made in order that the gaussian variational approximation works for the polymer case. However, their improvement results in that the 2-dimensional self-avoiding tethered membrane in 4-dimension is in the crumpled phase, which contradicts with the results of the numerical simulations [25]. Therefore, we shall not pursuit such a direction.

2. Stress disorder only.

In this case, $\Delta_K(q) = 0$, which means the up-down symmetry of the membrane. Then $g_\Delta(k) = 0$ and the equality $\omega = \alpha$ holds. We only need to consider eq.(2.3.20). Introducing two positive constants c_1 and c_2, we can write eq.(2.3.20) as

$$g_K(k)^{-1} = c_1 k^{2+\theta} - c_2 k^{4-Z_\mu-\alpha}. \qquad (2.3.34)$$

If $4-Z_\mu-\alpha > 2+\theta$, then the disorder term becomes irrelevant and the infrared behavior is determined by the self-avoiding term. That is, the self-avoidance completely determines the behavior. Then, we can use the result of the case 1 (no disorder) and we obtain $\omega = 8/d$. We put this result in the above condition to obtain the following constraint:

$$2 - Z_\mu > \frac{16}{d}. \qquad (2.3.35)$$

Then we may ask what happens when the above constraint does not hold, that is, when $16/d \geq 2 - Z_\mu$ and the stress disorder becomes relevant. At first sight, the second term in eq.(2.3.34) determines the infrared behavior of the membrane. However, this is not true. One should note that the coefficient of the second term in eq.(2.3.34) is negative implying the cancellation between the first term and the second term. Physically speaking, the second term comes from the stress disorder, and the fact that it becomes relevant means that the membrane tends to shrink. Then the exponent of the first term in eq.(2.3.34) becomes smaller and the infrared behavior of the membrane is determined

by the condition that the exponents of the first term and the second term become equal. From this condition, we obtain

$$\alpha = \frac{6 - Z_\mu}{2 + d/2}. \qquad (2.3.36)$$

This suggests that even in the short-range disorder case ($Z_\mu = 0$), ω at $d < 8$ is altered from the value $8/d$ of the pure case to $6/(2+d/2)$. We see that the self-avoiding tethered membranes with short-range stress disorder at $d > 2$ are in the crumpled phase. This conclusion seems to contradict with the result that for $T > 0$ (short-range) stress and spontaneous curvature disorders are irrelevant in the flat phase of the membrane. It is not so. Our conclusion means only that the self-avoiding tethered membrane with short-range stress disorder is in the crumpled phase. It does not exclude its transition to the flat phase. Therefore if the strength of the disorder is weak enough and we increase the rigidity of the membrane, there may occur the phase transition to the flat phase. In a previous work, we gave a conjecture that the self-avoiding tethered membranes with short-range stress disorder is in the flat phase or in the crumpled-glass phase and it is not in the crumpled phase. There, we assumed that the stress disorder is irrelevant even at finite d-case. This, however, does not hold as we have seen above. We note that in the long-range disorder case ($Z_\mu > 0$), the membrane does not become flat even at $d = 2$. It is a drawback of the variational method.

3. Curvature disorder only.

From eq.(2.3.21) we find that $\alpha' = Z_K + 2\alpha - 2$. And the equality $\alpha = \theta$ holds. That is,

$$\alpha = -4 + (1 + \frac{d}{2})\omega, \text{ and } \omega = \max(\alpha, \alpha'). \qquad (2.3.37)$$

In the temperature-dominated phase ($\alpha > \alpha'$), we find that $\omega = \alpha = \frac{8}{d}$ and the condition $\alpha > \alpha'$ reduces to $\frac{8}{d} < 2 - Z_K$. In the disorder-dominated phase ($\alpha' > \alpha$), the equality $\omega = \alpha'$ holds and

$$\alpha = \frac{4 - (1 + d/2)(Z_K - 2)}{1 + d}. \qquad (2.3.38)$$

For the short-range curvature disorder ($Z_K = 0$), at $d > 4$, $\omega = 8/d$ and at $d < 4$, $\omega > \alpha = (6 + d)/(1 + d) > 2$. This means that the crumpled phases do not exist at $d < 4$ and the self-avoiding tethered membrane with short-range curvature disorder at $d < 4$ is in the flat phase. However, long-range curvature disorder can destroy the flat phase. For example, in the case $Z_K = 1$, $\omega = \alpha' = 9/(1 + d)$ at $d < 8$. From this, we see that the self-avoiding tethered membrane with long-range curvature disorder ($Z_K = 1$) at $d = 4$ can be in the crumpled phase.

4. General case.

At first, we determine the value of the exponent α'. Introducing two positive constants d_1 and d_2, we can write eq.(2.3.21) as

$$k^{2+2\alpha-\alpha'} = d_1 k^{4-Z_K} + d_2 k^{4-Z_\mu-\alpha'}. \tag{2.3.39}$$

Then, if $Z_K > Z_\mu + \alpha'$ the infrared behavior is determined by the first term of this equation and $\alpha' = Z_K + 2\alpha - 2$. Inserting this value in the above condition, we obtain the following constraint:

$$0 > Z_\mu + 2\alpha - 2. \tag{2.3.40}$$

If $Z_K < Z_\mu + \alpha'$ the second term determine the infrared behavior. Since

$$k^{2+2\alpha-\alpha'} \sim k^{4-Z_\mu-\alpha'}, \tag{2.3.41}$$

we find that $2 - Z_\mu - 2\alpha = 0$. That is, the above constraint is not broken and the equality $\alpha' = Z_K + 2\alpha - 2$ holds always. However, as we shall see below, the constraint(2.3.40) is not necessarily conserved.

The process of determining the exponent α is essentially same with the previous cases. The different phases are characterized by whether the second term in eq.(2.3.34) (the contribution of the stress disorder) is relevant or not and whether the phase is in the temperature-dominated phase or in the disorder-dominated phase; four cases are a priori possible.

(1) Temperature-dominated ($\alpha > \alpha'$) and irrelevant stress disorder phase, $\alpha = 8/d, \alpha' = Z_K + 16/d - 2$. Then $K(\sigma) \sim \sigma^\alpha$. This phase exists for $16/d < 2 - Z_\mu$ and $Z_K < 2 - 8/d$.

(2) Temperature-dominated ($\alpha > \alpha'$) and relevant stress disorder phase, $\alpha = (6 - Z_\mu)/(2 + d/2), \alpha' = Z_K + (8 - d - 2Z_\mu)/(2 + d/2)$. Then $K(\sigma) \sim \sigma^\alpha$. This phase exists for $16/d > 2 - Z_\mu$ and $Z_K < (d - 2 + Z_\mu)/(2 + d/2)$.

(3) Disorder-dominated ($\alpha < \alpha'$) and irrelevant stress disorder phase, $\alpha = (6 + d - (1 + d/2)Z_K)/(1 + d), \alpha' = (10 - Z_K)/(1 + d)$. Then $K(\sigma) \sim \sigma^{\alpha'}$. This phase exists for $Z_K > 10/(2 + d) + (1 + d)Z_\mu/(2 + d), Z_K > 2 - 8/d$ and $8 - Z_K < 2d$.

(4) Disorder-dominated ($\alpha < \alpha'$) and relevant stress disorder phase, $\alpha = (8 + d - Z_\mu - (1 + d/2)Z_K)/(3 + d), \alpha' = (Z_K + 10 - 2Z_\mu)/(3 + d)$. Then $K(\sigma) \sim \sigma^{\alpha'}$. This phase exists for $Z_K < 10/(2+d) + (1+d)Z_\mu/(2+d), Z_K > (d-2+Z_\mu)/(2+d/2)$ and $Z_K + 4 - 2Z_\mu < 2d$.

In Figures 2, we summarize the phase diagrams of the restricted cases of the general result. Figure 2a shows the phase diagram of the crumpled phases in (d, Z_K) plane for the case of the short-range stress disorder ($Z_\mu = 0$). The region where the above crumpled phases do not occupy is considered to be the flat phase or the crumpled-glass phase. Figure 2b shows the phase diagram of the crumpled phases in (Z_μ, Z_K) plane for the case when the embedding dimension d is three. In ref.[38], the phase diagram of the flat

phases and flat glass phases of tethered membrane in (Z_μ, Z_K) plane for $d = 3$ case is given. Our conclusion is that the tethered membrane with disorder exponents (Z_μ, Z_K) with no rigidity is in the associated crumpled phase of Figure 2b. Following the first scenario presented in the introduction, when we increase the rigidity of the membrane there occurs the phase transition to the flat phases presented in the ref.[36] or to the crumpled glass phase depending on whether the strength is weak or strong. If we follow the second scenario [38], the exponents (Z_μ, Z_K) must be larger than the critical values in order that there occur the phase transition to the crumpled-glass phase. Otherwise, the rigid membrane is in the flat phase.

Large distance behaviors of the crumpled-glass phases (short-range disorders)

In the crumpled-glass phase ($q \neq 0$), we need to study the saddle point equations (2.3.26) and (2.3.27). The analysis goes in the same way with the previous subsection. From eq.(2.3.27), we find that the infrared behavior of $g_\Delta(k)$ is completely determined by the last term $2\Delta_\mu q k^2$. Then, we have $\alpha' = 2\alpha$, indicating that the membrane is in the disorder-dominated phase ($\alpha > \alpha'$). This is very natural, because the membrane is in the crumpled-glass phase and the infrared behavior is determined by the disorder of the ground state. With the above result ($\omega = \alpha' = 2\alpha$), the analysis can be done as in the stress disorder only case. We present the results. At $d > 3$, the stress disorder is irrelevant and $\omega = 8/(1 + d)$. At $d \leq 3$, both the self-avoidance and the disorder are relevant. However ω becomes larger than two and we believe that the crumpled-glass phase does not exist at $d \leq 3$. These situations entirely coincide with the previous ones [40] by changing γ with d. The fluctuation of the spin-glass operator does not modify the previous result in contrast to the crumpled phases.
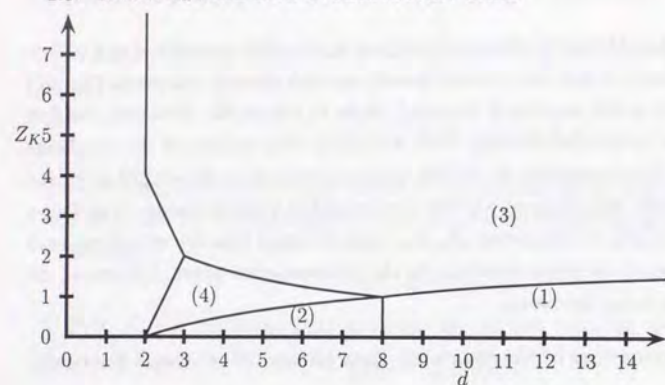
Figure 2a: The crumpled phases of the self-avoiding tethered membrane with short-range stress disorder ($Z_\mu = 0$) and long-range curvature disorder with exponent Z_K in d-dimensional space.

(1) Temperature-dominated and irrelevant stress disorder phase; (2) Temperature-dominated and relevant stress disorder phase; (3) Disorder-dominated and irrelevant stress disorder phase; (4) Disorder-dominated and relevant stress disorder phase.
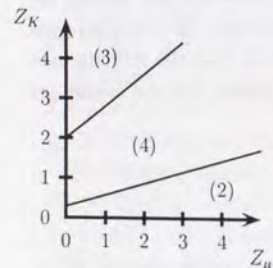

Figure 2b: The crumpled phases of the self-avoiding tethered membrane with long-range stress disorder with exponent Z_μ and long-range curvature disorder with exponent Z_K in 3-dimensional space.

(2) Temperature-dominated and relevant stress disorder phase; (3) Disorder-dominated and irrelevant stress disorder phase; (4) Disorder-dominated and relevant stress disorder phase.

2.3.3 Summary

In this section, we have studied the crumpled phases of the self-avoiding tethered membrane with disorders. We have shown that even a short-range stress disorder is relevant at $d < 8$ and the crumpled phase exists even at $2 < d \leq 4$. This result is in contrast with the crumpled phase of the phantom tethered membrane [28]. There, a short-range stress disorder merely causes to swell the membrane slightly and should not affect the universal property. We have given the exponent for the radius of gyration. Furthermore, we have considered the case where the disorders have long-range correlations. The membrane's behavior is characterized by whether the stress disorder is relevant or not and by whether the membrane is in the temperature-dominated phase or in the disorder-dominated phase. Specifying which phases the membrane with the disorder exponents (Z_μ, Z_K) in d-dimension belongs to, we have given the exponent for the radius of gyration. The phase diagrams in two special cases are presented (Fig.2a, Fig.2b). We have also studied the behavior of the crumpled-glass phase in the case of short-range disorders. In this case, the contribution from stress disorder can be seen as the fluctuations of the spin-glass operator. This fluctuation does not modify the behaviors of the crumpled-glass phase. However, the analysis is restricted to the replica symmetric solution and the improvement is left for a future study.

2.4 Discussions and Concluding Remarks

In this chapter, we have reviewed theoretical approaches to the self-avoiding randomly polymerized membranes. The model for randomly polymerized membranes with long-range interactions $r^{-\gamma}$ can be solved exactly using the large-d limit and we found that the flat phase becomes unstable and the crumpled glass phase takes over. We have obtained the phase diagram in the (γ, D) plane and several possible phase transitions. The exponents for the radius of gyration in the crumpled and the crumpled glass phase are also given.

In order to discuss the ordinary "short-range" self-avoiding tethered membrane with randomnesses, Sec.2.3 is devoted to the analysis of the generalized Edwards model with quenched randomnesses. The model is studied using the replica field theory. We have found that the randomnesses are relevant on the crumpled membrane and its behavior. In particular, the analysis has proposed the possibility that the self-avoiding tethered membrane with random stress can be crumpled when its bending rigidity is small. In the next chapter, we will study this possibility by Monte-Carlo method.

Chapter 3

Self-Avoiding Randomly Polymerized Membrane II: Numerical Studies

3.1   Genesis

Self-avoiding polymerized membrane is asymptotically flat when it is embedded in three dimensional space. Now it is understood that it is the result of crumpling transition caused by the "entropic" bending rigidity from self-avoiding interaction [10]. This means that the flat phase of the self-avoiding tethered membrane is described by the fixed point (Aronovitz-Lubensky fixed point) associated with the flat phase of the phantom polymerized membrane [30]. When one consider the stability of the flat polymerized membrane by some effect, a natural approach is to discuss the stability of the fixed point by the effect.

Recently, studies on the effect of quenched in-plane disorder have been extensively performed. And the ϵ-expansion analyses about the stability of the fixed point by the quenched inplane disorders, such as preferred metric and spontaneous curvature, concluded that the flat phase is stable with respect to weak these randomnesses at finite temperature $T > 0$ [27, 28, 34, 35]. This means that the flat phase of self-avoiding polymerized membrane is stable when the membrane is very rigid. Because, when the membrane is very rigid, and flat, it is possible to neglect the self-avoiding interaction and the above result also applies in this case. However, when the membrane is very soft or its bending rigidity is small, the only apprach to study the stability of the flat phase is to discuss the membrane's crumped phase. From this point of view, the crumpled phase of generalized Edwards model with quenched in-plane disorders has been discussed in the previous chapter and it was concluded that the membrane with random stress can be

crumpled at $d = 3$ [42]. The validity of the approach is not clear, however as has been discussed in Chapter 1, it gives good estimate about the behavior of the membrane without disorder embedded in higher dimensional space. In addition, the dimension four, which is the "upper" critical dimension for the flat phase of self-avoiding tethered membrane, has a meaning in the same frame work.

In this chapter, we study the above possibility of crumpled self-avoiding polymerized membrane with random stress by numerical methods [44, 45]. As a model for numerical studies, we have employed two types of models. (1) The first one is a randomly tethered membrane model [43] and (2) the second model is a model tethered membrane with random bond length [47]. In particular, we will study the membrane with small bending rigidity. In order to do so, we use the hard sphere model with smaller diameter "(weak self-avoiding case)". In this case we cannot prohibit the self-intersection of the membrane. Even if the membrane is found to be crumpled or large conformational transformation, it may be an artifact of the model. That is, if the self-intersection is completely forbidden, such behavior may not occur. However, if there occurs some instability and the universality changes, it means that the random stress is relevant on the flat polymerized membrane and the results of the above perturbation theory that the flat phase of (phantom) polymerized membrane is stable with respect to random stress breaks down. Therefore, in our numerical studies we concentrate on the weak self-avoiding case.

The organization of this chapter is as follows. In Sec.3.2, we describe the model and numerical procedures. We study two type of self-avoiding tethered membrane with random stress. (1) The first model is a randomly tethered membrane model. By the random polymerization, the membrane has dislocations and disclinations and they cause quenched random stress [43]. (2) The second model is a tethered membrane with random bond length [47]. The membrane is excised from regular hexagonal lattice and it has no dislocation or disclination. Every atom i was independently assigned a random number $p_i = \pm 1$, representing big or small atoms and the bond length between atom i and neighboring atom j was set as $b_{ij} = b + (p_i + p_j)v$. Then the membrane has random stress. When we consider the rigid membrane, we fix $b = 1.7$ and when we consider a membrane with small bending rigidity we use $b = 3.0$. We call the former case "strong" self-avoiding one, however, even in this case the self-intersection is not necessarily prohibited. The only difference from the latter one is its bending rigidity and flexibility. The results of the simulations are presented and analyzed in Sec.3.3. The membrane with weak self-avoidance ($b = 3.0$) shows large shrink by buckling transitions in both models. (1) The randomly tethered membrane is crumpled and the exponent for the radius of gyration R_G is 0.84 ± 0.01. For the second model (2) the fact that there occurs large shrink is

right even if the strength of disorder is small ($v \sim 0.2$). About its asymptotic form, the membrane with weak disorder ($v \sim 0.52$) is asymptotically flat and roughness exponent $\nu_\perp$ is small in our data ($\nu_\perp \simeq 0.3 \pm 0.1$). The membrane with strong disorder ($v = 0.75$) is crumpled and the exponent for the radius of gyration R_G is 0.90 ± 0.04. The membranes with strong self-avoidance are asymptotically flat in both models and their shrinkages are small. For the second random bond length model, we have studied its cooling process for strong self-avoiding case. Even if the temperature decreases, the shape of the membrane does not show large folding, which is observed in the phantom case. On the contrary, the membrane becomes flatter and flatter. In Sec.3.4, we discuss the implications of the results and suggest a direction of further study.

3.2 Model Systems and Simulation Procedure

We study two kinds of self-avoiding tethered membranes with quenched internal disorders. The first one is randomly tethered membrane model and the second one is random bond length model. The models which we study consists of hard spheres with diameter $\sigma = 1$ connected in a fixed geometry by flexible bonds. Hereafter, we will explain them in detail.

3.2.1 S.-A. randomly tethered membrane

For the randomly tethered membrane case, the initial states were two-dimensional random configuration of hard spheres. In order to prepare a random configuration of monomers, we first equilibrated systems of $N = 721$ monomers in a circle of radius 24 (density is about 0.4 particle per unit area) by standard Metropolis method. As the potential between monomers, we use

$$U(r) = \begin{cases} 0 & r > \sigma \\ \infty & \text{otherwise} \end{cases} \tag{3.2.1}$$

An elementary move in such Monte Carlo simulation consists of randomly choosing an atom and attempting to move it by an amount s in a randomly chosen direction. In the simulation we have taken the displacement $s \leq 0.2$. A trial move is accepted or rejected according to the conventional procedure of comparing $\exp(-\Delta\beta E)$, where ΔE is the energy difference between the configuration before and after the trial move, with a random number chosen from the interval $0 - 1$. During one Mnote Carlo time unit an attempt is made to move every atom of the surface. We performed $5 * N^2$ Monte-Carlo steps. We then "polymerized" the configuration by adding a tethering potential

$$U_{NN}(r) = k(r^2 - b^2)^2. \tag{3.2.2}$$

to all nearest neighbors which were identified by Delaunay triangulation [51]. The force constant k of the springs connecting the nearest neighbors is the same everywhere. Typical connectivity of the membrane with $N = 721$ monomers is shown in Figure 1. In the configuration, roughly 40% of monomers have six nearest neighbors. Membranes are excised from the network with monomer number $N = 169, 271, 397$ and 547 [1]. The tethering potential has a parameter b that determines the reference length at which potential becomes minimum. We take $b = 3$ or $b = 1.7$ for all nearest-neighbor pairs, independent of the distance between monomers. The case $b = 1.7$ corresponds to a rigid membrane and the case $b = 3.0$ corresponds to a membrane with small bending rigidity.
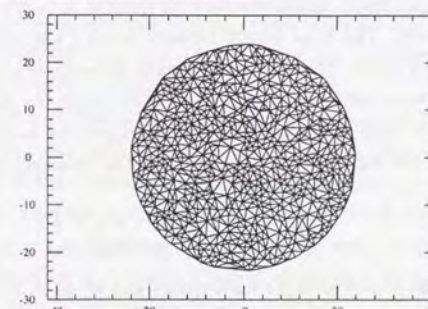
Initial Configuration for R.T.M. with N=721

Figure.1. Planar configuration of a randomly tethered membrane with 721 monomer. The solid lines represent flexible bonds.

We then allow the membrane to reequilibrate in three dimensions. We have fixed the force constant $k\beta(= k/k_B T) = 1$. At this temperature, the fluctuation of the distances between monomers is small. Of course, in the reequilibration, the hard core potential (3.2.1) also works with $\sigma = 1.0$.

3.2.2 S.-A. tethered membrane with quenched random internal disorder (Random bond length model)

The model which we study consists of hard spheres with diameter $\sigma = 1$ connected in a two-dimensional triangular array embedded in a three dimensional space. I-th atom of

---

[1] In our previous study, a different procedure for preparing initial configurations is used. In this paper, we have also modified the initial density of monomers and obtained better data.

such network is described by $\vec{r}_i$. In the simulation a hexagonal sheet (L $\leq$ 27 monomers across) with $N = (3L^2+1)/4$ monomers excised from the triangular lattice has been used. The connectivity of the system was fixed by keeping nearest neighbor atoms on the lattice connected by a tethering potential [2]

$$U_{NN}(r_{ij}) = k(r_{ij}^2 - b_{ij}^2)^2. \tag{3.2.1}$$

Here r_{ij} means the distance between i-th and j-th monomers and b_{ij} means the equilibrium distance (bond length), which varies among atom pairs but is kept frozen during the simulation. The force constant k of the springs connecting the nearest neighbors is the same everywhere and it is represented as $\kappa = \epsilon_0/\sigma^2$ in terms of an arbitrary energy unit ϵ_0. The bond lengths have been chosen by the following procedure [47]: every atom i was independently assigned a random number $p_i = \pm 1$, representing big or small atoms, respectively. The bond length between atom i and neighboring atom j was set as $b_{ij} = b + (p_i + p_j)v$. Thus the bond length between two big atom was $b + 2v$, the bond length between two small atoms was $b - 2v$, while the distance between a big and small atom was b. Such choice maintains an average bond length b. In order to take into account the effect of self-avoidance, we also add the following potential between all pairs of monomers,

$$U(r)_{S.A.} = \begin{cases} 0 & r > \sigma \\ \infty & \text{otherwise} \end{cases} \tag{3.2.2}$$

Here, σ means the diameter of the hard sphere and we fix $\sigma = 1$. The tethering potential does not restrict the length between nearest neighbor monomers. Even if we take $b < \sqrt{3}$ and $v = 0$, we cannot completely forbid the self-intersection at finite temperature. In the simulation we have studied two cases: The first case is $b = 3.0$ ((1):"Weak" self-avoidance) and the second one is $b = 1.7$ ((2):"Strong" self-avoidance). The case (1) corresponds to a membrane with small bending rigidity and the case (2) corresponds to a rigid membrane. About the strength of disorder, in the case (2), we have fixed $v = 0.3$ which is close to the maximal contrast between the long and the short bonds as allowed by the algorithm. In the case (1), we have at first studied two cases $v = 0.3 \times 3.0/1.7 \sim 0.52$(weak disorder) and $v = 0.75$(strong disorder) extensively. Then we have varied the strength of disorder in the range $0.0 < v < 0.95$. For comparison, we have also performed the Monte-Carlo study of hexagonal lattice with no disorder, $(b, v) = (3.0, 0.0)$ and $(b, v) = (1.7, 0.0)$. About the force constant k, we have studied the behavior of the membrane at one temperature $k/k_B T = 1.0$ and used the unit $T = 1.0(k/K_B = 1.0)$. At this temperature, the fluctuation of the distances between monomers is small. When we decrease the temperature, the

---

[2]In the model by Kantor [47], a slightly different potential was used.

simulation begin at $T = 10.0$, which was decreased from time to time by a factor 3. This is rapid cooling and there remains the danger that the membrane is trapped in some local minimum. However, we think that even with such rapid cooling we can see whether there occurs buckling instability, which results in a large conformational transformation of the membrane.

3.2.3 Simulation procedure

An elementary move in a Monte-Carlo simulation consists of randomly choosing an atom and attempting to move it by an amount s in a randomly chosen direction. In all the simulation we have taken the displacement $s \leq 0.2$. A trial move is accepted or rejected according to the conventional procedure of comparing $\exp(-\Delta\beta E)$, where ΔE is the energy difference between the configuration before and after the trial move, with a random number chosen from the interval $0 - 1$. We define the one Monte-Carlo time unit as a time required to perform N elementary moves.

In order to investigate the number of time steps (defined in terms of Monte-Carlo steps) required for thermalization, we have estimated the relaxation time by calculating the autocorrelation function of the observables such as radius of gyration and eigenvalues of the inertia tensor. Figure 2 depicts an example of such measurement for $L = 27(N = 547)$ surface at temperature $T = 1.0$. The line ($\times$), the line ($\diamond$) and the line ($\square$) correspond to the autocorrelation function $A_{Rg}(t)$ of the radius of gyration for $(b, v) = (3.0, 0.75)$, $(b, v) = (3.0, 0.0)$ and randomly tethered membrane ($b = 3.0$).
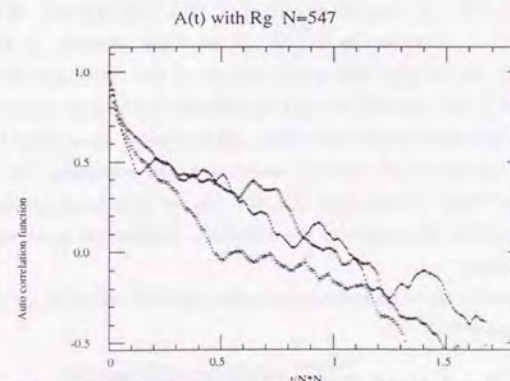
A(t) with Rg N=547

Figure 2. Time dependence of autocorrelation A_{Rg} for the radius of gyration with

$N = 547$. The Curve ($\times$) depicts A_{Rg} for $(b,v) = (3.0, 0.75)$ (weak self-avoidance and strong disorder), the curve ($\diamond$) represents A_{Rg} for $(b,v) = (3.0, 0.0)$ (Regular hexagonal membrane) and the curve ($\square$) represents shows A_{Rg} for randomly tethered membrane with $b = 3.0$.

The autocorrelation function of the radius of gyration is defined as $A_{Rg}(t) = (< [Rg(t'+t)Rg(t) > - < Rg(t') >][Rg(t') - < Rg(t') >] >)/ < [Rg(t')^2 - < Rg(t') >]^2 >$, where the average $<>$ is performed over the time t'. From the figure we see N^2 Monte-Carlo time units is sufficient for equilibration and independence between samples at the system size. In all the simulation, we have used N^2 Monte-Carlo steps as our time unit and we have performed equilibrium process over times ranging between $30N^2$ and $500N^2$ Monte-Carlo time units. We have also performed the disorder average for $N \le 169$ with some samples with random bond length model. For the randomly tethered membrane model, we have used the samples which are excised from the same initial configuration. When we vary the temperature or the strength of disorder, we have used a hexagonal sheet with 271 monomers.

3.3   Results

We show typical spatial conformations of the membranes with several cases in Figure 3 and Figure 4 ($N = 547$). Figures 3 correspond to the conformations of self-avoiding randomly tethered membrane with $b = 1.7$ (Fig.3a) and $b = 3.0$ (Fig.3b). Figures 4 correspond to the conformations of random bond length model case $(b,v) = (1.7, 0.3)$(Fig.4a),$(3.0, 0.75)$(Fig.4b) and $(b,v) = (3.0, 0.52)$(Fig.4c). We also depict the conformation without disorders in Figs.5. From these pictures, in the random bond length model, we can see that the configurations of the membrane with "strong" self-avoidance ($b = 1.7$) and disorder are not so different from those without disorders. On the other hand, the membranes with weak self-avoidance show large shrink and there occurs buckling transitions all over the membrane. In particular, the membrane with strong disorder seems to be crumpled (Fig.4b). On the othr hand, in the randomly tethered membrane model, we cannot see the difference between the weak self-avoidance and strong self-avoidance.

In order to quantify the shrinkage of the membrane with disorder, we define the following shrink parameter [44],

$$P_{shrink} = \frac{\text{Volume}_{\text{membrane with disorder}}}{\text{Volume}_{\text{hexagonal membrane}}} \qquad (3.3.1)$$

where, Volume is defined as

$$\text{Volume} = \sqrt{\lambda_1 * \lambda_2 * \lambda_3}. \qquad (3.3.2)$$

This shrink parameter means the inverse of the relative density of the membrane. In Figures 6, we show the shrink parameter as a function of the monomer number N for both models. Fig. 6a and Fig.6b correspond to the randomly tethered case and random bond length case. When the self-avoiding interaction is weak $b = 3.0$, large shrink occurs and its density changes $5 \sim 11$ times when $N = 547$. In what follows, we will study the conformation of the membrane more carefully.
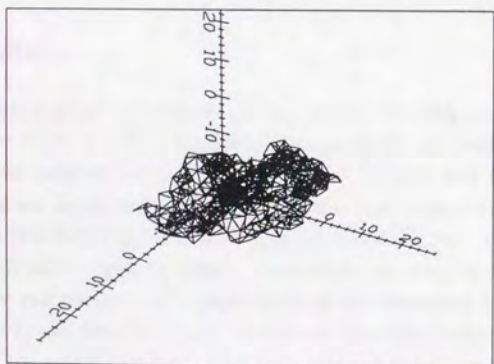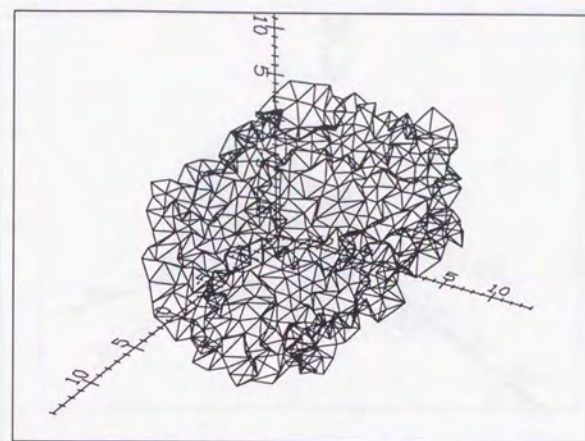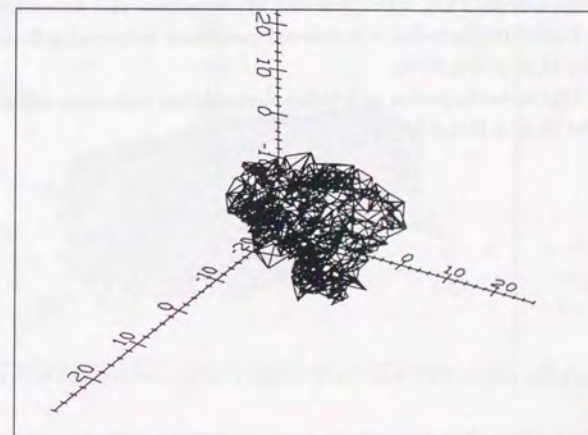
(a)

Config.
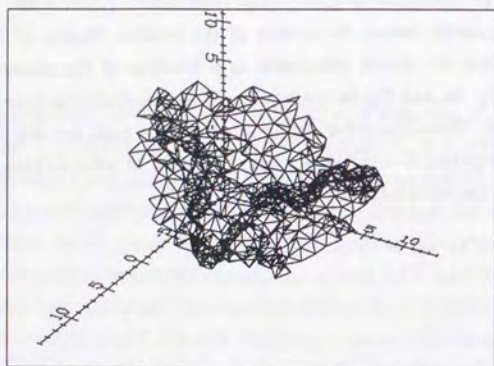
(b)

Config.

Fig.3.(a) Typical configuration of a randomly tethered membrane with strong self-avoidance $(b) = (1.7)$.

(b) Typical configuration of a randomly tethered membrane with weak self-avoidance and weak $(b) = (3.0)$.

(a)

$(b,v)=(1.7,0.3)$

(b)

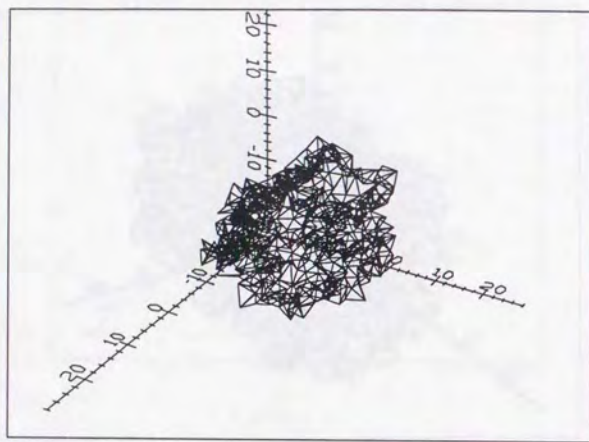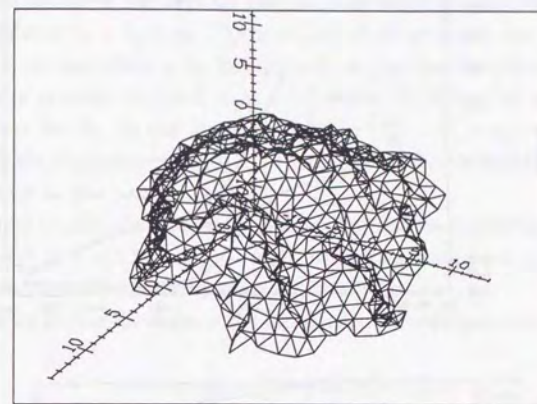Configuration with $(b,v)=(3.0,0.75)$

(c)

$(b,v)=(3.0,0.52)$

Figure 4.(a) Typical configuration of a tethered membrane with strong self-avoidance and weak disorder $(b,v) = (1.7, 0.3)$ and 547 monomers in 3 dimensional space.

(b) Typical configuration of a tethered membrane with weak self-avoidance and strong disorder $(b, v) = (3.0, 0.75)$.

(c) Typical configuration of a tethered membrane with weak self-avoidance and weak disorder $(b, v) = (3.0, 0.53)$.
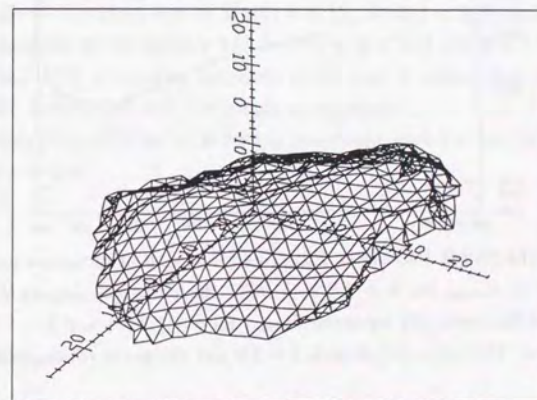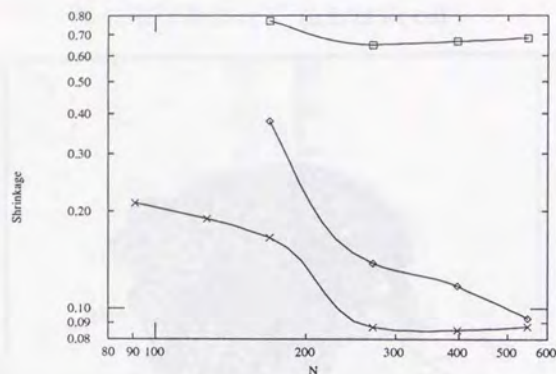
(a)

$(b,v)=(1.7,0.0)$

(b)

$(b,v)=(3.0,0.0)$

Figure 5.(a) Typical configuration of a tethered membrane with strong self-avoidance $(b, v) = (1.7, 0.0)$.

(b) Typical configuration of a tethered membrane with weak self-avoidance $(b, v) = (3.0, 0.0)$.
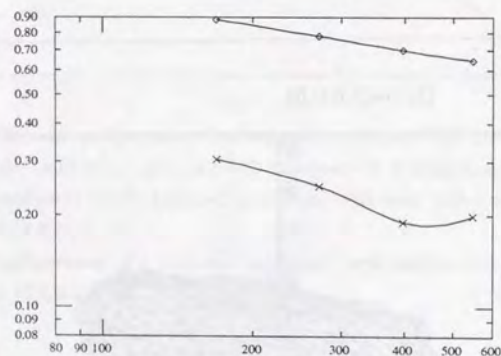
(a)

(b)

Figure 6 (a) The Shrink Parameter P_{shrink} as a function of monomer number N. The Curve ($\times$) depicts P_{shrink} for $b = 3.0, v = 0.75$, the curve ($\diamond$) depicts P_{shrink} for $b = 3.0, v = 0.52$ and the curve ($\square$) represent P_{shrink} for $b = 1.7.0, v = 0.3$.

(b) R.T.M.case. The curve ($\times$) depicts $b = 3.0$ and the curve ($\diamond$) depicts $b = 1.7$.

3.3.1 Randomly tethered membrane case

As in previous works [17, 18, 19], the inertia tensor of the system was diagonalized for each configuration in the data set and the eigenvalues are numbered according to their magnitudes as $\lambda_1 > \lambda_2 > \lambda_3$. The directions of the principal axes are given by the eigenvectors $\vec{e}_j$ corresponding to λ_j. In Figures 7, we plot the eigenvalues and the square of the radius of gyration $R_G{}^2(= \lambda_1 + \lambda_2 + \lambda_3)$ versus N. When the membrane is flat, the exponents ν for R_G, λ_1 and λ_2 should coincide ($R_G^2 \sim \lambda_1 \sim \lambda_2 \sim L^{2\nu}$). And it is different from the roughness exponent $\nu_\perp(\lambda_3 \sim L^{2\nu_\perp})$. When the membrane is crumped, the exponent for λ_3 also coincides with ν.

In the case $(b) = (3.0)$, the exponent ν is about 0.82 and the membrane is crumpled. In the case $(b) = (1.7)$, $\nu \sim 0.94$ and $\nu_\perp \sim 0.47$. The data are not good, anisotropic nature is clear and we think the membrane is asymptotically flat.

In order to see further the shape of the membrane, we investigate the structure factors defined by

$$S(\vec{k}) = \frac{1}{N^2} < \sum_{i,j} \exp i\vec{k} \cdot [\vec{r}_i - \vec{r}_j] > \qquad (3.3.3)$$

where i, j are the indices of the N particles on the network and $\vec{r}_i$ is the position of particles i. The angular bracket indicates the average over equilibrated configurations. In Figs.8, we show the structure factors $S(k\vec{e}_1) = S_1(k), S(k\vec{e}_2) = S_2(k)$ and $S(k\vec{e}_3) = S_3(k)$, plotted as a function of the variable kL^ν for $271 \leq N \leq 547$ and $b = 1.7$. The Structure factor $S(1)$ and $S(2)$ are scaling functions of kL and it means that the membrane is flat. From the behavior of $S(3)$ the roughness exponent $\nu_\perp = 0.55$. Figs.9 depicts the structure factors $S(1), S(2)$ and $S(3)$ for the membrane with $b = 3.0$. From these figures, the exponent $\nu = 0.85$.
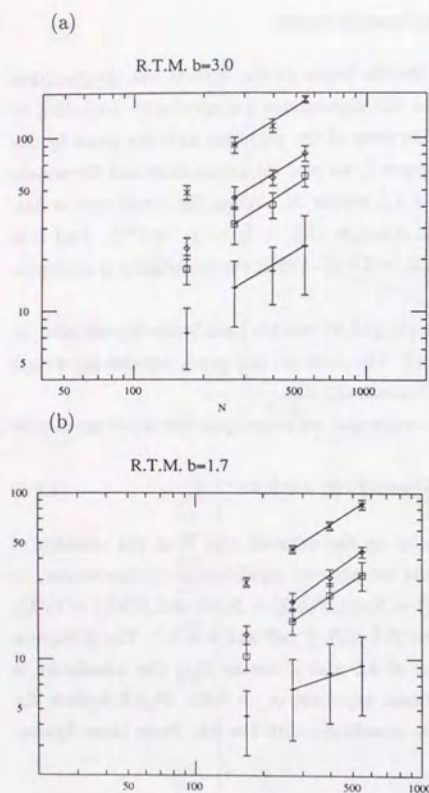
(a)

R.T.M. b=3.0

(b)

R.T.M. b=1.7

Figure 7. Scaling plot of the mean square
radius of gyration $< R_G^2 > (\times)$ and expec-
tation values $< \lambda_1 > (\diamond), < \lambda_2 > (\square), <
\lambda_3 > (+)$ of the eigenvalues of the moment
of inertia tensor for R.T.M. with $(b) = (3.0)$
(a) and $(b) = (1.7)$ (b). (a) The solid lines
have slopes 0.82,0.82,0.85, 0.80 from top to
bottom. (b) 0.90,1.0,0.91,0.47.

(a)

S(1) with R.T.M. with b=1.7

(b)

S(2) with R.T.M. with b=1.7 nu=1.0

(c)
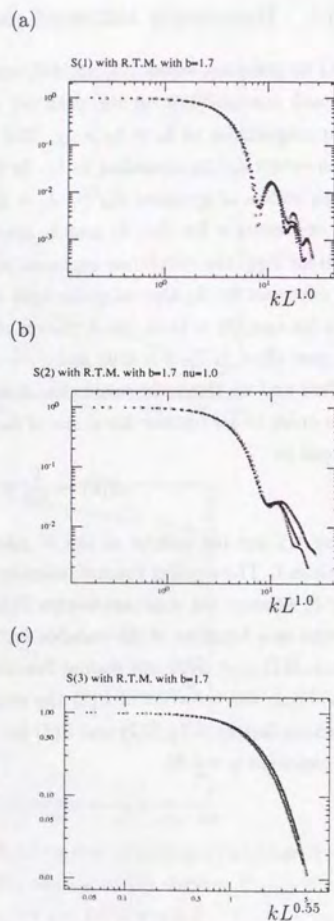
S(3) with R.T.M. with b=1.7

Figure 8.(a) The structure factor $S_1(kL^{1.0})$
for $N = 271(\times), 397(\diamond)$ and $547(\square)$. R.T.M.with
$b = 1.7$.

(b) The structure factor $S_2(kL^{1.0})$.

(c) The "perpendicular" structure factor
$S_3(kL^{0.55})$.

(a)

S(1) with R.T.M. with b=3.0

(b)

S(2) with R.T.M. with b=3.0 nu=0.85

(c)
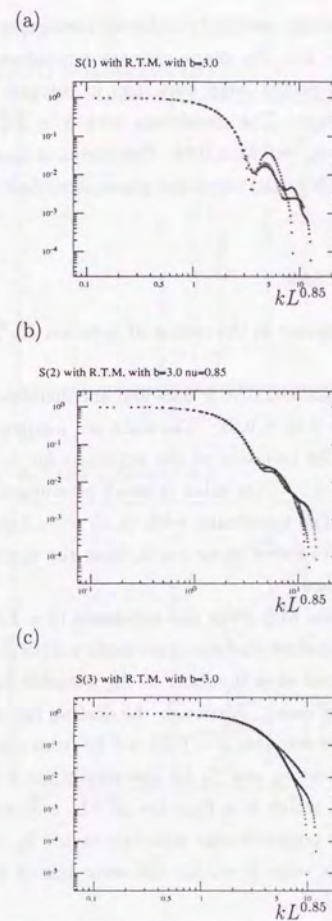
S(3) with R.T.M. with b=3.0

Figure 9.(a) The structure factor $S_1(kL^{0.85})$.R.T.M.with
$b = 3.0$.

(b) The structure factor $S_2(kL^{0.85})$.

(c) The "perpendicular" structure factor
$S_3(kL^{0.85})$.

In summary, we have found that the self-avoiding randomly tethered membrane is crumpled with exponent $\nu = 0.84 \pm 0.01 (R_G \sim L^\nu$). Its shape changes dramatically and becomes highly crumpled. In addition there occurs large bucklings in contrast to the previous results in the strong self-avoiding case. The membrane with $b = 1.7$ is asymptotically flat and the roughness exponent is $\nu_\perp = 0.51 \pm 0.04$. The shrink is small. From these behavior, the membrane with $b = 1.7$ is in the usual flat phase described by AL fixed point.

3.3.2 Random bond length model case

In Figures 10, we plot the eigenvalues and the square of the radius of gyration $R_G{}^2 (= \lambda_1 + \lambda_2 + \lambda_3)$ versus N.

In the case $(b, v) = (3.0, 0.75)$, the exponent ν is about 0.90 ± 0.04 and the membrane is crumpled. In the case $(b, v) = (3.0, 0.52)$, $\nu = 0.98 \pm 0.07$. The data are not good, we think the membrane is asymptotically flat. The behavior of the exponent for λ_3 is singular and the roughness exponent $\nu_\perp = 0.3 \pm 0.1$. This value is small as compared with the tethered membrane without disorders. The membrane with $(b, v) = (1.7, 0.3)$ behaves as $\nu = 0.95 \pm 0.01$. The exponent $\nu \sim 0.95$ seems to be small, from the spatial conformation (Fig.4a) we think the membrane is flat.

In order to see further the shape of the membrane with weak self-avoidance $(b = 3.0)$, we investigate the structure factors. In Figs.11, we show the structure factors $S(k\vec{e}_1) = S_1(k), S(k\vec{e}_2) = S_2(k)$ and $S(k\vec{e}_3) = S_3(k)$, plotted as a function of the variable kL^ν for $271 \leq N \leq 547$ and $v = 0.75$(Strong disorder case). Although the scaling for the "perpendicular" structure factor S_3 is not good, we estimate $\nu = 0.90 \sim 0.85$ from other structure factors. Figs.12 depict the structure factors S_1 and S_3 for the membrane with $(b, v) = (3.0, 0.52)$. The scaling behavior for S_1, which is a function of kL, indicates that the membrane is flat. From the scaling of the perpendicular structure factor S_3, we estimate the roughness exponent $\nu_\perp = 0.21$. This value is within the error bar of the previous estimate from the scaling λ_3 and is reliable [3].

---

[3]The behavior of structure factors for the membrane with $(b, v) = (1.7, 0.3)$ are not good. The reason is not clear and our conclusion that the membrane is flat is only from the spatial conformation (Fig.4a) and that the shrink is small(Fig.6b)

(a)

Rg and Li for (b,v)=(3.0,0.75)

(c)

(b,v)=(1.7,0.3)

(b)

Rg Li for (b,v)=(3.0,0.52)
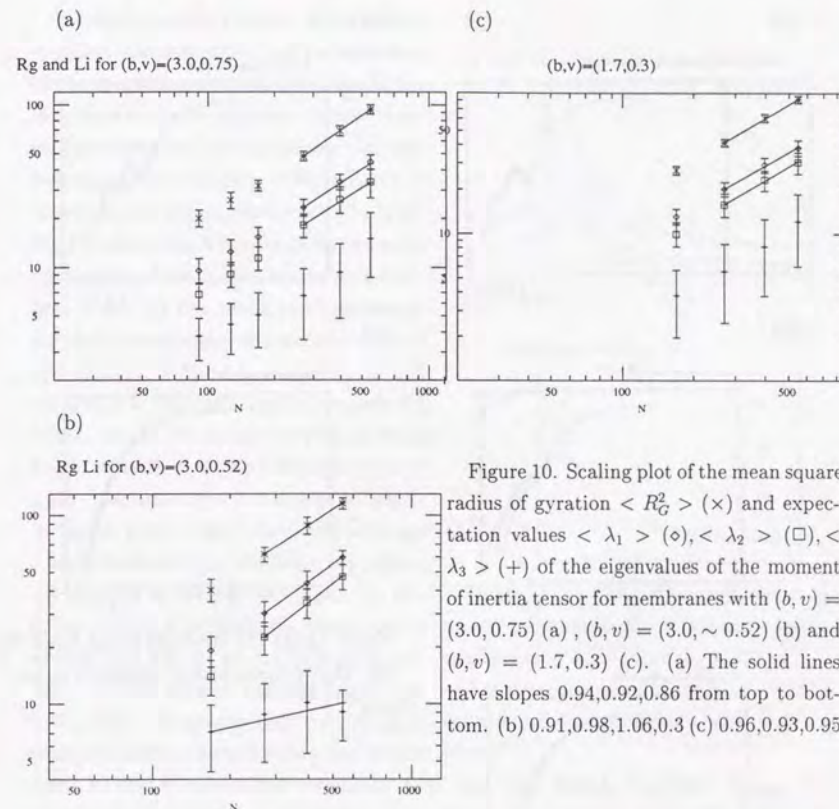
Figure 10. Scaling plot of the mean square radius of gyration $< R_G^2 >$ ($\times$) and expectation values $< \lambda_1 >$ ($\diamond$), $< \lambda_2 >$ ($\square$), $< \lambda_3 >$ ($+$) of the eigenvalues of the moment of inertia tensor for membranes with $(b, v) = (3.0, 0.75)$ (a) , $(b, v) = (3.0, \sim 0.52)$ (b) and $(b, v) = (1.7, 0.3)$ (c). (a) The solid lines have slopes $0.94, 0.92, 0.86$ from top to bottom. (b) $0.91, 0.98, 1.06, 0.3$ (c) $0.96, 0.93, 0.95$.

(a)   (a)

S(1) with (b,v)=(3.0,0.75) 271<N<547   S1 with (b,v)=(3.0,0.53)

$kL^{0.90}$ $kL^{1.0}$

(b)   (b)

S(2) with (b,v)=(3.0,0.75)   S3 with (b,v)=(3.0,0.53)

$kL^{0.85}$ $kL^{0.21}$

(c)   Figure 12.(a) The structure factor $S_1(qL^{1.0})$.
                                       (b) The "perpendicular" structure factor
S(3) with (b,v)=(3.0,0.75) $S_3(qL^{0.21})$.

$kL^{0.95}$

Figure 11.(a) The structure factor $S_1(qL^{0.90})$.

(b) The structure factor $S_2(qL^{0.85})$.

(c) The "perpendicular" structure factor

$S_3(qL^{0.95})$.

In order to see the behavior of the conformational transformation and the shrinkage of the membrane with weak self-avoidance caused by the random stress, we have studied the behaviors of the membrane with various strength of disorder. The strength of disorder is in the range $0.0 < v < 0.95$. Fig.13a depicts the behavior of R_G and other eigenvalues of the inertia tensor as a function of v. Fig.13b shows the corresponding shrink parameter, respectively. Even if the strength of disorder is small $v \sim 0.2$, the shrink is large and density becomes 2.5 times. That is, the membrane's shape changes much. After that, the shrink parameter and other quantities does not change so much. In figures 14, we depict the conformational transformation of the membrane as we change the strength of disorder v. When the disorder is weak $v = 0.05$, the membrane is smooth and we can see its anisotropic nature. As the disorder becomes large, $v = 0.30 \sim 0.50$, the membrane's conformation changes dramatically and we see large shrink, which is induced by buckling transitions. And the membrane with strong disorder $v = 0.95$ seems to be crumpled and takes isotropic conformation.

(a)

Rg^2 and Li with b=3.0 and (v=0.0 to 0.95)

(b)

Shrink Parameter vs v=0.0 to 0.95

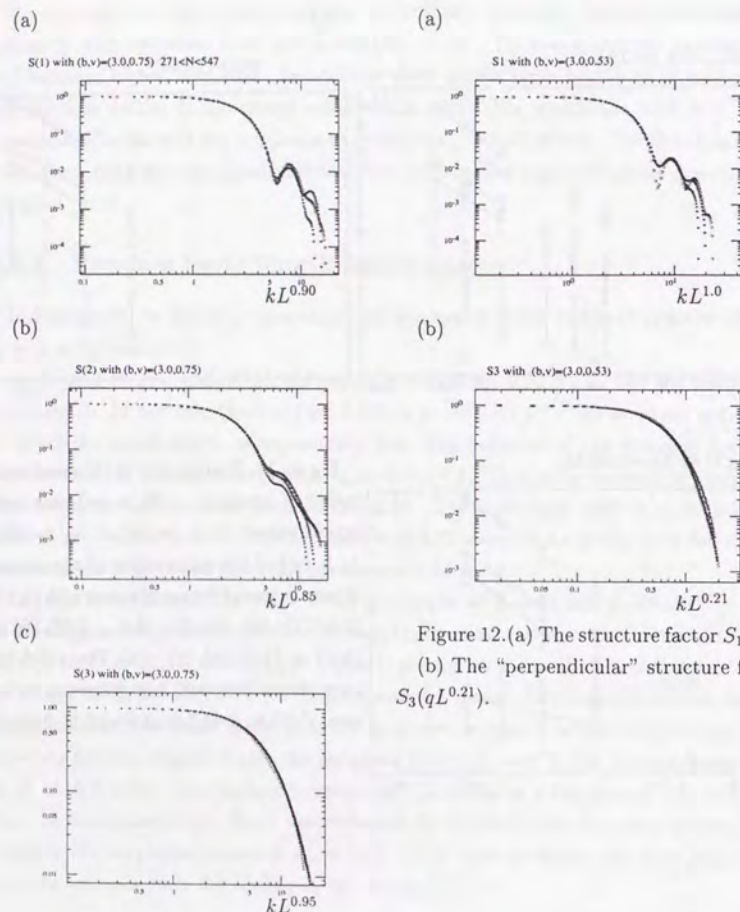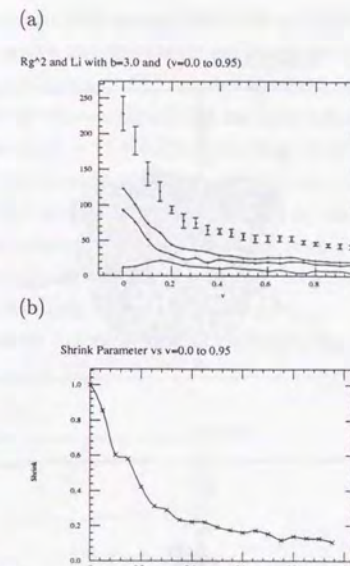Figure 13 (a) Plot of the mean square radius of gyration $< R_G^2 >$ ($\times$) and expectation values $< \lambda_1 >$ ($\diamond$), $< \lambda_2 >$ ($\square$), $< \lambda_3 >$ (+) of the eigenvalues of the moment of inertia tensor for membranes with $(b, N) = (3.0, 271)$

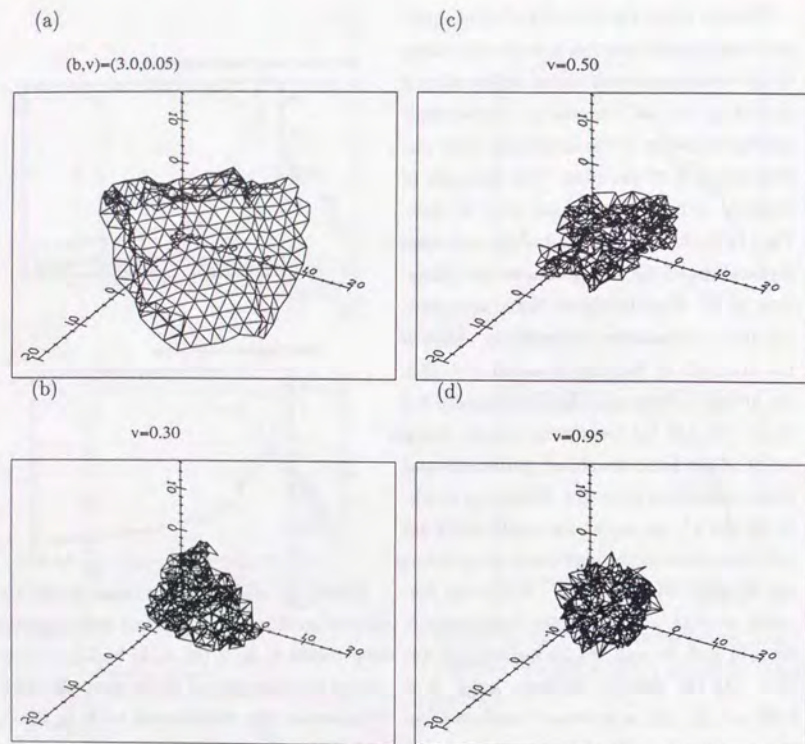(b) The Shrink Parameter P_{shrink} as a function of strength of disorder v. $N = 271$ and $b = 3.0$.

(a)

(b,v)=(3.0,0.05)

(b)

v=0.30

(c)

v=0.50

(d)

v=0.95

Figure 14. Typical spatial conformation of the two-dimensional membrane with weak self-avoidance $(b = 3.0)$ and (a)$v = 0.05$, (b)$v = 0.3$, (c)$v = 0.50$ in flat, and (d)$v = 0.95$ in crumpled.

Secondly, we study the cooling of the membrane with strong self-avoidance and weak disorder $(b, v) = (1.7, 0.3)$. If the bending rigidity and the elastic constants change as we decrease the temperature T, the buckling condition (2.1.1) may be satisfied. At the temperature $T = 1$, the membrane is flat from the above analysis. On the other hand, the membrane with the same strength of disorder $(b, v) = (3.0, 0.52)$ shows large shrink. If buckling transition occurs as T decreases, the membrane with $(b, v) = (1.7, 0.3)$ also shows large shrink. The temperature dependence of the spatial conformations of the membranes are depicted in Figure 15. As the temperature decrease, at $T \sim 0.3$, some peak occurs in λ_3, however overall the membrane becomes flatter and flatter. We see no apparent evidence of foldings or large buckling, which was seen in the phantom case near $T = 0$ [47]. We have also obtained other thermodynamic functions such as internal energy and specific heat. We do not find any singurality in the data.
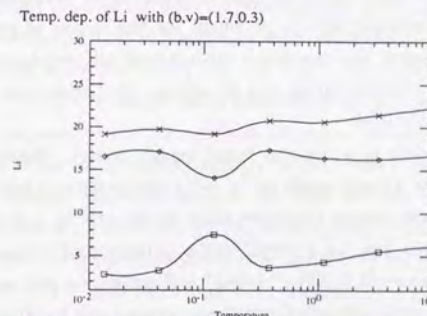
Temp. dep. of Li with (b,v)=(1.7,0.3)

Figure 15. Temperature dependence of the three (ordered) eigenvalues $\lambda_1 > \lambda_2 > \lambda_3$ of the inertia tensor of the membrane with $(b, v) = (1.7, 0.3)$ and $N = 271$.

We can interpret this result as follows. Even if the temperature decreases, the bending rigidity does not become enoughly small and the buckling condition is not satisfied. This means that the "entropic" bending rigidity in the flat phase, contributes as a remnant one to the total bending rigidity and it does not depend on the temperature. This explanation seems to contradict with the picture that the induced "entropic" rigidity is proportional to temperature and we cannot give any clear answer [10]. If the above interpretation is not right, we can propose two other possibilities. One is that the large shrink is an atrifact of the model and if the self-intersection is completely prohibited, such behavior including large buckling transition cannot occur. The second possibility is the difference in the local

flexibility of the membrane. That is, the large shrink or buckling transition occurs only if the membrane is very flexible case. Otherwise, even if the bending rigidity becomes small enough, buckling transition cannot occur and large shrink does not apppear. However, within our study we cannot determine which one is true.

3.4 Discussions and Concluding Remarks

In this chapter, we have performed simulations of the self-avoiding tethered membrane model with quenched disorders. As a model for randomly polymerized membrane we have studied two types.

[1] The first model is a randomly tethered membrane model. The membrane with weak self-avoidance $b = 3.0$ shows large shrink and takes highly crumpled conformation. The asymptotic form ts isotropic anf the exponent for the radius of gyration is $\nu = 0.84 \pm 0.01$. On the other hand, the membrane with strong self-avoidance does not show any large conformational transformation and its anisotropic behavior is clear. The roughness exponent is $\nu_\perp = 0.51 \pm 0.04$.

[2] The second model is a random bond length model. Introducing two kinds of monomers (big $(p_i = 1)$ and small $(p_i = -1)$) ,the reference length between i-th and j-th monomers b_{ij} varies among monomer pairs by the rule $b_{ij} = b + (p_i + p_j)v$. We have studies the model with $b = 3.0$ ("weak" self-avoidance and various strengths of disorder)(1) and with $(b, v) = (1.7, 0.3)$ ("strong" self-avoidance and weak disorder)(2). (1) For membranes with weak self-avoidance there occurs large buckling transitions and the membrane shows large shrinkage. The relative density with the $v = 0.0$ case becomes $8 \sim 9$ times even if the strength of disorder is small $v \sim 0.52$ (Fig.6). When the disorder is small ($v \sim 0.52$), the membrane is asymptotically flat and the roughness exponent is small ($\nu_\perp = 0.30 \pm 0.10$). About the membrane with strong disorder ($v = 0.75$), it is crumpled with the exponent for the radius of gyration $\nu = 0.90 \pm 0.04$. Theoretical prediction is $\nu = 6/7$ [42], however more large system size is necessary in order to estimate the exponent and to determine whether these results are cross-over effect or not. We also note that these findings may arise from that the model does not completely forbid the self-intersection. That is, if the self-intersection is completely prohibited, such behaviors may not occur. However, even if the self-intersection is completely forbidden, highly crumpled and floppy conformation is possible in self-avoiding plaquette membrane model [20, 21]. We think that large shrinkage can occur in complete self-avoiding tethered membrane when the bending rigidity is small. (2) A membrane with strong self-avoidance and weak disorder $(b, v) = (1.7, 0.3)$ is asymptotically flat and its shrinkage is small. On

the other hand the membrane with the same strength of disorder and weak self-avoidance $(b, v) = (3.0, 0.52)$ shows large shrink. One possible reason for the difference is that the former one has large bending rigidity than the latter one. The condition (2.1.1) is not satisfied and buckling transition does not occur in the strong self-avoidance case. In oreder to see whether there occurs some large conformational transformation by thermal bucklings transition, we have performed the cooling of the membrane. The membrane becomes flatter and flatter as the temperature decreases and we find no folding or large buckling between the temperature about $0.01 < T < 10.0$. This means that the bending rigidity cannot be so small even if the temperature is very low. That is, as the "entropic" rigidity contribution to the total bending rigidity of the membrane does not depend on the temperature and the buckling condition is not satisfied even if the temperature becomes small.

From these results, we propose the possibility of thermal conformational transformation of the "weak" self-avoiding tethered membrane with quenched disorder. Introducing the "bare" bending energy κ in the model, we can make the membrane smooth and flat again. Then we may be able to see the large buckling of the membrane by decreasing the temperature [29]. Because, as the temperature decreases the effective rigidity becomes smaller and smaller. If the total bending rigidity, which is the sum of the "entoropic" one and the thermally induced one which include the bare bending rigidity, becomes small enough and the constant K_0 becomes large, the buckling condition (2.1.1) is satisfied and there occurs bucklings. Such transformation is possible only for the weak self-avoidance case, otherwise remnant entropic rigidity prevent the condition (2.1.1) to be satisfied in the strong self-avoidance case. This possibility may be relevant to the understanding of the wrinkling transition in partially polymerized vesicles [32].

We also propose the following possibility which may correspond to the wrinkling transition [28]. In the experiment, the partial polymerization at high temperature presumably results in sparse but percolating network of covalent bonds and the flat shape is stable. As the temperature decreases, crystalline order sets in within these lipid area and quenched random stress will appear. This process corresponds to the increase in v in our model and large transformation occurs and wrinkled structure appears. That is, the wrinkling transition may be a mechanical buckling transition which we found in this work.

Chapter 4

Phase Transitions of Polymerized Membrane with Attractive Interactions

4.1 Genesis

Recently there has been considerable interest in the phase transition of polymerized (tethered) membranes [1] with attractive interactions [10, 52, 53, 9]. In a pioneer work [10], Abraham and Nelson found by molecular dynamics simulations that the introduction of attractive interactions between monomers leads to a collapsed membrane with fractal dimension 3 at sufficiently low temperature. Subsequently, Abraham and Kardar [52] showed that for open membranes with attractive interactions, as temperature decreases, there exists a well defined sequence of folding transitions and then the membrane ends up in the collapsed phase. They also presented a Landau theory of the transition and in addition, they discussed that the folding transition is related to the unbinding transition of bimembranes. Liu and Plischke [53] carried out Monte Carlo simulations for a similar model and found that the membrane undergoes a phase transition from the high temperature flat phase to the low temperature collapsed phase passing through an intermediate crumpled phase. The intermediate crumpled phase exists over a certain range of temperature and its fractal dimension is estimated as $d_f = 2.5$. Following this work, Grest and Petsche [9] extensively carried out molecular dynamics simulations of closed membranes. They considered flexible membranes; the nodes of the membrane are connected by a linear chain of n monomers. For short monomer chains, $n = 4$, there occurs a first order transition from the high temperatures flat phase to the low temperature collapsed phase, but no intermediate crumpled phase. For longer chains, $n = 8$, the transition is either continuous or weakly first order. With the assumption of the continuous transition, the fractal di-

mension of the membrane at the transition is estimated as $d_f = 2.4$. Mori and Wadati [54] discussed the phase transition of $D-$dimensional (phantom) polymerized membrane with long-range attractive interaction (r^γ) and showed that there are several types of phase transition from a flat phase to a compact phase depending on the type of the interaction (γ) and the dimension of the membrane (D). Especially, when the interaction is short-ranged, the transition is continuous. Based on this result, they discussed the possibility of the complete cancellation between the "entropic" rigidity from self-avoidance [10] and the negative rigidity from attractive interaction which causes the crumpling transition of the membrane. This cancellation does only occur when the membrane is very flexible case. Otherwise, the flat phase becomes unstable before the cancellation becomes complete and the membrane shows the sequential folding transition. About the sequential folding transition, Mori and Kajinaga [55] have presented a simple model, a square lattice model with attractive interactions, and has succeeded in constructing a model which describe the transition.

In this chapter, we review theoretical approaches to the phase transitions of polymerized membranes with attractive interactions. The balance of this chapter is as follows. In Sec.4.2, we review the Landau theory for the phase transitions of polymerized membranes with attractive interactions. Sec.4.3 is devoted to a theory for $(D-$dimensional$)$ polymerized membrane with attractive long-range $(r^{-\gamma})$ interactions. Using the large-d limit, we solve the model and discuss the possible phases and phase transitions in the (γ, D) plane. When the interaction is short-ranged, the membrane shows a continuous transition from the flat phase to the compact phase passing through a crumpled phase. Based on the result, we propose a theoretical interpretation about the above numerical results. In particular, we emphasize on the cancellation between the "entropic" bending rigidity from self-avoiding interaction and the negative bending rigidity from attractive interactions. We define the square lattice model with bending rigidity (u) and interactions (ω) in Sec.4.4. We consider two types of interaction; the first one is a potential which is proportional to the contact area of the lattice (CA type) and the second one is proportional to the number of pairs of elementary squares which occupy the same place in the plane (CP type). We analyze these models theoretically and we obtain the phase diagrams in the (u, ω) plane for each potential. In particular, for the CA type interaction, we find a partially folded state in the region $(u > 0, \omega < 0)$. Numerical studies for the model with the CA type interaction shows a sequential folding transition of the lattice. In Sec.4.5, we conclude with remarks on the viewpoint of the cancellation between the "entropic" bending rigidity and the negative bending rigidity.

4.2 Landau Theory for Attractive Polymerized Membrane

Here we will explain the Landau theory for tethered membranes with attractive interactions [52]. An effective free energy is constructed for $\vec{X}(\sigma)$, which is a coarse-grain version of the coordinate $\vec{X}(m,n)$ of the monomers in the network. On the basis of symmetry consideration, the lowest order terms in a gradient-density expansion for the Hamiltonian $\beta\mathcal{H}$ are

$$
\begin{aligned}
\beta\mathcal{H}[\vec{X}(\sigma)] &= \int d^2\sigma[\frac{t}{2}\partial_i\vec{X}\cdot\partial_i\vec{X} + u(\partial_i\vec{X}\cdot\partial_j\vec{X})(\partial_i\vec{X}\cdot\partial_j\vec{X}) \\
&+ v(\partial_i\vec{X}\cdot\partial_i\vec{X})(\partial_j\vec{X}\cdot\partial_j\vec{X}) + \frac{\kappa}{2}\triangle\vec{X}\cdot\triangle\vec{X}] \\
&+ \frac{b}{2}\int d^2\sigma\int d^2\sigma'\delta^3[\vec{X}(\sigma)-\vec{X}(\sigma')] \\
&+ \frac{c}{6}\int d^2\sigma\int d^2\sigma'\int d^2\sigma''\delta^3[\vec{X}(\sigma)-\vec{X}(\sigma')]\delta^3[\vec{X}(\sigma')-\vec{X}(\sigma'')].
\end{aligned}
$$
$$(4.2.1)$$

The parameters t, u, v, κ, b, c depend on temperature and the microscopic potential. The local term represents the nonlinear elasticity of the membrane and the non-local terms are due to long-range interactions, such as self-avoidance. If we ignore thermal fluctuations, we can evaluate the free energy $\mathcal{F}$ at mean field level in terms of a uniform density $n(\sim L^2/R^3)$ and tangent vector $\vec{m}$. Here L is the linear size and R is the radius of gyration. The free energy is evaluated as,

$$\beta\mathcal{F}/L^2 = \min[(\frac{t}{2}m^2 + 2(u+2v)m^4) + (\frac{b}{2}n + cn^2)]_{m,n}. \tag{4.2.2}$$

The signs of the lowest order term (that is, t and b) determine the phase of the membrane and there are four phases (flat, crumpled, compact, folded) corresponding to the signs of the parameters b, t (Fig.1).

In the first quadrant ($t > 0, b > 0$), the membrane is in the crumpled phase and $R \sim L^{4/5}$. In the fourth quadrant ($t < 0, b > 0$), the membrane is flat ($m \neq 0$). In the region ($t > 0, b < 0$), the order parameter m is 0 and the density n becomes finite ($L^2/R^3 \sim n$). The membrane is in the compact phase ($R \sim L^{2/3}$). In the third quadrant ($t < 0, b < 0$), both m and n tend to be nonzero. Physical meaning of the phase is not so clear, it seems to correspond to a folded structure, because this phase can be obtained by regularly folding the flat membrane into a compact structure. Based on this results, Abraham and Kardar think that as the temperature decreases the membrane proceeds along the trajectory indicated in Fig.1 and it corresponds to the sequential folding transition. In

the following sections, we study several models of attractive polymerized membranes and their relations with the Landau model.
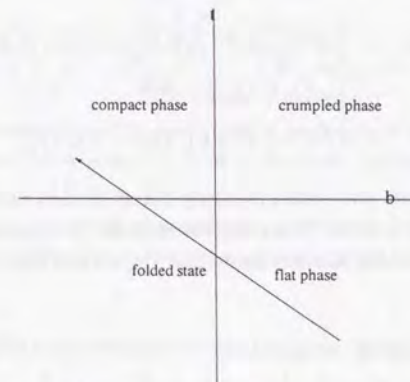

Figure 1. Phase diagram of the Landau theory. The arrow on the line indicate the possible trajectory which corresponds to the sequential folding transition.

4.3 Polymerized Membrane with Long-range Attractive Interactions

In this section, we study the phase transition of phantom polymerized membrane with attractive interactions. This model can be solved exactly using the large-d limit and we can discuss their phase transitions.

4.3.1 Polymerized membrane with attractive interactions

We prepare some notations. The position of the D-dimensional membrane in a d-dimensional space is described by d bulk coordinates $X^i(\sigma^\alpha)(i = 1,\cdots,d)$, where $\sigma^\alpha(\alpha = 1,\cdots,D)$ are the internal manifold coordinates. We denote the bending rigidity of the membrane by κ and the elastic Lamé coefficients by μ and λ. The interaction between

different positions, which is rotationally-invariant, is represented by V. We take

$$V(r^2) = u/(r^2)^{\frac{\gamma}{2}}, \tag{4.3.1}$$

where r is the distance, and u and γ are some constants. The Hamiltonian of the tethered membrane with long-range interaction is given by

$$
\begin{aligned}
\mathcal{H}[\vec{X}(\sigma)] &= \int d^D\sigma [\frac{d}{2}\kappa\triangle\vec{X}\cdot\triangle\vec{X} + \frac{1}{4}\mu d\{\partial_\alpha\vec{X}\cdot\partial_\beta\vec{X} - \delta_{\alpha\beta}\}^2 \\
&+ \frac{1}{8}\lambda d\{\partial_\alpha\vec{X}\cdot\partial_\alpha\vec{X} - D\}^2] \\
&+ d\int d^D\sigma \int d^D\sigma' V((\vec{X}(\sigma) - \vec{X}(\sigma'))^2).
\end{aligned} \tag{4.3.2}
$$

The first term represents the bending elasticity, the second and third terms the stretching elasticity and the last term the long-range interactions. To investigate the large-d limit, it is useful to introduce the auxiliary fields $\chi_{\alpha\beta}$, $A(\sigma,\sigma')$ and $B(\sigma,\sigma')$[22, 24] and rewrite the Hamiltonian as

$$
\begin{aligned}
&\mathcal{H}[\vec{X}, \chi_{\alpha\beta}, A, B] \\
&= \int d^D\sigma [\frac{d}{2}\kappa\triangle\vec{X}\cdot\triangle\vec{X} + \frac{1}{2}\chi_{\alpha\beta}(\partial_\alpha\vec{X}\cdot\partial_\beta\vec{X} - \delta_{\alpha\beta}) - \frac{1}{2}\rho(\chi_{\alpha\beta})^2 - \frac{1}{2}\eta(\chi_{\alpha\alpha})^2] \\
&-d\int d^D\sigma \int d^D\sigma'(\frac{1}{4}([\vec{X}(\sigma) - \vec{X}(\sigma')]^2 - A(\sigma,\sigma'))B(\sigma,\sigma') - V(A(\sigma,\sigma')),
\end{aligned} \tag{4.3.3}
$$

where $\rho = 1/2\mu$ and $\eta = -\lambda/(2\mu(2\mu + d\lambda))$. We define the flatness order parameter ζ; for the flat phase $\vec{X}(\sigma) = \zeta\sigma^\alpha\vec{e}_\alpha$. We assume that $\chi_{\alpha\beta} = \chi\delta_{\alpha\beta}$, $A(\sigma,\sigma') = A(\sigma-\sigma')$, $B(\sigma,\sigma') = B(\sigma - \sigma')$ because of isotropy and translational invariance.

Now we can derive the following set of saddle point equations [24],

$$K(k) \equiv \kappa k^4 + \chi k^2 + 4\gamma u \int d^D\sigma [1 - \cos(\vec{k}\cdot\vec{\sigma})](\frac{1}{A(\sigma)})^{1+\gamma/2}, \tag{4.3.4}$$

$$A(\sigma) = \zeta^2\sigma^2 + 2\int \frac{d^D k}{(2\pi)^D}[1 - \cos(\vec{k}\cdot\vec{\sigma})]\frac{1}{K(k)}, \tag{4.3.5}$$

$$\zeta^2 = 1 + 2\chi(\rho + \eta D) - \frac{1}{2D}\int \frac{d^D k}{(2\pi)^D}\frac{k^2}{K(k)}, \tag{4.3.6}$$

$$\zeta = 0 \quad \text{and/or} \quad \partial K(q)/\partial q^2 = 0. \tag{4.3.7}$$

Equation (4.3.7) indicates that the solution with the broken symmetry ($\zeta > 0$) is possible only if the coefficient of the k^2 term in $K(k)$ is 0. These saddle point equations have been analyzed in the repulsive force case ($u > 0$) [22, 24]. We also recall that, in the phantom

case, that is $V(r^2) = 0$, eqs.(4.3.6) and (4.3.7) survive and flat phase ($\zeta > 0$) exists only for $D > 2$ [22]. By a formal expansion of eq.(4.3.4) in powers of k, we obtain

$$K(k) = \tau_{eff}k^2 + \kappa_{eff}k^4, \quad \text{for small } k, \tag{4.3.8}$$

where the effective surface tension τ_{eff} and the effective rigidity κ_{eff} are given by

$$\tau_{eff} = \chi - \frac{\gamma u}{D}\int d^D\sigma\sigma^2[A(\sigma)]^{-1-\frac{\gamma}{2}}, \tag{4.3.9}$$

$$\kappa_{eff} = \kappa + \frac{\gamma u}{4(D^2 + 2D)}\int d^D\sigma\sigma^4[A(\sigma)]^{-1-\frac{\gamma}{2}}. \tag{4.3.10}$$

We find that in the attractive force case $u < 0$, a correction to the rigidity is negative, while in the repulsive force case $u > 0$, it is positive. And in the flat phase, from eqs.(4.3.7),(4.3.8) and (4.3.9), $\chi = \frac{\gamma u}{D}\int d^D\sigma(A(\sigma))^{-1-\frac{\gamma}{2}}$. Depending on the sign of u, we see from eq.(4.3.6) there is a positive or negative contribution to the order parameter ζ^2. Hereafter, we shall consider these saddle point equations in the attractive interaction case $u < 0$.

4.3.2 Large distance behavior and phase transitions

First, we consider the crumpled phase. In the phantom case, it is known that the behavior of the membrane is governed by $\tau_{eff}k^2$ and two-point function $A(\sigma)$ behaves as

$$A(\sigma) \sim \frac{1}{\tau_{eff}}\sigma^{(2-D)} \quad \text{for} \quad D < 2, \tag{4.3.11}$$

$$A(\sigma) \sim \frac{1}{\tau_{eff}} \quad \text{for} \quad D > 2. \tag{4.3.12}$$

Let the interaction be switched on ($u < 0$). Equation (4.3.9) shows that τ_{eff} diverges positively in the region $D > \frac{\gamma}{2+\gamma/2}$ and the membrane shrinks to a point. In actual membranes, there is a three-body interaction that forbids the membrane to shrink to a point [50] and such collapsed phase should be interpreted as the compact phase. However, in the discussion of the flat phase and its instability, the three-body interaction is irrelevant and we may neglect it.

Second, we consider the flat phase and its instability caused by the attractive interaction. In this case, the most important relation is eq.(4.3.10). By inserting the large distance behavior of the two-point function $A(\sigma) \sim \zeta^2\vec{\sigma}^2$, we observe that the second term, the contribution from the interaction, diverges when $\gamma - D < 2$. That is, in the region, the flat phase becomes unstable by even a weak attractive interaction. In the region $D > 2$ and $\gamma - D > 2$, the flat phase exists and remains stable when the interaction is very weak. Then, it is interesting to ask the following question : what will happen in

this coexistence region between the flat phase and the compact phase when we increase the magnitude of u. From eqs.(4.3.7) and (4.3.8), we have $K(k) \sim \kappa_{eff} k^4$. Rewriting ζ^2 by $B(u)$, we have the large distance behaviors of the two-point function as

$$A(\sigma) \sim B(u)\sigma^2 + C\sigma^{4-D} \quad \text{for} \quad D < 4, \quad (4.3.13)$$

$$A(\sigma) \sim B(u)\sigma^2 + C \quad \text{for} \quad D > 4. \quad (4.3.14)$$

The former one ($D < 4$) corresponds to the usual flat phase and the latter ($D > 4$) to the super flat phase [22]. Let us discuss the behavior of $B(u)$ when the parameter u changes. We suppose that $B(u)$ vanishes continuously at $u = u_c$. Then by inserting the above infrared behavior of $A(\sigma)$ into eq.(4.3.10), we know that the second term diverges in the region $\gamma < \frac{D}{1-D/4}$ at $u = u_c$ and is convergent in the region $\gamma > \frac{D}{1-D/4}$ at $u = u_c$. This means that in the region ($\gamma < \frac{D}{1-D/4}$), the transition from the flat phase to the compact phase cannot be continuous. In order to see the situation more clearly, we introduce the following "toy" model for the order parameter $B(u)$,

$$B(u) = 1 - C_1 \frac{1}{\kappa_{eff}(u)}, \quad (4.3.15)$$

$$\kappa_{eff}(u) = \kappa + uC_2 B(u)^{-\delta}. \quad (4.3.16)$$

Here, we have considered the infinite elastic constant limit in the original saddle point equations and introduced some constants C_1, C_2 and δ. These equations are used to determine self-consistently the order parameter. The behavior of $B(u)$ is schematically drawn in Fig.2.
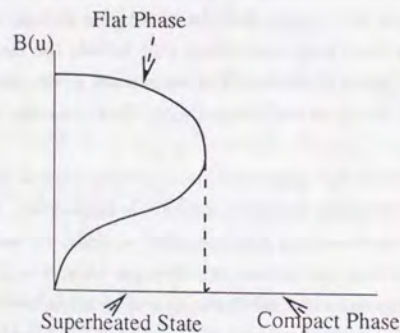

Figure 2. Behavior of the order parameter in the (B, u) plane. B is the square of the

order parameter ζ and u is the strength of attractive interaction.

From this, we find that there exists a first-order transition from the flat phase to the compact phase at a certain value u_c. The transition from the compact phase to the flat phase requires a further investigation, but it seems that there is a "superheated" compact phase. Phase diagram in terms of γ and D is summarized in Fig.3. Recall that γ signifies the decaying power of the interaction and D is the dimension of the membrane. From these analysis, it is clear that, if the attractive interaction is finite-ranged, then the membrane exhibits a continuous crumpling transition from the flat phase to the compact phase and there exists a critical crumpled state at the transition point.
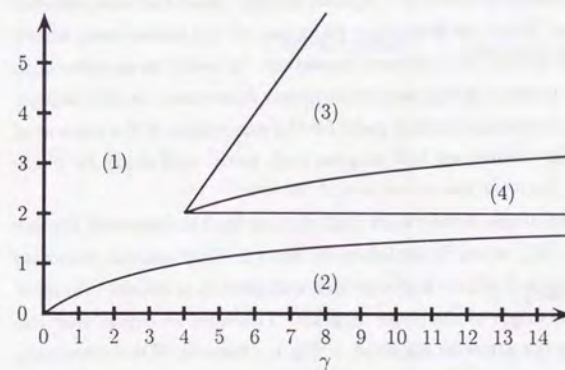
Phase Diagram

Figure 3. Phase diagram in the (γ, D) plane: (1) compact state; (2) crumpled state; (3) flat state + compact state; (4) flat state + critical state + compact state.

4.3.3 Discussions

In what follows, we discuss the implication of the above analysis, in particular to the numerical studies and the Landau model. Our analysis deals mainly with the instability of the flat phase of the phantom membrane caused by the attractive interaction. On the other hand, numerical simulations treat the self-avoiding tethered membranes with short-range attractive interaction. The self-avoidance induces the entropic rigidity [10] and because of its effect, the membrane is in the flat phase. When the membrane is in the flat phase, it is widely believed that the self-avoidance is irrelevant and can be ignored. In other words, the bare rigidity κ in the Hamiltonian (eq.(4.3.2)) include the effect of the self-avoidance and this contribution does not depend so much on the temperature. Therefore, the analysis in the present paper corresponds to the numerical simulations before the phase transition to the collapsed phase occurs. This transition is a continuous crumpling transition and there exists a critical crumpled state, which explains the result of the recent numerical simulation [9] that the phase transition seems to be continuous in the $n = 8$ case. However, our model treats the very flexible membrane and in the less flexible case the transition may be discontinuous. The reason is that: when the membrane is not flexible, before the cancellation becomes complete, the flat phase becomes unstable by the attractive interactions. Then the first order transition to the folded state occurs and the unbinding transition nature [52] becomes important. In order to describe such process, the folding degree of freedom of the membrane is very important. In this respect, the square lattice model is a convenient starting point for the description of the sequential folding transition. In the next section, we will propose such model and study its phase transitions.

Now, we discuss the relation of the above result with the one by Abraham and Kardar based on the Landau model [52], which is explained in Sec.4.2. Our analysis indicates that the change in the parameter b causes a change in t and there is a critical crumpled state which corresponds to the origin of the phase diagram. Therefore we expect that the phase transition occurs along the arrow as depicted in Fig.4. However, if the membrane is less flexible, the route considered by Abraham and Kardar is also possible. With these considerations, we propose the following relation between the parameters b and t.

$$b \equiv (T - T_\theta),$$
$$t = -b - t_0. \qquad (4.3.17)$$

Here, T_θ is the transition temperature and the positive constant t_0 differentiates the two cases: $t_0 = 0$ correspond to the flexible membrane (continuous transition case) and $t_0 > 0$ correspond to the less flexible membrane (first order transition case). These relations enable us to discuss the properties of the membranes' solution. The detailed analysis is

left for a future study.

Finally we make a comment on an experimental situation of our model. It is known that attractive forces (short-range or long-range) appear when a system of polymers is in a critical fluid [57]. The conformation of the polymers change drastically due to these forces. If we consider the same situation for the polymerized membrane we can imagine two possibilities. First, the phase transition of the membrane occurs when the surrounding fluid is far from critical point. In this case, the attractive force is short-ranged and phase transition may be smooth. Second, if the phase transition occurs when the fluid is near the critical region, the transition is discontinuous because the attractive force is long-ranged. Then the correlation length of the fluid exceeds the size of the membrane, the membrane expands to the original flat shape. We think that this situation should be also interesting for numerical studies.
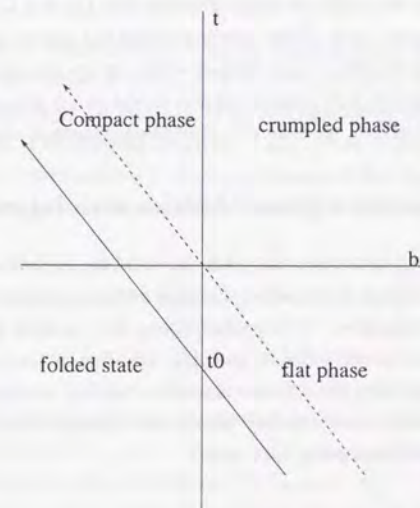

Figure 4. Phase diagram of the Landau theory and the possible trajectories; the arrow ($t_0 = 0$) indicates the continuous crumpling transition proposed in this section; the line ($t_0 > 0$) is suggested by Abraham and Kardar.

4.4 Square Lattice with Attractive Interactions

This section is devoted to a simple model which describes the sequential folding transition of the polymerized membrane with attractive interaction. In order to describe the transition of the membrane, the folding degrees of freedom of the membrane are important. Square lattice model was at first introduced by David and Guitter [12] as a simple model for polymerized membrane. The model is a discrete rigid-bond square lattice, which is allowed to fold on itself along its bonds in a two-dimensional embedding space. By changing the bending rigidity u, it shows a first order transition from a completely flat phase ($u > 0$) to a completely folded state ($u < 0$) [12, 59]. Triangular lattice case was also studied [58, 60, 59]. Here, we would like to study a square lattice model with attractive ($\omega < 0$) or repulsive interactions ($\omega > 0$) as a simple model which describes the sequential folding transition of the tethered membrane. As an interaction between different parts of the lattice, we study two types of interaction: the first one is a potential which is proportional to contact area of the membrane and the second one is proportional to the number of pairs of the elementary squares which occupy the same place in the plane. We discuss possible phases and phase diagrams in the (u, ω) plane for each interaction. For the first type interaction, we have also performed numerical studies.

4.4.1 Model system : Square Lattice with interactions

We consider a model of foldings of a two-dimensional square lattice with $L \times L$ size. We consider all possible foldings of the lattice and each folding maintains the correct distances between the neighboring sites. Two configurations are identical if the positions of all corresponding sites (or vertex) coincide and this definition of the identical configuration does not distinguish between the different manners of folding which lead to the same final state. Figure 5a) depicts such a lattice before the folding, while figure 5b) shows the section of it in a folded state along its x-axis.
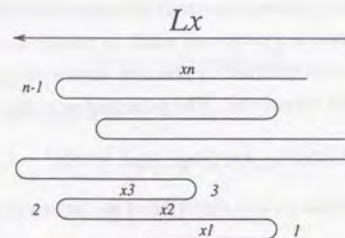
a)
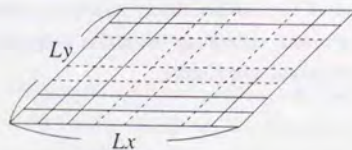
b)

Figure 5: a) Stretched form of a square lattice of size $L \times L$.

b) Typical configuration of a section of the lattice. The folds have a vanishing length. The lattice is not completely folded to clearly indicate the configuration.

The membrane has of course two such sections. The membrane is constrained to a plane and the section is represented by a line of zero thickness which folds in $N = 1, 2, \cdots, L$ segments of successive lenght $x_1, x_2, \cdots x_N$ [61]. Correspondingly, the other section, which folds in M segments, is represented by $y_1, y_2, \cdots y_M$. These segments' lenghts x_i and y_j are multiples of lattice constant $a = 1$. For convenience, in the theoretical calculation, we treat them as continuous quantities with U.V. cutoff (lattice constant $a = 1$). The total lengths are fixed:

$$\sum_{i=1}^{N} x_i = L$$
$$\sum_{j=1}^{M} y_j = L. \qquad (4.4.1)$$

A configuration of the system is thus determined by a set of natural numbers (N, M) and a set of positive numbers $x_1, x_2, \cdots, x_N; y_1, y_2, \cdots, y_M$. Let the potential energy for a configuration of the square lattice be denoted by $U_{N,M}(x_1, x_2, \cdots, x_N; y_1, y_2, \cdots, y_M)$.

The potential energy will be taken to consist of the sum of two terms. First, as a bending energy, we assign energy κ per unit length of a fold. We denote an interaction between the elementary squares of the lattice as U_I and the potential energy for the system is written as,

$$U_{N,M}(x_1, x_2, \cdots, x_N; y_1, y_2, \cdots, y_M)$$
$$= (N-1)\kappa L + (M-1)\kappa L + U_I \qquad (4.4.2)$$
$$= U'_{N,M} + U_I. \qquad (4.4.3)$$

As an interaction between different parts of the square lattice, we consider two types of interaction. The first one is a potential which is proportional to $\overline{C}$ontact $\overline{A}$rea of the lattice. The contact area is determined by the area difference between the initial stretched form and the configuration considered. The potential is written as,

$$U_{I,CA}(x_1, \cdots, x_N; y_1, \cdots, y_M) = w(L^2 - L_x L_y). \tag{4.4.4}$$

Here, L_x and L_y are the widths in each direction of the lattice (Fig. 5b) and are represented as,

$$
\begin{aligned}
L_x &= \text{Max}(x_1, x_1 - x_2 + x_3, \cdots) - \text{Min}(0, x_1 - x_2, \cdots) \\
L_y &= \text{Max}(y_1, y_1 - y_2 + y_3, \cdots) - \text{Min}(0, y_1 - y_2, \cdots).
\end{aligned} \tag{4.4.5}
$$

We also consider a potential which is proportional to the number of pairs of elementary squares that share the same place in the plane ($\overline{C}$ontact $\overline{P}$air).

$$U_{I,CP}(x_1, \cdots, x_N; y_1, \cdots, y_M) = w(\text{Number of pairs of contact elementary squares}). \tag{4.4.6}$$

In the usual discussion of polymer with attractive interaction, the second type is usually employed [50]. However, the attractive interaction of a polymer in poor solvent comes from the fact that solute-solute and solvent-solvent contacts are preferred to solute-solvent contacts. From this point of view, we think the contact area potential $U_{I,CA}$ is more natural than the contact pairs potential $U_{I,CP}$ and we will discuss the difference between these potentials in the square lattice model.

For convenience we will use the reduced bending rigidity and potential strength,

$$u = \kappa/k_B T \quad ; \quad \omega = w/k_B T. \tag{4.4.7}$$

The partition function is given as,

$$
\begin{aligned}
Z(u, \omega, L) &= \sum_{N,M=1}^{\infty} \int_a^{\infty} dx_1 \int_a^{\infty} dx_2 \cdots \int_a^{\infty} dx_N \int_a^{\infty} dy_1 \int_a^{\infty} dy_2 \cdots \int_a^{\infty} dy_M \\
&\quad \delta(\sum_{i=1}^{N} x_i - L) \delta(\sum_{j=1}^{M} y_j - L) \exp(-U_{N,M}/k_B T).
\end{aligned} \tag{4.4.8}
$$

The evaluation of the configuration sum is very difficult, we would like to treat the interaction term U_I at mean field level. At first we evaluate the partition function with the potential $U'_{N,M}$. By using Laplace transform [61], the partition function can be calculated easily and the expression is,

$$Z(u, \omega = 0, L) = \exp(2\eta_* L). \tag{4.4.9}$$

Here η_* is a solution of the following equation,

$$\exp(a\eta_*)\eta_* = \exp(-uL) \tag{4.4.10}$$

Then the free energy of the system is

$$
\begin{aligned}
\mathcal{F}_0 &\equiv -\ln Z^2(u, \omega = 0, L) \\
&= -2\eta_* L.
\end{aligned} \tag{4.4.11}
$$

The condition (4.4.10) is rewritten as,

$$\ln \eta_* + a\eta_* = -uL. \tag{4.4.12}$$

In the thermodynamic limit $L \to \infty$, the solution η_* is estimated as ($a = 1$),

$$
\eta_* = \begin{cases} \exp(-uL) & u > 0 \\ -uL & u < 0. \end{cases} \tag{4.4.13}
$$

Free energy $\mathcal{F}_0$ is

$$
\mathcal{F}_0 = \begin{cases} -2L \exp(-uL) & u > 0 \\ -2uL^2 & u < 0. \end{cases} \tag{4.4.14}
$$

The total number of folds N_{Total} is,

$$
\begin{aligned}
N_{Total} &\equiv <N + M - 2> \equiv \frac{\partial}{L \partial u} \mathcal{F}_0 \\
&= \begin{cases} 2L \exp(-uL) \to 0 \ (L \to \infty) & u > 0 \\ 2L & u < 0. \end{cases}
\end{aligned} \tag{4.4.15}
$$

This behavior completely coincides with the previous results [12, 59].

In the following we would like to study the effect of interactions on these results. From the above analysis, the lattice is in a completely flat phase ($u > 0$) or completely folded state ($u < 0$). When the lattice is in the flat state, the attractive interaction is considered to break the flat state like in the figure 6a.
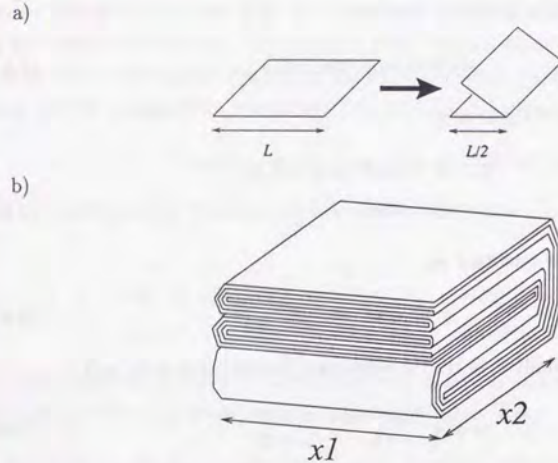
a)

b)

Figure 6: a) Folding transition of a flat membrane. Attractive interaction is considered to break the flat phase like in the figure.

b) Uniformly folded state of a square lattice. Each segment has equal length $x = L/N$.

We assume the broken flat state is an uniformly folded state with $N = 1 + \frac{1}{2}N_{Total}$ segments in each direction (fig 6b), that is each segment has equal length $\bar{x} \equiv L/N$. We estimate the effect of attractive interactions as,

$$< U_{CA} > = \omega(L^2 - \bar{x}^2) \tag{4.4.16}$$

$$< U_{CP} > = \frac{1}{2}\omega N^2(N^2 - 1)\bar{x}^2. \tag{4.4.17}$$

On the other hand, when the repulsive force breaks completely folded state, it is not clear how the folded state becomes unstable. We assume the above estimation holds even in this case. And in what follows, we also take the lattice constant $a = 0$ for the convenience of calculation. Then $\eta_* = \exp(-uL)$ and $N_{Total} = 2L\exp(-uL)$. However, when one interprets the results physically, the U.V.cutoff has to be taken into account. The total free energy is evaluated as

$$\mathcal{F}(u, \omega, L) = \begin{cases} -2\eta_* L + \omega(L^2 - \bar{x}^2) & \text{CA case} \\ -2\eta_* L + \frac{1}{2}\omega N^2(N^2 - 1)\bar{x}^2 & \text{CP case.} \end{cases} \tag{4.4.18}$$

From the relation $N_{Total} = 2L\exp(-uL)$, we can express u in terms of N_{Total},

$$uL = -\ln(N_{Total}/2L). \tag{4.4.19}$$

In the above estimation of interactions (4.4.17), we use the fold number $N = 1 + \frac{1}{2}N_{Total}$ which is a function of u. In order to rewrite the free energy $\mathcal{F}_0(u, \omega, L)$ in terms of (N_{Total}, ω, L), we perform the Legendre transform with respect to u. Then the free energy $\mathcal{G}(N_{Total}, \omega, L)$ is,

$$\mathcal{G}(N_{Total}, \omega, L) = uLN_{Total} - \mathcal{F}(u, \omega, L)$$
$$= \begin{cases} -N_{Total}\ln N_{Total}/2L + N_{Total} - \omega L^2(1 - N^{-2}) & \text{CA case} \\ -N_{Total}\ln N_{Total}/2 + N_{Total} - \frac{1}{2}\omega L^2(N^2 - 1). & \text{CP case.} \end{cases} \tag{4.4.20}$$

This free energy $\mathcal{G}$ has the following relation,

$$\frac{\partial \mathcal{G}}{\partial N_{Total}} = uL. \tag{4.4.21}$$

4.4.2 Phase diagram of square lattice with interactions

In what follows, we discuss the effect of interactions on the completely flat phase and on the completely folded state. At first, we discuss the effect of attractive interactions on the completely flat phase. In this case, N_{Total} is very small (~ 0) and the free energy $\mathcal{G}$ is roughly estimated as,

$$\mathcal{G}(N_{Total}, \omega, L) = uL < N_{Total} > -\mathcal{F}(u, \omega, L)$$
$$= \begin{cases} -N_{Total}\ln(N_{Total}/2L) + N_{Total} - \omega L^2 N_{Total} & \text{CA case} \\ -N_{Total}\ln(N_{Total}/2L) + N_{Total} - \frac{1}{2}\omega L^2 N_{Total}. & \text{CP case.} \end{cases} \tag{4.4.22}$$

Here we have discarded terms which are higher order in N_{Total} or which do not depend on N_{Total}. From the relation (4.4.21), N_{Total} is given by

$$N_{Total} = \begin{cases} 2L\exp(-(uL + \omega L^2)) & \text{CA case} \\ 2L\exp(-(uL + \frac{1}{2}\omega L^2)) & \text{CP case .} \end{cases} \tag{4.4.23}$$

This means that the completely flat phase becomes unstable with respect to both attractive interactions and the critical values $\omega_{critical}$ are

$$\omega_{critical} = \begin{cases} -u/L & \text{CA case} \\ -2u/L & \text{CP case .} \end{cases} \tag{4.4.24}$$

These values goes to zero in the thermodynamic limit $L \to \infty$, which is very natural. Because the free energy difference between the completely flat state and the one fold state with a crease at its center is $\delta F = \frac{1}{2}\omega L^2 + uL - \ln 2$ and it becomes negative for

$\omega < -2u/L$ [52]. However, after some sequential foldings, the behaviors of the membrane are different for each interaction. In this case N_{Total} is not small and eq.(4.4.21) becomes

$$uL \sim \begin{cases} -\omega L^2/N^3 & \text{CA case} \\ -\omega L^2 N & \text{CP case} . \end{cases} \qquad (4.4.25)$$

In the CP case, the effect of interaction becomes more and more important as N becomes large. And in the thermodynamic limit ($L \to \infty$), the bending ridity becomes irrelevant and the membrane is in the completely folded state.

We also note that the equation (4.4.21) has the following form

$$uL = -\ln(N_{Total}/2L) - \frac{1}{4}\omega L^2 N_{Total}. \qquad (4.4.26)$$

When ω is negative, the right hand side has a minimum. If u is small enough, the equation has no solution. The reason is that the free energy has no minimum and the model predicts a complete collapse of the membrane ($N \to \infty$). In order to avoid this catastrophe [50], we need to introduce three-body repulsive interactions like

$$U_{I,CT}(x_1, \cdots, x_N; y_1, \cdots, y_M) = w'(\text{Number of trios of contact elementary squares}).$$
$$(4.4.27)$$

Then the free energy has the following additional term,

$$< U_{I,CT} > = \frac{1}{6}\omega' L^2 (N^2 - 1)(N^2 - 2). \qquad (4.4.28)$$

Then the equation (4.4.21) is roughly,

$$-\omega = \frac{4u}{N_{Total}L} + \frac{4}{L^2 N_{Total}}\ln(N_{Total}/2L) + \frac{1}{6}\omega' N_{Total}^2. \qquad (4.4.29)$$

This equation has solutions N_{Total} for any value of ω when $\omega' > 0$. Especially, depending on the value of ω', there is the possibility that the equation has two solutions for some value of ω. Following the discusion about the coil-globule transition of a polymer, it corresponds to a discontinuous transition (change in N becomes discontinuous) [50].

On the other hand, in the CA case, the interaction becomes small as N becomes large and balancing the effect of bending rigidity and that of attractive interaction ($eq.$(4.4.25)), N behaves as $L^{1/3}$. The behavior of mean area is estimated to be $< L_x \times L_y >\sim \overline{x}^2 \sim L^{4/3}$. That is, the number of folds is small and the membrane is not in the completely folded state. We call this phase partially folded state and analyze its behavior by a numerical method later.

Secondly, we study the stability of the completely folded state with respect to repulsive interactions. In this case, N_{Total} is large ($\sim 2L$). In the CA case, the interaction is

irrelevant and the completely flat phase is stable with respect to the weak repulsive interaction. However, the situation is not so simple. In the completely folded state, the free energy per elementary square is $f_{fold} = 2u + \omega$ and in the flat phase $f_{flat} = 0$. From the discussion given in [59], the free energy of the system is given by

$$f_{square} = \text{Min}(f_{fold}, f_{flat}). \qquad (4.4.30)$$

Consequently, there occurs a first order phase transition between a completely flat phase ($2u + \omega > 0$) and a completely folded state ($2u + \omega < 0$). Intermediate folded state ($0 < N_{Total} < 2(L - 1)$) does not appear. [1]

In the CP case, the repulsive interaction becomes very large and the completely folded phase becomes unstable. Even if N and ω are small, the repulsive interaction wins over negative bending energy in the thermodynamic limit ($L \to \infty$) and we think that the membrane is flat. However in this case, the above estimation of the interaction (4.4.17) is not good. Because, when the membrane is almost flat, negative bending energy causes a crease at the edge of the membrane not at its center. Even if the system size is large a fold can occur at its edge and the membrane is not in the completely flat phase.

Phase diagrams for both interactions are summarized in Figures 7. Fig. 7a and 7b correspond to the phase diagrams of the system with CA interaction and that of the system with CP interaction. In the domain ($u > 0, \omega > 0$), the membrane is in the completely flat phase ($N_{Total} = 0$) and in the domain ($u < 0, \omega < 0$), the membrane is completely folded ($N_{Total} = 2L$) for both interactions. The completely flat phase ($u > 0$) becomes unstable by both attractive interactions ($\omega < 0$), however the resulting phases are different. In the CA case the membrane is partially folded and $N_{Total} \sim L^{1/3}$ and the mean area behaves $< L_x \cdot L_y >\sim L^{4/3}$. In the CP case, the membrane is completely folded. When the system size is finite ($L < \infty$), both system show the sequential folding transition. In the domain ($u < 0, \omega > 0$), the folded state also becomes unstable in both system. In the CA case, there occurs a first order phase transition from the completely folded phase to the completely flat phase at the line ($2u + \omega = 0$). In the CP case, the completely folded state becomes unstable by any amount of repulsive interaction and the membrane becomes flat.

---

[1]The free energy difference with system size $L \times L$ between the completely flat phase and the one folded state with a crease at its edge is $\delta F = (u + \omega)L$ and it is positive in the region $2u + \omega > 0$ and $\omega > 0$. Before the one folded state appears, the completely folded state appears at the line $2u + \omega = 0$ and the intermediate folded state does not occur.
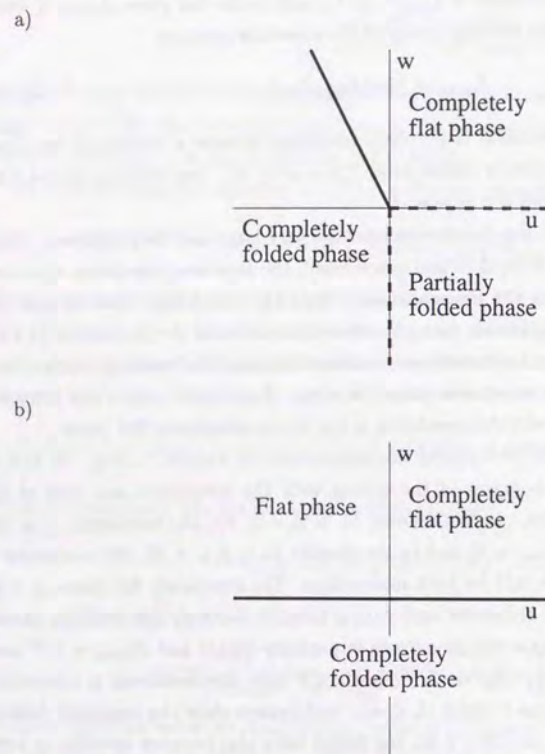
a)

b)

Figure 7: a) Phase diagram in the (u, ω) plane for the square lattice with CA type interaction. Three first order transition lines $\omega = -2u(u < 0), u = 0(\omega < 0)$ and $\omega = 0(u > 0)$ separate the three phases, completely flat phase, completely folded phase and partially folded state.

b) Phase diagram for the square lattice with CP type interaction. One first order line $\omega = 0$ separates the completely folded state from the flat phase.

4.4.3 · Numerical Studies

In this section, we will study the square lattice with CA interaction numerically. In the previous section, we have treated the segment lengths as continuous quantities. Hearafter, we return to the original discrete system.

The potential we consider is,

$$U_{N,M} = U'_{N,M} + U_{I,CA}(L_x, L_y), \qquad (4.4.31)$$

and we perform the configuration sum directly. From the definition of $U_{I,CA}$ (eq.(4.4.4)), the above potential only depends on the folding number $(N - 1, M - 1)$ and the width of each section (L_x, L_y). We can interpret each section as one-dimensional random walk with $L - 1$ steps and it has 2^{L-1} states. Main part of numerical calculation is the number counting of states which is specified by the final length l ($= L_x, L_y$ in the previous section) and the bending number b ($= N - 1, M - 1$). Table 1 shows such numbers which represent the degeneracies of corresponding (l, b) states for the $L = 12$ case. Hearafter, we denote such number as $D(l, b)$.

$l \backslash b$	0	1	2	3	4	5	6	7	8	9	10	11
1	0	0	0	0	0	0	0	0	0	0	0	1
2	0	0	0	0	0	1	7	20	30	25	11	0
3	0	0	0	1	10	56	102	140	80	30	0	0
4	0	0	1	16	74	139	192	100	55	0	0	0
5	0	0	6	38	84	140	84	70	0	0	0	0
6	0	1	13	38	86	70	77	0	0	0	0	0
7	0	2	8	34	32	56	0	0	0	0	0	0
8	0	2	12	20	44	0	0	0	0	0	0	0
9	0	2	4	18	0	0	0	0	0	0	0	0
10	0	2	11	0	0	0	0	0	0	0	0	0
11	0	2	0	0	0	0	0	0	0	0	0	0
12	1	0	0	0	0	0	0	0	0	0	0	0

Table 1: The number $D(l, b)$ of the states which have the length l and the b times folds for a 11 step random walk, obtained by exact enumeration on the computer.

Then we execute the following "standard" calculation to evaluate the partition function and other thermodynamic quantities for each set of parameters (u, ω). The partition function is evaluated as

$$Z(u, \omega, L) \equiv \sum_{L_x, L_y = 1}^{L} \sum_{N, M = 0}^{L-1} D(L_x, N) D(L_y, M) \exp\left[-U_{N,M}(N, M; L_x, L_y)\right] \quad (4.4.32)$$

where

$$U_{N,M}(N, M; L_x, L_y) = uL(M + N - 2) - \omega L_x L_y. \qquad (4.4.33)$$

Note that we have moved the energy origin by a constant $-wL^2$ from the definition of the previous section. The thermal average $< \quad >$ of some physical quantity $O(N, M, L_x, L_y)$ is defined as

$$< O(N, M, L_x, L_y) > \quad \equiv \quad \sum_{L_x, L_y=1}^{L} \sum_{N,M=0}^{L-1} D(L_x, N) D(L_y, M) O(N, M, L_x, L_y)$$
$$\exp\left[-U_{N,M}(N, M; L_x, L_y)\right] / Z[u, \omega, L]. \qquad (4.4.34)$$

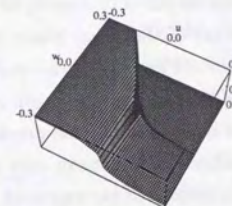The specific heat, mean area, mean folding number are calculated as,

$$\text{Specific Heat} \quad \equiv \quad <U_{N,M}{}^2> - <U_{N,M}>^2$$
$$\text{Mean Area} \quad \equiv \quad <L_x \times L_y>$$
$$\text{Mean Bending Number} \quad \equiv \quad <N_{Total}> \equiv <N + M - 2>.$$

In what follows, we presents the results of numerical studies. Figures 8 depict the mean bending number, the mean area and the specific heat for membranes of size $L = 30 \times 30$ for parameters u and ω in the range $-0.3 < u, \omega < 0.3$. These seem to imply that there are (at least) three different phases.
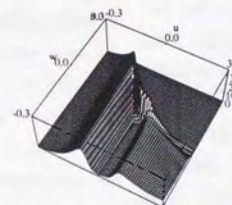
a)

b)
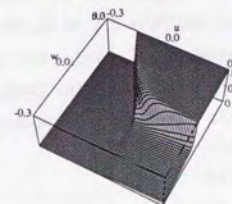
c)

Figure 8: Mean bending number (a), mean area (b) and specific heat (c) for square lattice of size $L = 30$ for parameters u and ω in the range $-0.3 < u, \omega < 0.3$. The first two are normalized by their maximum values.

In the region $\omega > 0$ and $\omega > -2u$, the membrane is in the completely flat phase. The mean bending number is zero and the mean area is maximum L^2. In the region $u < 0$ and $\omega < -2u$, the membrane is in the completely folded state. The mean bending number is

$2(L-1)$ and the mean are is 1. In the remaining region ($u > 0, \omega < 0$), the membrane is in the partially folded state. Both the mean bending number and the mean area are small but nonzero. We also find a first order transition from the completely flat to the completely folded state at the line $2u + \omega = 0$. Among of all, the emergence of "partially folded state" on the forth quadrant of the (u, ω) plane is interesting. In this region, in order to minimize the potential of the system, both bending number and lengths L_x, L_y have to be small. From the table 1, we can see that such configuration does not exist and equilibrium configuration has to manage it. In the previous section, by balancing these energies, the mean bending number and the mean area are estimated as $N_{Total} \sim L^{1/3}$ and $< L_x \times L_y > \sim L^{4/3}$. We have estimated the exponent μ of the mean bending number $< N_{Total} > \sim L^\mu$ as $\mu \simeq 0.39 \pm 0.05$. We also evaluated the exponent ν of the mean area $< L_x \times L_y > \sim L^\nu$ as $\nu \simeq 1.30 \pm 0.07$ (figures 9). The prediction of the mean field theory is good. When there is no interaction ($u = 0, \omega = 0$), the membrane is a direct product of two random walks in one dimension [12]. In this free case, the mean bending number is of course $\frac{1}{2}L$ and the exponent $\mu = 1.0$. From the figure 9c, the exponent for the mean area is $\nu = 1.55$. This means that the swell of the partially folded state is smaller than that of the free case.
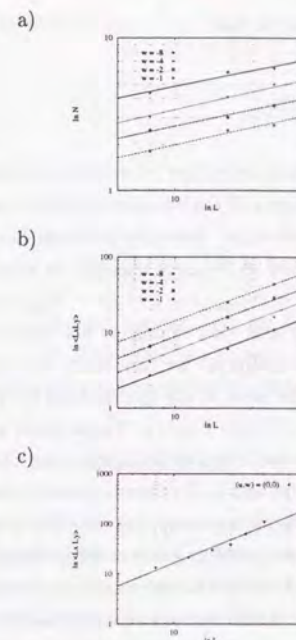
Figure 9: System size dependence of mean bending number a) and of mean area b). Bending rigidity u is fixed at $u = 0.5$. The lines indicate a fit of the data yielding exponents μ and ν (Mean bending number $\sim L^\mu$ and Mean area $\sim L^\nu$). The exponents are $\mu = 0.39 \pm 0.05$ and $\nu = 1.30 \pm 0.07$.

c) System size dependence of mean area for free system $(u, \omega) = (0,0)$.($\nu = 1.55$).

Nextly, we will discuss the phase transition between these phases. Previously we have discussed the phase transition between the completely flat phase and the completely

folded phase at a line $2u + \omega = 0$, we will discuss other two cases. At first, we study the transition from the completely flat phase to the partially folded phase. In the previous section, we have discussed that the membrane with finite L shows a sequential folding transition. Figures 10 show the behavior of the membrane. We have fixed the bending rigidity at $u = 0.5$. Figure 10a shows the behavior of the mean bending number as we change the strength of attractive interaction ω, which is scaled with u/L, for system size $L = 8, 16, 24$. In each system size, the curve runs up in a rather discrete manner like a staircase and its value at each plateau is almost integers. The length of each plateau becomes longer as ω becomes large. More detailed graph around the origin for the membrane of size $L = 30 \times 30$ is shown in other figures (Fig 10b), with the behavior of the mean area (Fig 10c). One notices that the first "jump" of the bending number from zero to one occurs at $w = -2u/L$ while the area becomes half of L^2, which implys that the membrane folds on itself and a crease neatly divides it in half. This can be easily understood from the view point of the energetic competition between flat and singly folded state in the previous section. As the bending number becomes large, the energy gain by a fold becomes small and the length of plateau becomes longer. We conclude that these behavior of the membrane is a sequential folding transition of the membrane.
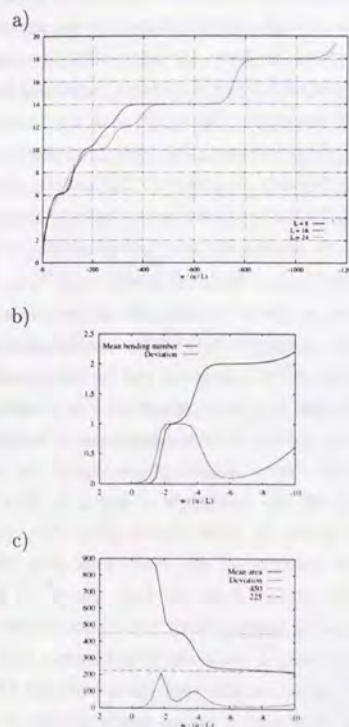
Figure 10: a) Mean bending number $< N_{Total} >$ versus strength of attractive interaction ω, which is scaled with u/L for $L = 8, 16, 24$ at $u = 0.5$. Mean bending number are quantized and plateaus emerge.

b,c) More detailed graphs for mean bending number and mean area around the origin for $L = 30$. When a first folding transition occurs, the mean area becomes half. This means that a crease neatly divides the

membrane in half.

The phase transition between the partially folded state and the completely folded state is discontinuous. Because the mean bending number $< N_{Total} >$ changes its behavior from $< N_{Total} > \sim L^{1/3}$ to $< N_{total} > = 2(L-1)$ and this change is not continuous. In addition, we can easily describe the double peak in the specific heat for the case $\omega = 0$ [2](see Fig.11). These peaks approaches each other as the system size L becomes large and in the thermodynamic limit $(L \to \infty)$, it becomes δ-function like peak and it correspond to a first order transition. These two peaks clearly remains in the domain $\omega < 0$ and we think that the transition from the partially folded $(u > 0)$ to a completely folded state $(u < 0)$ is a first order

---

[2]In the free case $\omega = 0$, we can calculate the partition function and other thermodynamic quantities for the discrete system as,

$$
\begin{aligned}
Z[u, \omega = 0, L] &= \{1 + \exp(-uL)\}^{2(L-1)} \\
N_{Total} &= 2(L-1)/\{1 + \exp(uL)\} \text{ (4.4.35)} \\
&\to \begin{cases} 0 & \text{as } u \to \infty \\ L-1 & u \to 0 \\ 2(L-1) & u \to -\infty \end{cases} \\
C \text{ (specific heat)} &= u^2 \frac{\partial^2}{\partial u^2} \ln Z(u, \omega = 0, L) \\
&= 2(L-1) \frac{(uL/2)^2}{\cosh^2 uL/2} \quad \text{(4.4.36)}
\end{aligned}
$$

These results suit very well with numerical studies on the u-axis (Fig.11).
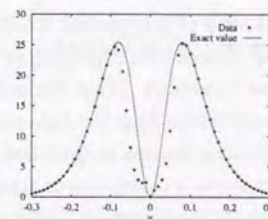
---

transition.

Figure 11: Specific heat for $L = 30$ with $\omega = 0$. The solid line is exact results and the dots are from numerical data.

4.4.4 Discussions

In this section, we have studied the square lattice with bending rigidity u and interaction ω. As an interaction between different elementary squares of the lattice, we have discussed two types. The first one is a potential which is proportional to contact area (CA), and the second one is a potential that is proportional to the number of contact pairs of elementary squares (CP). Especially, we have analyzed the stability of the completely flat phase $(u > 0)$ with respect to attractive interactions $(\omega < 0)$ and that of completely folded state $(u < 0)$ with respect to repulsive interactions $(\omega > 0)$. Both attractive interactions destroy the flat phase and these systems show a sequential folding transition when the system size is finite. However the resulting states are different. In the CA case the membrane is partially folded and in the CP case the membrane is completely folded. Repulsive interactions also destroy the completely folded state. In the CA case, there occurs a first order phase transition between a completely folded state to a completely flat state at the line $2u + \omega = 0$. In the CP case, any amount of repulsive interaction makes the membrane flat. These results are summarized in Figures 7.

We have also performed numerical studies for the CA case and confirmed several theoretical results. Especially, there occurs a sequential folding transition. This means that we can use the square lattice model with attractive interactions as a simple model for the sequential folding transition of tethered membrane. Thermodynamical behavior of the partially folded state is also studied and its total folding number and its area behave as $N_{Total} \sim L^{0.39}, < L_x \cdot L_y > \sim L^{1.30}$. This phase is more "compact" than the phase of the free membrane $(u, \omega) = (0.0, 0.0)$. On the other hand, the behavior of the membrane with CP interaction in the region $(u > 0, \omega < 0)$ is not clear when the three-body force exists. We cannot compare the behavior of the membrane with these interactions. Experiments on the polymerized membrane in poor solvent showed that the membrane is in a compact phase after several foldings [62, 63, 64]. However, we cannot decide which interaction is better than the other interaction in our analysis. From this point of view, the square lattice model with bending rigidity and CP interaction and three-body interaction deserves for future study.

4.5 Concluding Remarks

In this chapter, we have discussed the phase transition of polymerized membrane with attractive interactions. Extensive numerical studies showed that depending on the flexibility of the membrane it shows two types of phase transitions. When the membrane is very flexible, it seems to show a continuous phase transition from the high temperature flat phase to the low temperature compact phase passing through an intermediate crumpled phase. When the membrane is less flexible, it shows a discontinuous transition. In particular, if the membrane has open boundary it shows the sequential folding transition.

In order to understand the difference between these phase transitions physically, we have studied several models of polymerized membrane with attractive interactions. Especially, we have investigated the instabilities of the flat polymerized membrane by attractive interactions. Then we identify the flat phase of a rigid (phantom) polymerized membrane with the flat phase of a self-avoiding polymerized membrane and conclude that the cancellation between the "entropic" bending rigidity from self-avoidance and the negative bending rigidity from attractive interactions plays the essential role in understanding the difference between the phase transitions. That is, if the cancellation is complete, the phase transition becomes continuous like the crumpling transition and it passes through a critical crumpled state. On the other hand, if the flat phase becomes unstable before the cancellation becomes complete, the membrane shows discontinuous transition.

However, we will note that the above identification of the two flat phase is not right in some cases. Here we present one counter example [26]. We consider a flat phantom polymerized membrane. If we decrease the bending rigidity, that is, if we subtract κ from the initial value, the membrane of course shows the crumpling transition to the crumpled state. If the identification is right, a flat self-avoiding polymerized membrane shows the same crumpling transition by subtracting bending rigidity. This point hase been discussed and studied by Mori and Komura [26] and their numerical study showed that the membrane shows a phase transition from the flat phase to another rigid flat phase. And there does not appear any isotropic state. This is true even if the membrane is flexible and they conclude that the cancellation between the entropic bending rigidity and negative bending rigidity does not occur. And the identification is not true in this case and it is true only if the membrane is very flexible and the negative bending rigidity is induced by attractive interaction.

This is a subtle and difficult point in understanding the properties of polymerized membranes. Especially, if one study the stability of the flat phase theoretically, such difficulty always occurs. At the present time it is possible only to analyze the stability of the

phantom polymerized membrane and we need to assume that the result can be applied to the real self-avoiding polymerized membrane. However, up to now, we have no complete theory to describe the crumpling transition like crossover of the self-avoiding tethered membrane and we cannot treat the stability of the "true" self-avoiding polymerized membrane [3].

---

[3] Same situation also arises in the instability of the flat phase by the random stress.

Bibliography

[1] D.R.Nelson, T.Piran and S.Weinberg, eds.,Proceedings of the Fifth Jerusalem Winter School,"Statistical Mechanics of Membranes and Surfaces", World Scientific, Singapore,1989.

[2] P.B.Canham, "The minimum energy of bending as a possible explanation of the biconcave shape of the human red blood cell", J.Theor.Biol.26(1970)61.

[3] W.Helfrich, "Elastic properties of lipid bilayers: theory and possible experiments",Z.Naturforsch.$28C$(1973)693.

[4] D.R.Nelson and L.Peliti, "Fluctuations in membranes with crystalline and hexatic order",J.Phys.(Paris)48(1986)1085.

[5] F.David, E.Guitter and L.Peliti, "Critical properties of fluid membranes with hexatic order", J.Phys.(Paris)48(1987)2059.

[6] L.Peliti and S.Leibler, "Effects of Thermal Fluctuations on Systems with Small Surface Tension",Phys.Rev.Lett.54(1985)690.

[7] Y.Kantor, M.Kardar and D.R.Nelson, "Statistical Mechanics of Tethered Surfaces",Phys.Rev.Lett.57(1986)791,

[8] Y.Kantor, M.Kardar and D.R.Nelson, "Tethered surfaces: Statics and dynamics", Phys.Rev.$A35$(1987)3056.

[9] G.S.Grest and I.B.Petsche, "Molecular dynamics simulations of self-avoiding tethered membranes with attractive interactions: Search for a crumpled phase",Phys.Rev.$E50$(1994)1737.

[10] F.F.Abraham and D.R.Nelson, "Fluctuations in the flat and collapsed phases of polymerized membranes",J.Phys.(Paris)51(1990)2653.

[11] Y.Kantor and K.Kremer, "Excluded-volume interactions in tethered membranes",Phys.Rev.$E48$(1993)2490.

[12] F.David and E.Guitter, "Crumpling Transition in Elastic Membranes: Renormalization Group Treatment",Europhys.Lett.5(1988)709.

[13] E.Guitter, F.David, S.Leibler and L.Peliti, "Thermodynamical behavior of polymerized membranes", J.Phys.(Paris)50(1989)1787.

[14] M.Paczuski, M.Kardar and D.R.Nelson, "Landau theory of the Crumpling Transition",Phys.Rev.Lett.60(1988)2639.

[15] Y.Kantor and D.R.Nelson, "Crumpling Transition in Polymerized Membranes",Phys.Rev.Lett.58(1987)774.

[16] Y.Kantor and D.R.Nelson, "Phase transitions in flexible polymeric surfaces",Phys.Rev.$A36$(1987)4020.

[17] M.Plischke and D.Boal, "Absence of a crumpling transition in strongly self-avoiding tethered membranes",Phys.Rev.$A38$(1988)4943.

[18] F.F.Abraham, W.Rudge and M.Plischke, "Molecular Dynamics of Tethered Membranes",Phys.Rev.Lett.62(1989)1757.

[19] D.Boal, E.Levinson, D.Liu and M.Plischke, "Anisotropic scaling of tethered self-avoiding membranes", Phys.Rev.$A40$(1989)3292.

[20] A.Baumgarter and W.Renz, "Crumpled Self-Avoiding Tethered Surfaces",Europhys. Lett.17(1992)381.

[21] D.M.Kroll and G.Gompper, "Floppy Tethered Networks",J.Phys.1(Paris)3(1993)1131.

[22] E.Guitter and J.Palmeri, "Tethered membranes with long range interactions",Phys.Rev.$A45$(1992)734.

[23] M.Goulian, "The Gaussian Approximation for Self-Avoiding Tethered Surfaces",J.Phys.2(Paris)1(1991)1327.

[24] P.Le Doussal, "Tethered membranes with long-range self-avoidance: large-dimension limit",J.Phys.A: Math.Gen.25(1992)L469.

[25] G.S.Grest,"Self-avoiding tethered membranes embedded in high dimensions",J.Phys.1(Paris)1(1991)1695.

[26] S.Mori and S.Komura, "Self-Avoiding Tethered Membrane with Negative Bending Rigidity",preprint.

[27] D.R.Nelson and L.Radzihovsky, "Polymerized Membranes with Quenched Random Internal Disorder",Europhys.Lett.**16**(1991)79.

[28] L.Radzihovsky and D.R.Nelson, "Statistical mechanics of randomly polymerized membranes", Phys.Rev.**A44**(1991)3525.

[29] C.Carraro and D.R.Nelson, "Grain-boundary buckling and spin-glass models of disorder in membranes",Phys.Rev.**E48**(1993)3082.

[30] J.Aronovitz and T.C.Lubensky, "Fluctuations of Solid Membranes",Phys.Rev.Lett.**60**2636.

[31] H.S.Seung and D.R.Nelson, "Defects in flexible membranes with crystalline order", Phys.Rev.**A38**(1988)1005.

[32] M.Mutz, D.Bensimon and M.J.Brienne, "Wrinkling Transition in Partially Polymerized Vesicles", Phys.Rev.Lett.**67**(1991)923.

[33] D.Bensimon, M.Mutz and T.Gulik, "Wrinkling transition in polymerized membranes", Physica**A194**(1993)190.

[34] D.C.Morse, T.C.Lubensky and G.S.Grest, "Quenched disorder in tethered membranes", Phys.Rev.**45**(1992)2151.

[35] D.C.Morse and T.C.Lubensky, "Curvature disorder in tethered membranes: A new flat phase at $T = 0$", Phys.Rev.**A46**(1992)1751.

[36] L.Radzihovsky and P.Le Dousaal, "Crumpled glass phase of randomly polymerized membranes in the large d limit",J.Phys.(Paris)**I 2**(1992)599.

[37] D.Bensimon, D.Mukamel and L.Peliti, "Quenched Curvature Disorder in Polymerized Membranes",Europhys. Lett.**18**(1992)269.

[38] P.Le Dousaal and L.Radzihovsky, "Flat Glassy phases and wrinkling of polymerized membranes with long-range disorder", Phys.Rev.**B48**(1993)3548.

[39] D.R.Nelson and L.Radzihovsky, "Grain-boundary instabilities and buckling in partially polymerized membranes", Phys.Rev.**A46**(1992)7474.

[40] S.Mori and M.Wadati, "Randomly polymerized membrane with long range interactions",Phys.Lett.**A185**(1994)206.

[41] S.Mori and M.Wadati, "Tethered Membranes with Quenched Random Internal Disorders and Long Range interactions",J.Phys. Soc.Jpn.**63**(1993)3864.

[42] S.Mori and M.Wadati, "Crumpled Phases of Self-Avoiding Randomly Polymerized Membranes",Phys.Rev.**E50**(1994)867.

[43] D.C.Morse, I.B.Petsche, G.S.Grest and T.C.Lubensky, "Disorder in polymerized fluid membranes", Phys.Rev.**A46**(1992)6745.

[44] S.Mori, " Conformation of Self-Avoiding Randomly Tethered Membrane", Phys.Lett.**A207** (1995)87.

[45] S.Mori, "Self-Avoiding Tethered Membranes with Quenched Random Internal Disorder",preprint submitted to Phys.Rev.**E**.

[46] S.Mori, "Conformation of Self-Avoiding Randomly Tethered Membrane",preprint submitted to J.Phys.Soc.Jpn.

[47] Y.Kantor, "Glassy State of Polymerized membranes",Europhys.Lett.**20**(1992)337.

[48] S.F.Edwards and P.W.Anderson, "Theory of spin glasses",J.Phys.(Paris)**F5**(1975)965.

[49] M.Mezard and G.Parisi, "Replica field theory for random manifolds",J.Phys.1(Paris)**1**(1991).

[50] J.des Cloizeaux and G.Jannink, "Polymers in Solution", Clarendon Press, Oxford(1990).

[51] R.Friedberg and H.-C.Ren, "Field Theory on a computationality constructed random lattice",Nucl.Phys.**B235**(1984)310.

[52] F.F.Abraham and M.Kardar, "Folding and Unbinding Transitions in Tethered Membranes",Science **252**(1991)419.

[53] D.Liu and M.Plischke,"Monte Carlo studies of tethered membranes with attractive interactions",Phys.Rev.**A45**(1992)7139.

[54] S.Mori and M.Wadati, "Phase transitions of polymerized membrane with attractive long-range interactions",Phys.Lett.**A201**(1995)61.

[55] S.Mori and Y.Kajinaga, "Square Lattice with Attractive Interactions", Phys.Rev.**E**(in press).

[56] F.F.Abraham and M.Goulian, "Diffraction from Polymerized Membranes: Flat vs. Crumpled",Europhys.Lett.**19**(1992)293.

[57] T.Vilgis, A.Sans and G.Jannink, "Conformation of a polymer chain dissolved in a critical fluid", J.Phys.(Paris)II**3**(1993)1779 and references therein.

[58] Y.Kantor and M.V.Jaric, "Triangular Lattice Folding – a Transfer Matrix Study",Europhys.Lett.**11**(1990)158.

[59] P.Di Francesco and E.Guitter, "Folding Transition of the triangular lattice",Phys.Rev.**E50**(1994)4418.

[60] P.Di Francesco and E.Guitter, "Entropy of folding of the triangular lattice",Europhys.Lett.**26**(1994)455.

[61] See the review by F.W.Wiegel, "Models of conformational phase transitions" in "Phase Transition and Critical Phenomena", C.Domb and J.L.Lebowitz, Eds. (Academic Press, London, 1988), vol 7, chap. 2.

[62] T.Hwa, E.Kokufuta and T.Tanaka, "Conformation of graphite oxide membranes in solution",Phys.Rev.**A**(1991)R2235.

[63] X.Wen,C.Garland, T.Hwa, M.Kardar, E.Kokufuta, Y.Li, M..Orkisz and T.Tanaka, "Crumpled and collapsed conformations in graphite oxide membranes", Nature(London)**355**(1992)426.

[64] M.S.Spector, E.Naranjo, S.Chiruvolu and J.Zasadzinski, "Conformation of a Tethered Membrane: Crumpling in Graphite Oxide ?", Phys.Rev.Lett.**21**(1994)2867.